Winter 1-1-2012

A New Pathway Responsible For 53BP1 Loss in Breast Cancer and Laminopathies

David Alan Grotsky
Washington University in St. Louis

WASHINGTON UNIVERSITY IN ST. LOUIS

Division of Biology and Biomedical Sciences

Molecular Genetics and Genomics

Dissertation Examination Committee:
Susana Gonzalo, Chair
Dennis Hallahan
David Piwnica-Worms
Barry Sleckman
Katherine Weilbaecher
Zhongsheng You

A New Pathway Responsible For 53BP1 Loss in Breast Cancer and Laminopathies

by

David Alan Grotsky

A dissertation presented to the
Graduate School of Arts and Sciences
of Washington University in
partial fulfillment for the degree
of Doctor of Philosophy

December 2012

St. Louis, Missouri

Table of Contents

List of Figures

List of Tables

Acknowledgements

First I must thank my mentor, Susana Gonzalo, a brilliant scientist and wonderful person who cared about both my scientific and personal growth. Her never ending enthusiasm and optimism for science and my project was the greatest thing that led to my success as a graduate student. I am truly privileged to have been able to work with her and have her as my mentor.

Next, I must thank past and present members of the Gonzalo Lab, especially Ignacio Gonzalez-Suarez, Abena Redwood, and Martin Neumann who I worked with for the majority of my graduate school career. Their assistance and friendships made the lab a great place to work and I greatly appreciated all of the help they gave me through the years. I am also thankful to everyone else in the lab who contributed to my project, including Monica Croke, Sylvia Ortega-Martinez, Ray Kreienkamp, Sree Yaddanapudi, Jesus Caceres, and Stephanie Perkins.

Thank you to everyone I collaborated with through the years, especially Adriana Dusso who always had ideas and words of encouragement for me throughout all of graduate school. Thanks to Anna Novell, Montserrat Martinez-Alonso and Xabier Matias-Guiu at the University of Lleida in Spain for their work on the immunohistochemistry of the tumor tissue microarray. Thanks to all other collaborators including Junran Zhang, now at Case Western Reserve University in Cleveland, Ohio and to the laboratories of David Piwnica-Worms, Katherine Weilbaecher, Buck Rogers, and Enrique Izaguirre at Washington University.

I must thank all of my friends, especially those who I met in St. Louis and helped me get through graduate school. I have truly made lifelong friendships with all of them. Finally, thanks to my entire family for raising me and loving me, and thanks to my wonderful wife Laura without whom I would be lost.

ABSTRACT OF THE DISSERTATION

A New Pathway Responsible For 53BP1 Loss in Breast Cancer and Laminopathies

by

David Grotsky

Doctor of Philosophy in Molecular Genetics and Genomics

Washington University in St. Louis, 2012

Susana Gonzalo, Chairperson

53BP1 is a tumor suppressor protein that is important in the non-homologous end joining (NHEJ) pathway for DNA double strand break repair. Mice lacking 53BP1 present with increased radiosensitivity and genomic instability and are cancer prone. Loss of 53BP1 has been implicated by our laboratory in causing genomic instability in cells that lack A-type lamins and work by others has shown that loss of 53BP1 is associated with breast cancers of the poorest prognosis - BRCA1-mutated and Triple Negative Breast Cancers (TNBC) - and contributes to their resistance to current therapies, such as PARP inhibitors (PARPi). Work in our laboratory had previously identified a novel mechanism for regulation of 53BP1 protein levels - degradation by the cysteine protease cathepsin L (CTSL). The main questions addressed in this dissertation are whether CTSL-mediated degradation of 53BP1 is a mechanism contributing to BRCA1-mutated and TNBC tumor progression and resistance to therapy and if activation of this pathway is responsible for genomic instability in progeria and other laminopathies.

We found that CTSL-mediated degradation of 53BP1 is activated upon loss of BRCA1, rescuing homologous recombination (HR) and proliferation defects. Inhibiting CTSL using CTSL inhibitors or vitamin D treatment stabilizes levels of 53BP1 protein, leading to an increase

in NHEJ and defects in HR. Stabilization of 53BP1 using CTSL inhibitors or vitamin D leads to increased genomic instability and compromises proliferation following ionizing radiation or treatment with PARPi, which could represent a novel therapeutic strategy for breast cancers with the poorest prognosis. Furthermore, we identified nuclear CTSL as a novel biomarker for TNBC, which correlated inversely with 53BP1. We also identified the signature of low nuclear vitamin D receptor (VDR) with low 53BP1 and high nuclear CTSL in TNBC and BRCA1-mutated tumors, revealing a novel triple biomarker for stratification of patients with these cancers. We hypothesize that these patients can be treated with vitamin D or cathepsin inhibitors to stabilize 53BP1 levels to render tumor cells susceptible to PARPi treatment or other DNA damaging strategies.

We also show that the Δexon9Lmna mouse model of progeria exhibits telomere shortening and defects of heterochromatin, but not an increase in telomere deletions or an increase in genomic instability as seen upon loss of A-type lamins. Interestingly, the levels of 53BP1 are maintained in cells from these mice. These results demonstrate that different lamins mutations present with varying phenotypes and that 53BP1 status could be an important determinant for maintenance of genomic instability in some lamins-related diseases.

CHAPTER ONE

Introduction

1.1 Early events in the DNA damage response pathway

Proper repair of DNA damage is essential for the maintenance of genomic stability. Improper or inefficient repair of DNA damage can lead to mutations, chromosomal translocations, or loss of genetic information that could ultimately lead to diseases, such as cancer (Jackson & Bartek, 2009). DNA double strand breaks are particularly dangerous to the cell and constantly arise from both endogenous and exogenous damaging agents (Wyman & Kanaar, 2006). The cell has evolved a complex pathway, the DNA damage response, to sense, signal, and ultimately repair double strand breaks (**Figure 1-1**). The current model suggests the MRN complex, made up of MRE11, RAD50, and NBS1, senses the DNA double strand break and recruits ATM to the site (Lee & Paull, 2004, 2005). ATM is a master regulator that is either activated by the MRN complex or autophosphorylated on S1981 resulting in its activation (Bakkenist & Kastan, 2003; So, Davis, & Chen, 2009). ATM then phosphorylates H2AX, a histone H2A variant, on S139 (Burma, Chen, Murphy, Kurimasa, & Chen, 2001; Fernandez-Capetillo et al., 2002) which helps with the recruitment and foci formation of various DNA repair factors including 53BP1, NBS1, BRCA1, and MDC1 (Fernandez-Capetillo et al., 2002; Fernandez-Capetillo, Lee, Nussenzweig, & Nussenzweig, n.d.; Paull et al., n.d.; Stewart, Wang, Bignell, Taylor, & Elledge, 2003). MDC1 is considered to be a master organizer for protein assembly at breaks and binds directly to γH2AX to protect it from dephosphorylation (Stewart et al., 2003; Stucki et al., 2005). MDC1 then directly interacts with NBS1, one of the components of the MRN complex (Lukas et al., 2004), to promote recruitment of the ubiquitin ligase RNF8 (Kolas et al., 2007; Mailand et al., 2007). RNF8 ubiquitylates histones H2A and H2AX leading to chromatin restructuring and recruitment of another ubiquitin ligase, RNF168 (Doil et al., 2009). The ubiquitylated histones serve as marks for recruitment of the downstream effectors of

DNA double strand break repair, BRCA1, which facilitates homologous recombination, and 53BP1, which facilitates non-homologous end joining (Doil et al., 2009; Kolas et al., 2007; Mailand et al., 2007; Stewart et al., 2009).

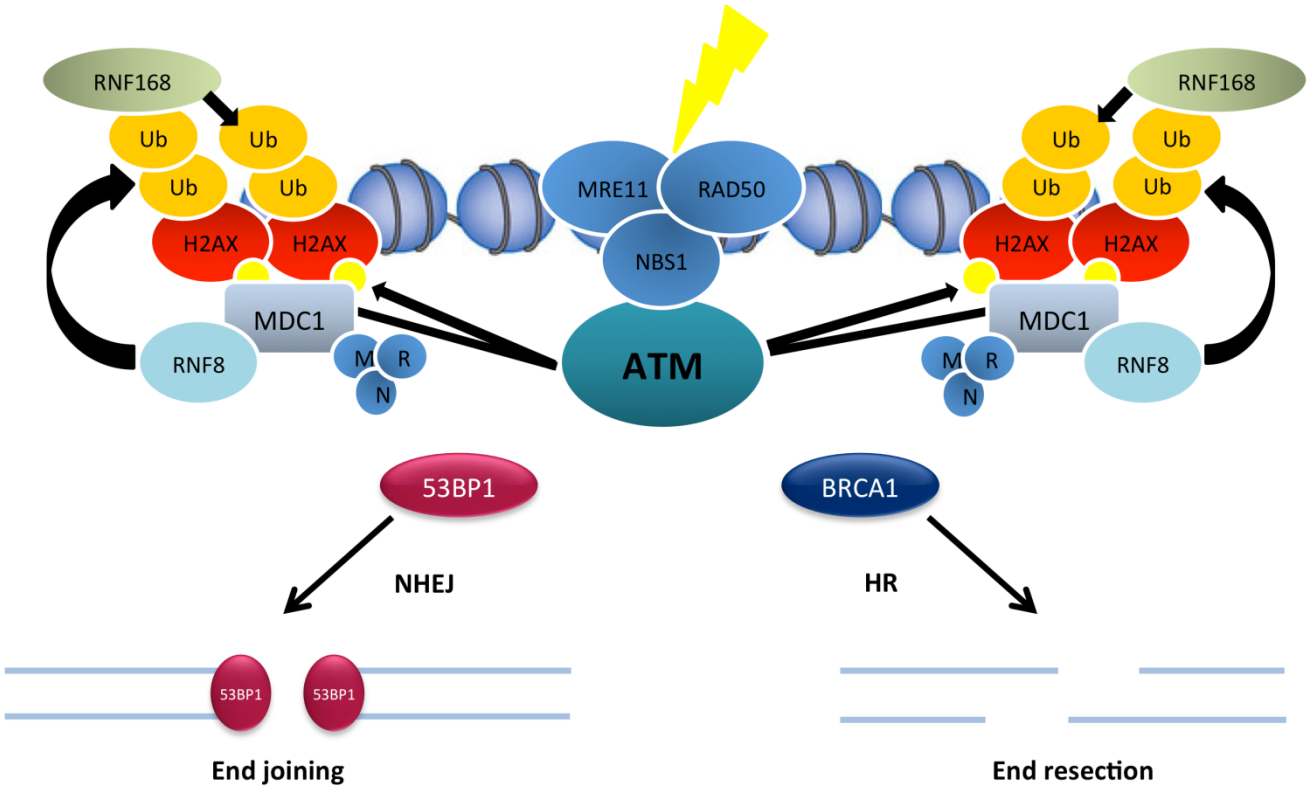

Figure 1-1. Important factors in the early stages of the DNA double strand break repair pathway. When a double strand break occurs, it is sensed by the MRN complex which recruits and activates ATM. ATM phosphorylates H2AX which targets MDC1 and other factors to the break. These factors attract RNF8 which ubiquitylates histones H2A and H2AX and leads to the accumulation of RNF168. The ubiquitylated histones serve as marks for localization of the downstream effectors, 53BP1 and BRCA1. 53BP1 facilitates non-homologous end joining while BRCA1 facilitates homologous recombination. See text for more detail.

The interaction of BRCA1 with RAP80, which contains a tandem ubiquitin-interacting motif, leads to BRCA1's direct binding to ubiquitylated histones at break sites (Kim, Chen, & Yu, 2007; Sobhian et al., 2007; B. Wang et al., 2007; Yan et al., 2007). 53BP1's tandem tudor

domains have been shown to interact with dimethylated histone H4 at lysine 20 to assist with its recruitment (Botuyan et al., 2006), providing further evidence that chromatin status is important in DNA repair. Also, 53BP1 and BRCA1 are both targets of sumoylation and the SUMO E3 ligases PIAS2 and PIAS4 are required for their recruitment to breaks (Galanty et al., 2009; Morris et al., 2009). Altogether, the DNA damage response is a multifaceted pathway that mobilizes and recruits a whole variety of nuclear factors to sites of DNA damage. This dissertation focuses specifically in the functional interplay of 53BP1 and BRCA1, two DNA repair factors with key roles in the choice of mechanism of DNA double strand break repair: homologous recombination or non-homologous end joining.

1.2 Homologous recombination

Homologous recombination (HR) is a key pathway in cells to repair DNA double strand breaks and is also important during meiosis. DNA repair by HR is mostly error free, and relies on the presence of a sister chromatid to serve as a template for recombination. Therefore, HR can only take place during the S/G2 phases of the cell cycle following replication of DNA.

A key initial step in HR is double strand break end resection to create long filaments of single stranded DNA. In yeast, the current view is that the nuclease Sae2 (as well as nucleases Exo1 and Dna2) is recruited to the break by the MRE11 subunit of the MRX (MRN in mammals) complex to conduct the resection (Huertas, Cortés-Ledesma, Sartori, Aguilera, & Jackson, 2008; Mimitou & Symington, 2009). Experiments have also shown that the human homolog of Sae2, CtIP, is required for end resection (Sartori et al., 2007).

Replication protein A (RPA) then binds to single stranded DNA to protect it from nucleases and hairpin formation (Fanning, Klimovich, & Nager, 2006). Next, RPA interacts with

the RAD51 recombinase followed by RAD51 displacement of RPA to form a RAD51-single stranded DNA coated filament (Golub, Gupta, Haaf, Wold, & Radding, 1998). In yeast, RAD51 associates with RPA to mediate RAD51 loading on RPA-coated DNA (Song & Sung, 2000) while in mammals there is evidence that BRCA2 assists with RAD51 recruitment to the single stranded DNA-double stranded DNA junction (H. Yang, Li, Fan, Holloman, & Pavletich, 2005). The RAD51 coated filament then performs homology search and strand invasion, followed by generation of a displacement loop (D-loop) to begin the synthesis of new DNA (Heyer, Ehmsen, & Liu, 2010; San Filippo, Sung, & Klein, 2008). The crossing over between homologous chromosomes to copy DNA ensures repair with high fidelity.

1.3 Breast cancer type 1 susceptibility protein (BRCA1)

BRCA1 is a tumor suppressor whose mutation of one allele in the germ line results in susceptibility to hereditary breast and ovarian cancer (HBOC) syndrome. This syndrome is associated with early onset breast cancer as well as a greater risk of pancreatic, stomach, laryngeal, fallopian tube, and ovarian cancer. BRCA1 mutations account for approximately 5% of all breast cancer cases and have a lifetime risk of breast cancer of 50-80% and ovarian cancer of 30-50% (Roy, Chun, & Powell, 2012).

The BRCA1 gene encodes a protein of 1863 amino acids and contains 24 exons (Miki et al., 1994), with a majority of amino acids being coded by exon 11. BRCA1 contains two functional domains: a tandem BRCT domain at the C-terminus and a Ring domain at the N-terminus. The Ring domain of BRCA1 has E3 ubiquitin ligase activity and can ubiquitylate other proteins (Panier & Durocher, 2009). BRCA1 normally forms a heterodimer with another protein containing BRCT and Ring domains, BARD1, which contributes to BRCA1's stability (Joukov,

Chen, Fox, Green, & Livingston, 2001). BRCA1 has been attributed to a whole host of cellular processes including maintenance of heterochromatin, regulation of epigenetic mechanisms such as DNA methylation, transcriptional regulation of several genes, control of centrosome numbers, and miRNA biogenesis (Kawai & Amano, 2012; Mullan, Quinn, & Harkin, 2006; Shukla et al., 2010; X. Xu et al., 1999; Zhu et al., 2011). However, BRCA1's most characterized role has been in its involvement in the DNA repair pathway. BRCA1 forms foci and localizes to sites of DNA double strand breaks (Scully et al., 1997) and loss of BRCA1 function leads to profound genomic instability characterized by unrepaired DNA breaks and complex chromosomal aberrations and rearrangements that compromise cell viability (Tirkkonen et al., 1997; X. Xu et al., 1999). As such, mouse strains with exon 11 of BRCA1 deleted are embryonic lethal (Evers & Jonkers, 2006), however, the lethality can be rescued by loss of ATM, Chk2, or p53, and these mice ultimately develop tumors (Cao et al., 2006)

BRCA1 is recruited to DNA double strand breaks through interaction of its BRCT repeats with a complex consisting of Abraxis and RAP80 (Kim et al., 2007; B. Wang et al., 2007). BRCA1 is thought to aid HR by facilitating end resection through its interaction with CtIP and the MRN complex, which in turn attributes a role for BRCA1 in DNA repair pathway choice (Chen, Nievera, Lee, & Wu, 2008; Yu, Wu, Bowcock, Aronheim, & Baer, 1998; Yun & Hiom, 2009). BRCA1, through its association with PALB2 and BRCA2 also plays an important role in RAD51 recruitment to single stranded DNA (Roy et al., 2012; F. Zhang et al., 2009).

BRCA1 is also involved in the activation of the G1/S, S-phase, and G2/M checkpoints. The BRCA1-BARD1 complex is required for ATM/ATR dependent phosphorylation of p53 at ser-15 following DNA damage (Fabbro et al., 2004). This BRCA1 dependent phosphorylation of p53 induces the CDK inhibitor p21 to promote the G1/S checkpoint following damage. Studies

have shown that the BRCA1-deficient cell line, HCC1937, has a defective S-phase checkpoint and reconstitution of BRCA1 in these cells restores this checkpoint (B. Xu, Kim St, & Kastan, 2001). BRCA1 has also been shown to regulate the G2/M checkpoint by activating Chk1 kinase following DNA damage (Yarden, Pardo-Reoyo, Sgagias, Cowan, & Brody, 2002). BRCA1 is clearly essential for DNA repair and many other cellular processes. Investigating the regulation and functions of BRCA1 and its interactions is important for understanding its role in the cell and how it contributes to tumorigenesis.

1.4 Non-homologous end joining

Non-homologous end joining (NHEJ) repairs DNA double strand breaks by ligation of two broken ends and is the dominant mechanism of DNA repair during G0, G1, and early S phases of the cell cycle (Lieber, Ma, Pannicke, & Schwarz, 2003). NHEJ also continues to repair breaks during late S and G2 phases when HR is occurring. Since no homologous chromosome is present as a repair template and broken ends are processed in NHEJ, it is considered to be error prone. Upon recognition of a double strand break, a heterodimeric complex of Ku70 and Ku80 binds to both ends of the broken DNA which promotes end alignment of the two ends (Walker, Corpina, & Goldberg, 2001). The Ku complex then recruits DNA-PK_{CS}, a member of the PIKKs (phosphoinositide 3-kinase-like family of protein kinases), and it is phosphorylated leading to inward movement of the DNA ends which allows two DNA-PK_{CS} molecules to form a synapse between the broken DNA ends (DeFazio, Stansel, Griffith, & Chu, 2002; Gottlieb & Jackson, 1993; Hartlerode & Scully, 2009).

Minimal end processing is required to prepare broken DNA strands for ligation. Artemis interacts with DNA-PK_{cs} to form 5'-phosphorylated ligatable ends that are required for repair

and is also able to cleave DNA loops, flaps, and gaps (Ma, Pannicke, Schwarz, & Lieber, 2002; Ma, Schwarz, & Lieber, 2005; Moshous et al., 2001). Other DNA gaps generated upon DNA damage are likely filled in by members of the DNA polymerase X family of polymerases, polymerase μ, polymerase λ, and terminal deoxyribonucleotidyltransferase (TdT) (Stephanie A Nick McElhinny & Ramsden, 2004; Walker et al., 2001). Ligation is carried out by a complex consisting of the ligase, DNA ligase IV, XRCC4, which forms a scaffold by interacting with Ku and DNA, and XLF, which is important for stimulating ligase activity (Grawunder et al., 1997; Grawunder, Zimmer, & Leiber, 1998; Gu, Lu, Tsai, Schwarz, & Lieber, 2007; S A Nick McElhinny, Snowden, McCarville, & Ramsden, 2000). Mice lacking Artemis or DNA-PK_{cs} are highly sensitive to ionizing radiation and present with immunodeficiency syndromes (Moshous et al., 2001; Rooney et al., 2002).

The core members of the NHEJ pathway are not only used to repair exogenous DNA damage but also for the deliberate formation and repair of DNA double strand breaks during class switch recombination and V(D)J (Variable, Diversity, and Joining) recombination (Dudley, Chaudhuri, Bassing, & Alt, 2005). NHEJ is also responsible for end joining of dysfunctional telomeres (Difilippantonio et al., 2008; Riha, Heacock, & Shippen, 2006), and paradoxically, Ku and DNA-PK_{cs} play roles in normal telomere length maintenance (Boulton & Jackson, 1998; Espejel et al., 2004). Thus, classical NHEJ is important for many cellular functions.

In addition to this classical form of NHEJ, new evidence is emerging about a pathway known as alternative or backup NHEJ (A-NHEJ or B-NHEJ) where end joining can occur in the absence of Ku, XRCC4, or DNA ligase IV. This pathway relies on microhomology-mediated end-joining, where CtIP resects DNA to reveal short regions of homology which are ligated primarily by DNA ligase III (Bennardo, Cheng, Huang, & Stark, 2008; Simsek et al., 2011; Y.

Zhang & Jasin, 2011). Since resected DNA in alternative NHEJ is not repaired with sequence from a homologous chromosome, A-NHEJ could be a more error prone pathway than classical NHEJ or HR. As such, it has been shown that A-NHEJ plays a major role in formation of chromosomal translocations in mouse embryonic stem cells (Y. Zhang & Jasin, 2011).

1.5 p53 Binding Protein 1 (53BP1)

53BP1 was originally discovered in a yeast two-hybrid screen looking for p53-interacting proteins (Iwabuchi, Bartel, Li, Marraccino, & Fields, 1994). Since 53BP1 contains tandem BRCT domains, it was associated with the DNA damage response pathway (Li & Zou, 2005). 53BP1 has no enzymatic function and is thought to serve as a platform for recruitment of other DNA damage response proteins. 53BP1 is rapidly recruited to ionizing radiation induced foci (IRIF) following double strand break induction, colocalizes with γH2AX and is a substrate for ATM (Anderson, Henderson, & Adachi, 2001; Rappold, Iwabuchi, Date, & Chen, 2001; Schultz, Chehab, Malikzay, & Halazonetis, 2000; Ward, Minn, van Deursen, & Chen, 2003). While 53BP1 does not appear to be necessary for core NHEJ, it is thought to be required for ATM-dependent NHEJ following DNA damage at heterochromatin, along with H2AX, NBS1, and MRE11 (FitzGerald, Grenon, & Lowndes, 2009; Goodarzi et al., 2008; Riballo et al., 2004). Cells deficient in 53BP1 are sensitive to irradiation and have a defect in the G2/M checkpoint following low doses of ionizing radiation, though not high doses (Fernandez-Capetillo et al., 2002; Nakamura et al., 2006). 53BP1 knockout mice exhibit radiosensitivity, growth retardation, cell cycle defects, chromosomal instability, and are cancer prone (Ward et al., 2003).

53BP1 has established roles in NHEJ during long range DNA double strand break repair, such as long range V(D)J recombination and class switch recombination. NHEJ plays a major

role in maturation of B and T lymphocytes by generating antigen response elements through breaking of DNA by the RAG1 and RAG2 endonucleases and rejoining by NHEJ proteins (Noon & Goodarzi, 2011). 53BP1 was found to have an essential role in the joining of distal ends of the V(D)J genes (Difilippantonio et al., 2008). As such, 53BP1 knockout mice exhibit growth retardation and immune deficiencies characterized by reduction in thymus size and reduced T cell count (Morales et al., 2003). 53BP1 acts similarly in class switch recombination during B cell activation to move and join distal ends of DNA (Bothmer et al., 2011).

The NHEJ pathway is activated in response to deprotected telomeres, which are recognized as DNA double strand breaks. 53BP1 was found to be important for the mobility and joining of telomeres upon disruption of the shelterin complex (Dimitrova, Chen, Spector, & de Lange, 2008). Studies in our laboratory have also implicated 53BP1 in end joining of dysfunctional telomeres (Gonzalez-Suarez et al., 2009).

1.6 53BP1 and BRCA1 compete for DNA double strand break repair pathway choice

Although HR can only take place during the late S and G2 phases of the cell cycle, and NHEJ predominantly takes place during G0/G1 and early S phases of the cell cycle, NHEJ still occurs during late S and G2 phases to repair double strand breaks formed during replication. A key question in the DNA repair field has been how are double strand breaks directed to repair by error free HR rather than error prone NHEJ. A study in 2009 suggested that phosphorylation of the end resection protein CtIP as cells enter S phase, along with the recruitment of BRCA1 serves as a switch to shift cells from NHEJ to HR (Yun & Hiom, 2009). This notion was supported by the finding that 53BP1 is able to inhibit HR by blocking end resection at double

strand breaks (Bothmer et al., 2011; Bunting et al., 2010). In concert with these findings, several studies have revealed that loss of 53BP1 rescues the embryonic lethality observed in mice with BRCA1 deleted of exon 11 without increasing tumorigenesis (Bouwman et al., 2010; Bunting et al., 2010; Cao et al., 2009). Loss of 53BP1 rescued HR, thereby alleviating the genomic instability and increased tumorigenesis normally observed in these mice. The current model suggests that when BRCA1 is absent, 53BP1 accumulates at DNA double strand breaks and blocks end resection, leading to aberrantly upregulated NHEJ and chromosomal instability that results in proliferation arrest or cell death **(Figure 1-2)**. When 53BP1 is lost in this context, end resection is allowed and HR is rescued, promoting error free DNA repair. Interestingly, downregulation of 53BP1 was observed in human BRCA1-mutated and triple-negative breast tumors (tumors with very poor prognosis that are often BRCA1-deficient) which could explain how these tumors overcome the genomic instability caused by HR defects (Bouwman et al., 2010). These results have very important implications for treatment of breast cancer.

HR deficient cells, such as BRCA1-mutated, are exquisitely sensitive to treatment with poly(ADP-ribose) polymerase inhibitors (PARPi) (Bryant et al., 2005; Farmer et al., 2005). PARP functions as a mediator in the base excision repair pathway, which is important for the repair of DNA single strand breaks and gaps (McCabe et al., 2006). If PARP is inhibited, single strand breaks are converted to double strand breaks which are repaired primarily by HR. Therefore, in HR deficient cells, double strand breaks generated after PARP inhibition are not properly repaired leading to genomic instability and cell death. These drugs are currently being used in clinical trials for BRCA1-mutated breast and ovarian cancers (Fong et al., 2009).

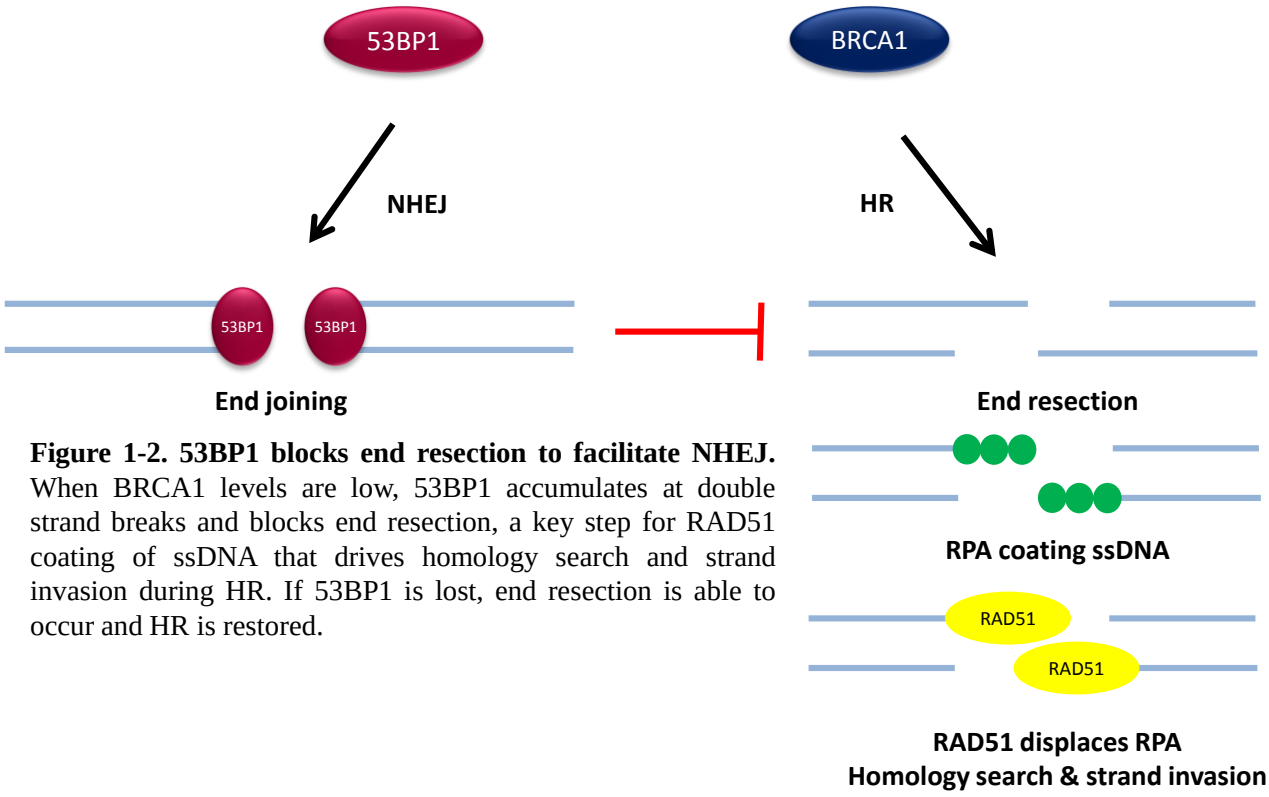

Figure 1-2. 53BP1 blocks end resection to facilitate NHEJ. When BRCA1 levels are low, 53BP1 accumulates at double strand breaks and blocks end resection, a key step for RAD51 coating of ssDNA that drives homology search and strand invasion during HR. If 53BP1 is lost, end resection is able to occur and HR is restored.

However, several studies have indicated that BRCA1 mutant cells can become resistant to PARPi by acquiring mutations in the BRCA1 gene that restores HR (Ashworth, 2008; Swisher et al., 2008; W. Wang & Figg, 2008). It was also shown that loss of 53BP1 in BRCA1-deficient cells increases resistance to PARPi and other DNA damaging strategies, which could be occurring in the human tumors with low 53BP1 (Bouwman et al., 2010; Bunting et al., 2010). Thus, doubly deficient cells in BRCA1 and 53BP1 are 'synthetically viable' (Aly & Ganesan, 2011). It is interesting to speculate that upregulating 53BP1 levels would render BRCA1-deficient cells and tumors 'synthetically lethal' to PARPi treatment and other DNA damaging strategies.

1.7 A-Type Lamins

A-type lamins are type V intermediate filaments that underlie the inner nuclear membrane and form a meshwork throughout the nucleoplasm, providing nuclear shape and stability (**Figure 1-3)** (Stuurman, Heins, & Aebi, 1998). A-type lamins have been implicated in many essential nuclear processes, including DNA replication and repair, gene transcription and silencing, positioning of nuclear pore complexes, chromatin remodeling, and nuclear envelope breakdown and assembly during mitosis (Goldman, Gruenbaum, Moir, Shumaker, & Spann, 2002; Gruenbaum, Margalit, Goldman, Shumaker, & Wilson, 2005). Four splice variants of A-type lamins are encoded by the *LMNA* gene (Lin & Worman, 1993). The major products are lamin A and the smaller lamin C, and the minor products are lamin AΔ10 and lamin C2, which is germline specific (Furukawa, Inagaki, & Hotta, 1994; Machiels et al., 1996). A-type lamins are only expressed in differentiated cells and are absent in mouse embryos until embryonic day 12 (Constantinescu, Gray, Sammak, Schatten, & Csoka, 2006). Almost all adult somatic cells in mice express lamin A/C, however A-type lamins were found to be absent from cells of the immune system such as B and T lymphocytes and cells isolated from the spleen, thymus, or bone marrow (Röber, Sauter, Weber, & Osborn, 1990).

Lamin A is first translated into prelamin A, which undergoes many processing steps to produce mature lamin A. First, the cysteine in the C-terminal CaaX motif of prelamin A is farnesylated, which likely targets the lamins to the inner nuclear membrane (Hennekes & Nigg, 1994). Then, the last three residues of the CaaX motif are cleaved and the cysteine undergoes methyl esterification. Finally, the farnesyl group and 15 C-terminal amino acids are cleaved by the zinc metalloproteinase Zmpste24 to produce mature lamin A (Mattout, Dechat, Adam,

Goldman, & Gruenbaum, 2006). Similarly to other intermediate filaments, lamins have a central α-helical coiled coil rod domain which is flanked by a non-helical N-terminal head domain and C-terminal tail domain (Stuurman et al., 1998). A-type lamins interact with several nuclear proteins that help lamins carry out their function, including lamins-associated proteins (LAP), emerin, nesprin, lamin B receptor (LBR), SUN proteins, and RING finger binding protein (RFBP) (Goldman et al., 2002).

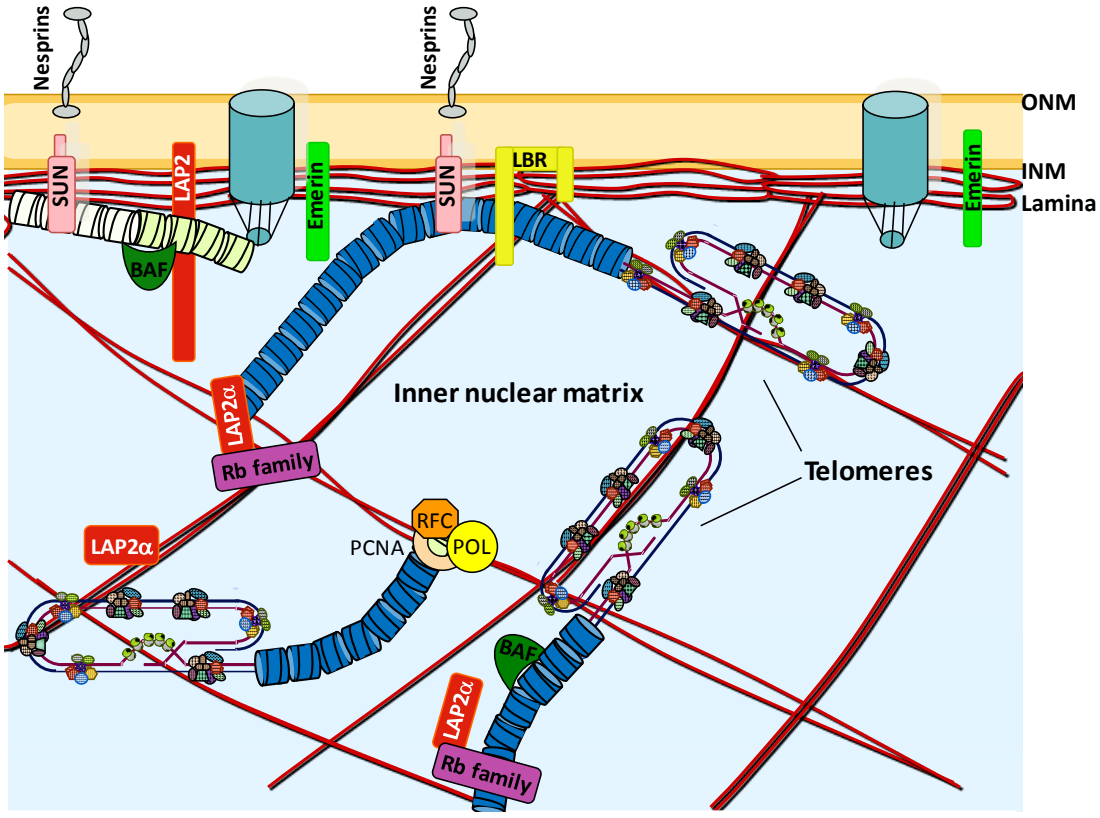

Figure 1-3. Nuclear distribution of A-type lamins. A-type lamins (in red) directly underly the inner nuclear membrane to give the nucleus structural support and shape, where they interact with several membrane proteins. They also form a meshwork throughout the nucleoplasm that associates with chromatin and nucleoplasmic proteins. We and others have found that A-type lamins interact with heterochromatic domains such as telomeres and centromeres.

More than 300 mutations in the human *LMNA* gene have been associated with a class of diseases termed laminopathies which display a wide range of pathologies (Dechat, Gesson, & Foisner, 2010). Laminopathies can affect adipose tissue, such as in partial lipodystrophy, muscle tissue, such as in several types of muscular dystrophy and cardiomyopathy, and axonal neurons, such as in Charcot-Marie-Tooth disorder (Mattout et al., 2006). *LMNA* mutations also lead to several early aging syndromes, the most dramatic and severe being Hutchinson-Gilford Progeria Syndrome (HGPS). Patients with HGPS appear normal at birth, but develop severe growth abnormalities by two years of age. Children with progeria continue to exhibit characteristics associated with aging, and generally die due to atherosclerosis at age 12 to 15. Most human progeria cases are caused by a splicing defect in exon 11 of the *LMNA* gene. A substitution of C to T at nucleotide -1824 (G608G) introduces a cryptic donor splice site that results in the deletion of 50 amino acids in prelamin A (De Sandre-Giovannoli et al., 2003; Eriksson et al., 2003). This altered form of lamin A is known as progerin and is toxic to the cells. Studies have shown that fibroblasts from progeria patients and expression of progerin in cells leads to telomere shortening (Decker, Chavez, Vulto, & Lansdorp, 2009; Huang, Risques, Martin, Rabinovitch, & Oshima, 2008), supporting the notion that telomere attrition is involved in the aging process.

Several mouse models to study laminopathies, including progeria, have been generated. The *LMNA* knockout mouse is one of the best characterized, providing data regarding the cellular and organismal consequences of loss of A-type lamins functions (Sullivan et al., 1999). These mice exhibit structural changes to the nuclear envelope and develop abnormalities that resemble the human laminopathy Emery-Dreyfuss muscular dystrophy. They die at two months of age with severe growth retardation and cardiomyopathy. A mouse model of progeria that expresses the mutant form of lamin A that is missing the final 50 amino acids (progerin) leads to

slow growth, bone abnormalities, and loss of fat, and ultimately mice die within 6 weeks (S. H. Yang et al., 2006). Cells from these mice exhibit misshapen nuclei and nuclear blebbing, and interestingly, treatment with fanesyltransferase inhibitors (FTI) to block progerin targeting to the inner nuclear membrane improved the nuclear abnormality phenotype (S. H. Yang et al., 2005). The first clinical trials testing the efficacy of FTI treatment in HGPS patients are currently ongoing (Gonzalez, Pla, Perez-Sala, & Andres, 2011). Early results indicate that FTI treatment led to weight gain in some children and all children participating in the clinical trial had at least one measureable improvement in cardiovascular stiffness, bone structure, or audiological status (Gordon et al., 2012).

Another premature aging mouse model is the *Zmpste24* knockout. These mice lack the metalloproteinase that is required to cleave the farnesylated tail of prelamin A to produce mature lamin A. In cells from these mice, mature lamin A is absent and farnesylated prelamin A accumulates at the nuclear periphery. These mice die at around five months of age and exhibit growth retardation, cardiomyopathy, muscular dystrophy, lypodystrophy, and a progeroid phenotype (Pendás et al., 2002; Varela et al., 2005). A mouse model of progeria has also been made by introducing a point mutation in exon 9 of the *LMNA* gene which was intended to generate the L530P substitution in amino acid sequence (Mounkes, Kozlov, Hernandez, Sullivan, & Stewart, 2003). This mutation caused mRNA splicing defects between exons 9 and 10 and deletion of exon 9 (Δexon9Lmna), which is accompanied by very low levels of mutant lamin A/C protein. Although the L530P point mutation is associated with muscular dystrophy in humans, the Δexon9Lmna mouse has a progeroid phenotype, with severe growth retardation and death within 4-5 weeks, but no evidence of muscular dystrophy. Thus, despite lower levels of A-type lamins, these mice present with a phenotype that is significantly different from that of

LMNA knockout mice, indicating distinct functional consequences of complete loss of A-type lamins and expression of low levels of mutant lamin A. Investigating the phenotypic difference between mouse models of laminopathies should reveal new insights into the pathogenesis of these diseases in humans.

A-type lamins have also been implicated in tumorigenesis. Differences in A-type lamins expression has been observed in several cancer types and has been linked to increased tumor aggressiveness (Prokocimer et al., 2009; Prokocimer, Margalit, & Gruenbaum, 2006). Methylation-induced silencing of the *LMNA* gene has been observed in leukemias, lymphomas, and small cell lung cancer, while over-expression is associated with colon carcinoma (Agrelo et al., 2005; Broers et al., 1993; Willis et al., 2008). Lamins have also been shown to affect pathways that regulate cancer. Importantly, loss of A-type lamins leads to increased proteasomal degradation and mislocalization of pRB and p107, key tumor suppressors (Johnson et al., 2004).

Studies in our own laboratory have revealed novel roles for A-type lamins in maintaining genomic stability and the DNA repair pathway (**Figure 1-4)**. *LMNA* null fibroblasts exhibit several telomere defects, including altered nuclear distribution of telomeres, telomere attrition, and defects in epigenetic heterochromatin status (Gonzalez-Suarez et al., 2009). We also observed an increase in genomic instability characterized by increases in signal free ends (telomere loss), chromosome and chromatid breaks, basal γH2AX foci formation characteristic of unrepaired DNA damage, and aneuploidy. Interestingly, although there was an increase in telomere deprotection, we did not observe an increase in chromosome end-to-end fusions, indicating a possible deficiency in the processing of dysfunctional telomeres by NHEJ. We found that loss of A-type lamins leads to a marked decrease in 53BP1 levels, due to upregulation of the cysteine protease cathepsin L (CTSL), and that this loss of 53BP1 is responsible for the lack of

chromosome end-to-end fusions that we observed (Redwood et al., 2011). Loss of A-type lamins also causes defects in DNA repair kinetics, specifically loss of the fast phase of repair corresponding to NHEJ, which are rescued by ectopic introduction of 53BP1. Furthermore, loss of A-type lamins impacts HR as well. We found that depletion of lamins leads to degradation of the Rb family members pRB and p107, but not p130. The increase in p130/E2F4 repressor complex formation was associated with transcriptional downregulation of BRCA1 and RAD51. Consistent with the defects in DNA repair mechanisms, lamins deficient cells exhibited increased radiosensitivity (Redwood et al., 2011). These studies demonstrated that A-type lamins promote genomic stability by maintaining the levels of key proteins involved in DNA repair mechanisms-HR and NHEJ-and in cell cycle regulation –Rb family members-.

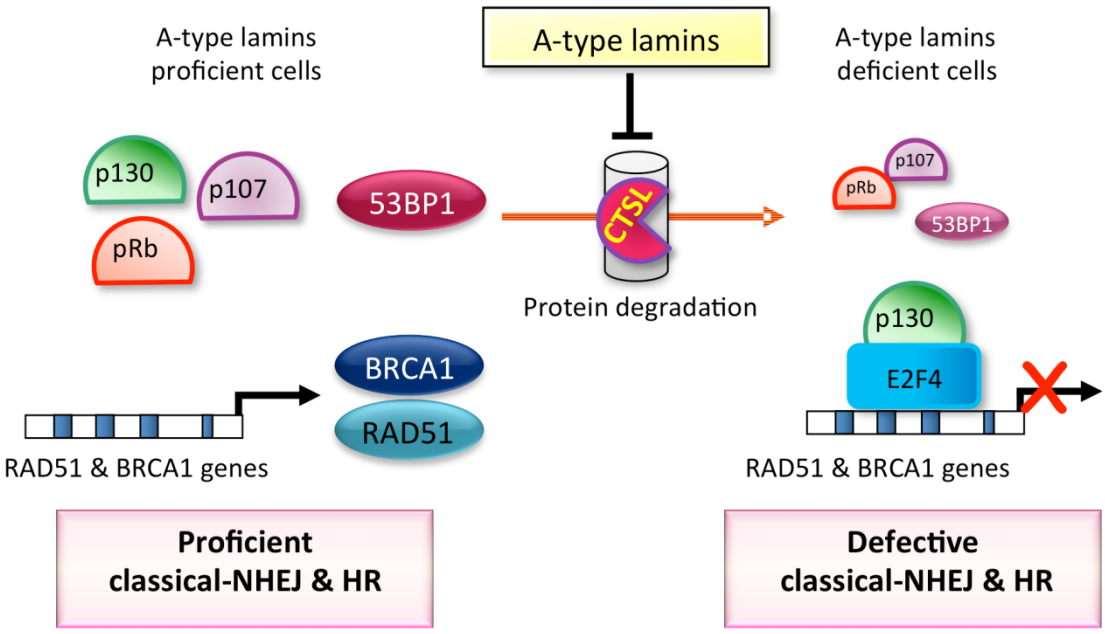

Figure 1-4. A-type lamins promote genomic stability by maintaining levels of key DNA repair proteins. A-type lamins stabilize levels of 53BP1 and Rb family members pRb and p107 by inhibiting CTSL-mediated degradation. The stabilization of 53BP1 facilitates classical non-homologous end joining (NHEJ). The reduction of pRb and p107 leads to increased formation of p130/E2F4 repressor complexes which repress BRCA1 and RAD51 transcription, compromising homologous recombination (HR).

1.8 Cathepsin L

Given that loss of A-type lamins leads to destabilization of 53BP1, we sought to determine how 53BP1 levels were being reduced. The loss of 53BP1 was due to a post-translational effect on protein stability, as 53BP1 transcripts levels in *LMNA* null cells remained constant. Therefore, we decided to test if the proteasome or a cysteine protease, cathepsin L (CTSL), could be responsible for the degradation of 53BP1. We investigated CTSL because a previous study had shown that in the *Zmpste24* knockout mouse model of progeria, levels of CTSL were elevated in liver and heart tissues (Varela et al., 2005). We showed that 53BP1 levels were stabilized in *LMNA* null cells when treated with a proteasome inhibitor and with an inhibitor specific for cathepsin L (Gonzalez-Suarez et al., 2011). The stabilization of 53BP1 with the CTSL inhibitor was more profound than with the proteasome inhibitor, so we decided to investigate the role of CTSL further. Indeed, we found that upon loss of A-type lamins the levels of 53BP1 were decreased concomitantly with transcriptional upregulation of CTSL. Depletion of CTSL in *LMNA* null cells rescued 53BP1 levels as well as the defect in DNA repair kinetics upon loss of A-type lamins, while overexpression of CTSL in wild type cells led to the degradation of 53BP1, unveiling a novel mechanism for regulation of 53BP1 protein levels (**Figure 1-5)** (Gonzalez-Suarez et al., 2011).

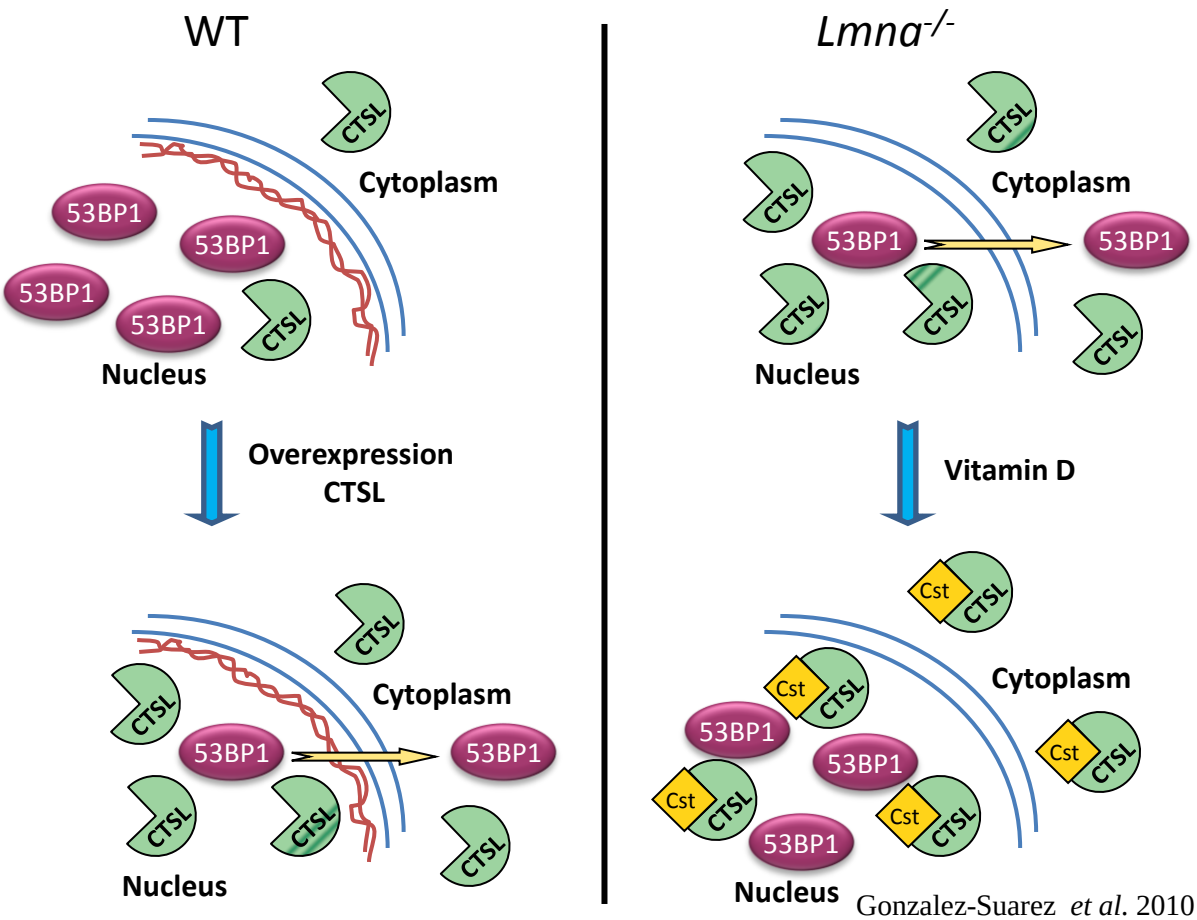

Gonzalez-Suarez *et al.* 2010

Figure 1-5. Cathepsin L regulation of 53BP1. (Left) A-type lamins prevent degradation of 53BP1 by stabilizing CTSL mRNA. Overexpression of CTSL promotes the transport of 53BP1 out of the nucleus and its degradation. (Right) Loss of A-type lamins leads to upregulation of CTSL and its accumulation in the nucleus, which leads to degradation of 53BP1 and its accumulation in the cytoplasm. Treatment with vitamin D inhibits CTSL activity, likely through upregulation of cystatins, and stabilizes 53BP1 levels.

Cathepsin L is a papain-like lysosomal cysteine protease, of which there are 11 currently known (Turk & Guncar, 2003). Cathepsin L is an endopeptidase that is produced as preprocathepsin L, transported to the endoplasmic reticulum and through the Golgi apparatus in secretory vesicles as procathepsin L and activated by autolysis at acidic pH in lysosomes, where it is stored (Lankelma et al., 2010). Cathepsin L knockout mice exhibit hair loss, thickening of

the skin, and abnormal spermatogenesis (Roth et al., 2000; Wright, Smith, Kerr, & Charron, 2003), and older mice develop dilated cardiomyopathy (Stypmann et al., 2002).

Cathepsin L has been shown to be upregulated in a wide variety of cancers, including colon, lung, gastric, breast, head and neck carcinomas, melanomas and gliomas (Jedeszko & Sloane, 2004; Kos et al., 1997). CTSL degrades components of the extracellular matrix such as fibronectin, laminin, and collagen types I and IV (Skrzydlewska, Sulkowska, Koda, & Sulkowski, 2005), which could help promote invasion and metastasis. In most studies, treatment with cathepsin inhibitors decreased invasion and metastasis of several types of cancer (Lankelma et al., 2010).

Cathepsin L has also been identified in the nucleus. A study showed that a truncated CTSL isoform is present in the nucleus where it proteolytically processes the CDP/Cux transcription factor to accelerate entry into S phase, indicating that CTSL could have a role in the cell cycle regulation and cell proliferation (Goulet et al., 2004). CTSL in the nucleus is also responsible for cleavage of the histone H3 N-terminal tail during mouse embryonic stem cell differentiation (Duncan et al., 2008). Studies in our laboratory have also revealed novel roles of CTSL in the nucleus. Loss of A-type lamins leads to upregulation of CTSL and accumulation of the active enzyme in the nucleus, which leads to the degradation of 53BP1 and its accumulation into the cytoplasm (Gonzalez-Suarez et al., 2011).

A study had previously shown that treatment of human colon cancer cells with the active metabolite of vitamin D (1α,25-dihydroxyvitamin D_3) induced vitamin D receptor (VDR) binding to the promoter of cystatin D, an endogenous inhibitor of CTSL, and led to increased levels of cystatin D mRNA and protein levels (Alvarez-Díaz et al., 2009). Interestingly, we

showed that inhibition of cathepsin L with vitamin D treatment in *LMNA* null cells stabilizes 53BP1 levels and rescues the defects in DNA repair kinetics and the processing of dysfunctional telomeres by NHEJ (**Figure 1-5)** (Gonzalez-Suarez et al., 2011). These studies provide an unprecedented method for regulating levels of 53BP1: inhibition of CTSL via treatment with vitamin D or cathepsin inhibitors.

1.9 Triple-negative breast cancer

Breast cancers have been divided into five main subtypes: two that are estrogen receptor positive (luminal A and luminal B) and three that have estrogen receptor negative tumors (normal-breast like, basal-like, and HER2 positive) (Constantinidou, Jones, & Reis-Filho, 2010; Sorlie et al., 2003; Sørlie et al., 2001). The luminal A and B subgroups have the best prognoses while the HER2 positive and basal-like tumors are more aggressive and have worse prognoses. The term basal-like refers to gene expression similarities between these types of tumors with normal basal epithelial cells of the breast and the increased expression of basal-like cytokeratins (Nanda, 2011). The triple-negative breast cancers (TNBC), which account for 15% to 20% of all breast cancers, are characterized by the absence of immunohistological staining of estrogen receptor, progesterone receptor, and HER2, and most TNBCs exhibit basal-like characteristics (Dent et al., 2007; Nanda, 2011). TNBCs are very aggressive and difficult to treat, as they cannot be treated with endocrine therapy or HER2 inhibitors due to the lack of hormone receptors and HER2 expression (Reis-Filho & Tutt, 2008). Additionally, up to 90% of tumors that have germline mutations in BRCA1 are triple-negative (Thompson & Easton, 2002). Triple-negative and BRCA1-mutated tumors tend to be more common in younger women and African American women, and have a higher risk of metastasis and recurrence than other breast cancers (Dent et

al., 2007; Nanda, 2011).

Although TNBCs are characterized by the lack of hormone receptors and HER2, and their tendency to be basal-like, there is clear histopathological evidence that there are many differences between individual TNBCs (Rakha et al., 2007; B Weigelt et al., 2008; Britta Weigelt, Baehner, & Reis-Filho, 2010; Britta Weigelt & Reis-Filho, 2009). While chemotherapy treatment has shown moderate success in treating TNBCs, the differential response of these tumors to chemotherapeutic drugs provides further evidence of the heterogeneity of this class of tumors (Constantinidou et al., 2010; Nanda, 2011). It is clear that identification of new diagnostic characteristics or markers of TNBCs or BRCA1-mutated cancers could serve to predict efficacy of different treatments based on individual tumor statuses.

One very promising treatment strategy for TNBCs and BRCA1-mutated cancers is the use of PARP inhibitors combined with chemotherapy or radiation to improve outcomes, given that these tumors commonly have defects in HR. However, many tumors become resistant to PARP inhibitor treatment. Recent evidence suggests that loss of 53BP1 is associated with TNBC and contributes to the resistance of these tumors to PARP inhibitors by partially rescuing the BRCA1-deficient phenotype (Bouwman et al., 2010; Bunting et al., 2010). Given that studies in our laboratory have identified a novel mechanism of regulation of 53BP1, that is, cathepsin L-mediated degradation, we investigated here whether activation of cathepsin L is one of the mechanisms responsible for lowering 53BP1 levels in TNBC and BRCA1-mutated tumor cells. Furthermore, we tested if upregulation of 53BP1 using cathepsin L as an effector leads to increased sensitivity to DNA damaging strategies, and as a consequence in tumor cell death. Lastly, we investigated whether cathepsin L can serve as a novel biomarker for TNBC and BRCA1 related tumors with potential predictive value for drug response.

1.10 References

Agrelo, R., Setien, F., Espada, J., Artiga, M. J., Rodriguez, M., Pérez-Rosado, A., Sanchez-Aguilera, A., et al. (2005). Inactivation of the lamin A/C gene by CpG island promoter hypermethylation in hematologic malignancies, and its association with poor survival in nodal diffuse large B-cell lymphoma. *Journal of clinical oncology : official journal of the American Society of Clinical Oncology*, 23(17), 3940–7. doi:10.1200/JCO.2005.11.650

Alvarez-Díaz, S., Valle, N., García, J. M., Peña, C., Freije, J. M. P., Quesada, V., Astudillo, A., et al. (2009). Cystatin D is a candidate tumor suppressor gene induced by vitamin D in human colon cancer cells. *The Journal of clinical investigation*, 119(8), 2343–58. Retrieved from http://www.pubmedcentral.nih.gov/articlerender.fcgi?artid=2719930&tool=pmcentrez&rendertype=abstract

Aly, A., & Ganesan, S. (2011). BRCA1, PARP, and 53BP1: conditional synthetic lethality and synthetic viability. *Journal of molecular cell biology*, 3(1), 66–74. doi:10.1093/jmcb/mjq055

Anderson, L., Henderson, C., & Adachi, Y. (2001). Phosphorylation and rapid relocalization of 53BP1 to nuclear foci upon DNA damage. *Molecular and cellular biology*, 21(5), 1719–29. doi:10.1128/MCB.21.5.1719-1729.2001

Ashworth, A. (2008). Drug resistance caused by reversion mutation. *Cancer research*, 68(24), 10021–3. doi:10.1158/0008-5472.CAN-08-2287

Bakkenist, C. J., & Kastan, M. B. (2003). DNA damage activates ATM through intermolecular autophosphorylation and dimer dissociation. *Nature*, 421(6922), 499–506. doi:10.1038/nature01368

Bennardo, N., Cheng, A., Huang, N., & Stark, J. M. (2008). Alternative-NHEJ is a mechanistically distinct pathway of mammalian chromosome break repair. *PLoS genetics*, 4(6), e1000110. doi:10.1371/journal.pgen.1000110

Bothmer, A., Robbiani, D. F., Di Virgilio, M., Bunting, S. F., Klein, I. A., Feldhahn, N., Barlow, J., et al. (2011). Regulation of DNA end joining, resection, and immunoglobulin class switch recombination by 53BP1. *Molecular cell*, 42(3), 319–29. doi:10.1016/j.molcel.2011.03.019

Botuyan, M. V., Lee, J., Ward, I. M., Kim, J.-E., Thompson, J. R., Chen, J., & Mer, G. (2006). Structural basis for the methylation state-specific recognition of histone H4-K20 by 53BP1 and Crb2 in DNA repair. *Cell*, 127(7), 1361–73. doi:10.1016/j.cell.2006.10.043

Boulton, S. J., & Jackson, S. P. (1998). Components of the Ku-dependent non-homologous end-joining pathway are involved in telomeric length maintenance and telomeric silencing. *The EMBO journal*, 17(6), 1819–28. doi:10.1093/emboj/17.6.1819

Bouwman, P., Aly, A., Escandell, J. M., Pieterse, M., Bartkova, J., van der Gulden, H., Hiddingh, S., et al. (2010). 53BP1 loss rescues BRCA1 deficiency and is associated with triple-negative and BRCA-mutated breast cancers. *Nature structural & molecular biology*, 17(6), 688–95. doi:10.1038/nsmb.1831

Broers, J. L., Raymond, Y., Rot, M. K., Kuijpers, H., Wagenaar, S. S., & Ramaekers, F. C. (1993). Nuclear A-type lamins are differentially expressed in human lung cancer subtypes. *The American journal of pathology*, 143(1), 211–20. Retrieved from http://www.pubmedcentral.nih.gov/articlerender.fcgi?artid=1886958&tool=pmcentrez&rendertype=abstract

Bryant, H. E., Schultz, N., Thomas, H. D., Parker, K. M., Flower, D., Lopez, E., Kyle, S., et al. (2005). Specific killing of BRCA2-deficient tumours with inhibitors of poly(ADP-ribose) polymerase. *Nature*, 434(7035), 913–7. doi:10.1038/nature03443

Bunting, S. F., Callén, E., Wong, N., Chen, H.-T., Polato, F., Gunn, A., Bothmer, A., et al. (2010). 53BP1 inhibits homologous recombination in Brca1-deficient cells by blocking resection of DNA breaks. *Cell*, 141(2), 243–54. doi:10.1016/j.cell.2010.03.012

Burma, S., Chen, B. P., Murphy, M., Kurimasa, A., & Chen, D. J. (2001). ATM phosphorylates histone H2AX in response to DNA double-strand breaks. *The Journal of biological chemistry*, 276(45), 42462–7. doi:10.1074/jbc.C100466200

Cao, L., Kim, S., Xiao, C., Wang, R.-H., Coumoul, X., Wang, X., Li, W. M., et al. (2006). ATM-Chk2-p53 activation prevents tumorigenesis at an expense of organ homeostasis upon Brca1 deficiency. *The EMBO journal*, 25(10), 2167–77. doi:10.1038/sj.emboj.7601115

Cao, L., Xu, X., Bunting, S. F., Liu, J., Wang, R.-H., Cao, L. L., Wu, J. J., et al. (2009). A selective requirement for 53BP1 in the biological response to genomic instability induced by Brca1 deficiency. *Molecular cell*, 35(4), 534–41. doi:10.1016/j.molcel.2009.06.037

Chen, L., Nievera, C. J., Lee, A. Y.-L., & Wu, X. (2008). Cell cycle-dependent complex formation of BRCA1.CtIP.MRN is important for DNA double-strand break repair. *The Journal of biological chemistry*, 283(12), 7713–20. doi:10.1074/jbc.M710245200

Constantinescu, D., Gray, H. L., Sammak, P. J., Schatten, G. P., & Csoka, A. B. (2006). Lamin A/C expression is a marker of mouse and human embryonic stem cell differentiation. *Stem cells (Dayton, Ohio)*, 24(1), 177–85. doi:10.1634/stemcells.2004-0159

Constantinidou, A., Jones, R. L., & Reis-Filho, J. S. (2010). Beyond triple-negative breast cancer: the need to define new subtypes. *Expert review of anticancer therapy*, 10(8), 1197–213. doi:10.1586/era.10.50

De Sandre-Giovannoli, A., Bernard, R., Cau, P., Navarro, C., Amiel, J., Boccaccio, I., Lyonnet, S., et al. (2003). Lamin a truncation in Hutchinson-Gilford progeria. *Science (New York, N.Y.)*, 300(5628), 2055. doi:10.1126/science.1084125

Dechat, T., Gesson, K., & Foisner, R. (2010). Lamina-independent lamins in the nuclear interior serve important functions. *Cold Spring Harbor symposia on quantitative biology*, 75, 533–43. doi:10.1101/sqb.2010.75.018

Decker, M. L., Chavez, E., Vulto, I., & Lansdorp, P. M. (2009). Telomere length in Hutchinson-Gilford progeria syndrome. *Mechanisms of ageing and development*, 130(6), 377–83. doi:10.1016/j.mad.2009.03.001

DeFazio, L. G., Stansel, R. M., Griffith, J. D., & Chu, G. (2002). Synapsis of DNA ends by DNA-dependent protein kinase. *The EMBO journal*, 21(12), 3192–200. doi:10.1093/emboj/cdf299

Dent, R., Trudeau, M., Pritchard, K. I., Hanna, W. M., Kahn, H. K., Sawka, C. A., Lickley, L. A., et al. (2007). Triple-negative breast cancer: clinical features and patterns of recurrence. *Clinical cancer research : an official journal of the American Association for Cancer Research*, 13(15 Pt 1), 4429–34. doi:10.1158/1078-0432.CCR-06-3045

Difilippantonio, S., Gapud, E., Wong, N., Huang, C.-Y., Mahowald, G., Chen, H. T., Kruhlak, M. J., et al. (2008). 53BP1 facilitates long-range DNA end-joining during V(D)J recombination. *Nature*, 456(7221), 529–33. doi:10.1038/nature07476

Dimitrova, N., Chen, Y.-C. M., Spector, D. L., & de Lange, T. (2008). 53BP1 promotes non-homologous end joining of telomeres by increasing chromatin mobility. *Nature*, 456(7221), 524–8. doi:10.1038/nature07433

Doil, C., Mailand, N., Bekker-Jensen, S., Menard, P., Larsen, D. H., Pepperkok, R., Ellenberg, J., et al. (2009). RNF168 binds and amplifies ubiquitin conjugates on damaged chromosomes to allow accumulation of repair proteins. *Cell*, 136(3), 435–46. doi:10.1016/j.cell.2008.12.041

Dudley, D. D., Chaudhuri, J., Bassing, C. H., & Alt, F. W. (2005). Mechanism and control of V(D)J recombination versus class switch recombination: similarities and differences. *Advances in immunology*, 86, 43–112. doi:10.1016/S0065-2776(04)86002-4

Duncan, E. M., Muratore-Schroeder, T. L., Cook, R. G., Garcia, B. a, Shabanowitz, J., Hunt, D. F., & Allis, C. D. (2008). Cathepsin L proteolytically processes histone H3 during mouse embryonic stem cell differentiation. *Cell*, 135(2), 284–94. doi:10.1016/j.cell.2008.09.055

Eriksson, M., Brown, W. T., Gordon, L. B., Glynn, M. W., Singer, J., Scott, L., Erdos, M. R., et al. (2003). Recurrent de novo point mutations in lamin A cause Hutchinson-Gilford progeria syndrome. *Nature*, 423(6937), 293–8. doi:10.1038/nature01629

Espejel, S., Martín, M., Klatt, P., Martín-Caballero, J., Flores, J. M., & Blasco, M. A. (2004). Shorter telomeres, accelerated ageing and increased lymphoma in DNA-PKcs-deficient mice. *EMBO reports*, 5(5), 503–9. doi:10.1038/sj.embor.7400127

Evers, B., & Jonkers, J. (2006). Mouse models of BRCA1 and BRCA2 deficiency: past lessons, current understanding and future prospects. *Oncogene*, 25(43), 5885–97. doi:10.1038/sj.onc.1209871

Fabbro, M., Savage, K., Hobson, K., Deans, A. J., Powell, S. N., McArthur, G. A., & Khanna, K. K. (2004). BRCA1-BARD1 complexes are required for p53Ser-15 phosphorylation and a G1/S arrest following ionizing radiation-induced DNA damage. *The Journal of biological chemistry*, 279(30), 31251–8. doi:10.1074/jbc.M405372200

Fanning, E., Klimovich, V., & Nager, A. R. (2006). A dynamic model for replication protein A (RPA) function in DNA processing pathways. *Nucleic acids research*, 34(15), 4126–37. doi:10.1093/nar/gkl550

Farmer, H., McCabe, N., Lord, C. J., Tutt, A. N. J., Johnson, D. a, Richardson, T. B., Santarosa, M., et al. (2005). Targeting the DNA repair defect in BRCA mutant cells as a therapeutic strategy. *Nature*, 434(7035), 917–21. doi:10.1038/nature03445

Fernandez-Capetillo, O., Chen, H.-T., Celeste, A., Ward, I., Romanienko, P. J., Morales, J. C., Naka, K., et al. (2002). DNA damage-induced G2-M checkpoint activation by histone H2AX and 53BP1. *Nature cell biology*, 4(12), 993–7. doi:10.1038/ncb884

Fernandez-Capetillo, O., Lee, A., Nussenzweig, M., & Nussenzweig, A. (n.d.). H2AX: the histone guardian of the genome. *DNA repair*, 3(8-9), 959–67. doi:10.1016/j.dnarep.2004.03.024

FitzGerald, J. E., Grenon, M., & Lowndes, N. F. (2009). 53BP1: function and mechanisms of focal recruitment. *Biochemical Society transactions*, 37(Pt 4), 897–904. doi:10.1042/BST0370897

Fong, P. C., Boss, D. S., Yap, T. A., Tutt, A., Wu, P., Mergui-Roelvink, M., Mortimer, P., et al. (2009). Inhibition of poly(ADP-ribose) polymerase in tumors from BRCA mutation carriers. *The New England journal of medicine*, 361(2), 123–34. doi:10.1056/NEJMoa0900212

Furukawa, K., Inagaki, H., & Hotta, Y. (1994). Identification and cloning of an mRNA coding for a germ cell-specific A-type lamin in mice. *Experimental cell research*, 212(2), 426–30. doi:10.1006/excr.1994.1164

Galanty, Y., Belotserkovskaya, R., Coates, J., Polo, S., Miller, K. M., & Jackson, S. P. (2009). Mammalian SUMO E3-ligases PIAS1 and PIAS4 promote responses to DNA double-strand breaks. *Nature*, 462(7275), 935–9. doi:10.1038/nature08657

Goldman, R. D., Gruenbaum, Y., Moir, R. D., Shumaker, D. K., & Spann, T. P. (2002). Nuclear lamins: building blocks of nuclear architecture. *Genes & development*, 16(5), 533–47. doi:10.1101/gad.960502

Golub, E. I., Gupta, R. C., Haaf, T., Wold, M. S., & Radding, C. M. (1998). Interaction of human rad51 recombination protein with single-stranded DNA binding protein, RPA. *Nucleic acids research*, 26(23), 5388–93. Retrieved from http://www.pubmedcentral.nih.gov/articlerender.fcgi?artid=148005&tool=pmcentrez&rendertype=abstract

Gonzalez, J. M., Pla, D., Perez-Sala, D., & Andres, V. (2011). A-type lamins and Hutchinson-Gilford progeria syndrome: pathogenesis and therapy. *Frontiers in bioscience (Scholar edition)*, 3, 1133–46. Retrieved from http://www.ncbi.nlm.nih.gov/pubmed/21622261

Gonzalez-Suarez, I., Redwood, A. B., Grotsky, D. a, Neumann, M. a, Cheng, E. H.-Y., Stewart, C. L., Dusso, A., et al. (2011). A new pathway that regulates 53BP1 stability implicates cathepsin L and vitamin D in DNA repair. *The EMBO journal*, 30(16), 3383–96. doi:10.1038/emboj.2011.225

Gonzalez-Suarez, I., Redwood, A. B., Perkins, S. M., Vermolen, B., Lichtensztejin, D., Grotsky, D. a, Morgado-Palacin, L., et al. (2009). Novel roles for A-type lamins in telomere biology and the DNA damage response pathway. *The EMBO journal*, 28(16), 2414–27. doi:10.1038/emboj.2009.196

Goodarzi, A. A., Noon, A. T., Deckbar, D., Ziv, Y., Shiloh, Y., Löbrich, M., & Jeggo, P. A. (2008). ATM signaling facilitates repair of DNA double-strand breaks associated with heterochromatin. *Molecular cell*, 31(2), 167–77. doi:10.1016/j.molcel.2008.05.017

Gordon, L. B., Kleinman, M. E., Miller, D. T., Neuberg, D. S., Giobbie-Hurder, A., Gerhard-Herman, M., Smoot, L. B., et al. (2012). Clinical trial of a farnesyltransferase inhibitor in children with Hutchinson-Gilford progeria syndrome. *Proceedings of the National Academy of Sciences of the United States of America*, 109(41), 16666–71. doi:10.1073/pnas.1202529109

Gottlieb, T. M., & Jackson, S. P. (1993). The DNA-dependent protein kinase: requirement for DNA ends and association with Ku antigen. *Cell*, 72(1), 131–42. Retrieved from http://www.ncbi.nlm.nih.gov/pubmed/8422676

Goulet, B., Baruch, A., Moon, N.-S., Poirier, M., Sansregret, L. L., Erickson, A., Bogyo, M., et al. (2004). A cathepsin L isoform that is devoid of a signal peptide localizes to the nucleus in S phase and processes the CDP/Cux transcription factor. *Molecular cell*, 14(2), 207–19. Retrieved from http://www.ncbi.nlm.nih.gov/pubmed/15099520

Grawunder, U., Wilm, M., Wu, X., Kulesza, P., Wilson, T. E., Mann, M., & Lieber, M. R. (1997). Activity of DNA ligase IV stimulated by complex formation with XRCC4 protein in mammalian cells. *Nature*, 388(6641), 492–5. doi:10.1038/41358

Grawunder, U., Zimmer, D., & Leiber, M. R. (1998). DNA ligase IV binds to XRCC4 via a motif located between rather than within its BRCT domains. *Current biology : CB*, 8(15), 873–6. Retrieved from http://www.ncbi.nlm.nih.gov/pubmed/9705934

Gruenbaum, Y., Margalit, A., Goldman, R. D., Shumaker, D. K., & Wilson, K. L. (2005). The nuclear lamina comes of age. *Nature reviews. Molecular cell biology*, 6(1), 21–31. doi:10.1038/nrm1550

Gu, J., Lu, H., Tsai, A. G., Schwarz, K., & Lieber, M. R. (2007). Single-stranded DNA ligation and XLF-stimulated incompatible DNA end ligation by the XRCC4-DNA ligase IV complex: influence of terminal DNA sequence. *Nucleic acids research*, 35(17), 5755–62. doi:10.1093/nar/gkm579

Hartlerode, A. J., & Scully, R. (2009). Mechanisms of double-strand break repair in somatic mammalian cells. *The Biochemical journal*, 423(2), 157–68. doi:10.1042/BJ20090942

Hennekes, H., & Nigg, E. A. (1994). The role of isoprenylation in membrane attachment of nuclear lamins. A single point mutation prevents proteolytic cleavage of the lamin A precursor and confers membrane binding properties. *Journal of cell science*, *107 (Pt 4*, 1019–29. Retrieved from http://www.ncbi.nlm.nih.gov/pubmed/8056827

Heyer, W.-D., Ehmsen, K. T., & Liu, J. (2010). Regulation of homologous recombination in eukaryotes. *Annual review of genetics*, 44, 113–39. doi:10.1146/annurev-genet-051710-150955

Huang, S., Risques, R. A., Martin, G. M., Rabinovitch, P. S., & Oshima, J. (2008). Accelerated telomere shortening and replicative senescence in human fibroblasts overexpressing mutant and wild-type lamin A. *Experimental cell research*, 314(1), 82–91. doi:10.1016/j.yexcr.2007.08.004

Huertas, P., Cortés-Ledesma, F., Sartori, A. A., Aguilera, A., & Jackson, S. P. (2008). CDK targets Sae2 to control DNA-end resection and homologous recombination. *Nature*, 455(7213), 689–92. doi:10.1038/nature07215

Iwabuchi, K., Bartel, P. L., Li, B., Marraccino, R., & Fields, S. (1994). Two cellular proteins that bind to wild-type but not mutant p53. *Proceedings of the National Academy of Sciences of the United States of America*, 91(13), 6098–102. Retrieved from http://www.pubmedcentral.nih.gov/articlerender.fcgi?artid=44145&tool=pmcentrez&rendertype=abstract

Jackson, S. P., & Bartek, J. (2009). The DNA-damage response in human biology and disease. *Nature*, 461(7267), 1071–8. doi:10.1038/nature08467

Jedeszko, C., & Sloane, B. F. (2004). Cysteine cathepsins in human cancer. *Biological chemistry*, 385(11), 1017–27. doi:10.1515/BC.2004.132

Johnson, B. R., Nitta, R. T., Frock, R. L., Mounkes, L., Barbie, D. A., Stewart, C. L., Harlow, E., et al. (2004). A-type lamins regulate retinoblastoma protein function by promoting subnuclear localization and preventing proteasomal degradation. *Proceedings of the*

National Academy of Sciences of the United States of America, 101(26), 9677–82. doi:10.1073/pnas.0403250101

Joukov, V., Chen, J., Fox, E. A., Green, J. B., & Livingston, D. M. (2001). Functional communication between endogenous BRCA1 and its partner, BARD1, during Xenopus laevis development. *Proceedings of the National Academy of Sciences of the United States of America*, 98(21), 12078–83. doi:10.1073/pnas.211427098

Kawai, S., & Amano, A. (2012). BRCA1 regulates microRNA biogenesis via the DROSHA microprocessor complex. *The Journal of cell biology*, 197(2), 201–8. doi:10.1083/jcb.201110008

Kim, H., Chen, J., & Yu, X. (2007). Ubiquitin-binding protein RAP80 mediates BRCA1-dependent DNA damage response. *Science (New York, N.Y.)*, 316(5828), 1202–5. doi:10.1126/science.1139621

Kolas, N. K., Chapman, J. R., Nakada, S., Ylanko, J., Chahwan, R., Sweeney, F. D., Panier, S., et al. (2007). Orchestration of the DNA-damage response by the RNF8 ubiquitin ligase. *Science (New York, N.Y.)*, 318(5856), 1637–40. doi:10.1126/science.1150034

Kos, J., Stabuc, B., Schweiger, A., Krasovec, M., Cimerman, N., Kopitar-Jerala, N., & Vrhovec, I. (1997). Cathepsins B, H, and L and their inhibitors stefin A and cystatin C in sera of melanoma patients. *Clinical cancer research : an official journal of the American Association for Cancer Research*, 3(10), 1815–22. Retrieved from http://www.ncbi.nlm.nih.gov/pubmed/9815568

Lankelma, J. M., Voorend, D. M., Barwari, T., Koetsveld, J., Van der Spek, A. H., De Porto, A. P. N. a, Van Rooijen, G., et al. (2010). Cathepsin L, target in cancer treatment? *Life sciences*, 86(7-8), 225–33. doi:10.1016/j.lfs.2009.11.016

Lee, J.-H., & Paull, T. T. (2004). Direct activation of the ATM protein kinase by the Mre11/Rad50/Nbs1 complex. *Science (New York, N.Y.)*, 304(5667), 93–6. doi:10.1126/science.1091496

Lee, J.-H., & Paull, T. T. (2005). ATM activation by DNA double-strand breaks through the Mre11-Rad50-Nbs1 complex. *Science (New York, N.Y.)*, 308(5721), 551–4. doi:10.1126/science.1108297

Li, L., & Zou, L. (2005). Sensing, signaling, and responding to DNA damage: organization of the checkpoint pathways in mammalian cells. *Journal of cellular biochemistry*, 94(2), 298–306. doi:10.1002/jcb.20355

Lieber, M. R., Ma, Y., Pannicke, U., & Schwarz, K. (2003). Mechanism and regulation of human non-homologous DNA end-joining. *Nature reviews. Molecular cell biology*, 4(9), 712–20. doi:10.1038/nrm1202

Lin, F., & Worman, H. J. (1993). Structural organization of the human gene encoding nuclear lamin A and nuclear lamin C. *The Journal of biological chemistry*, 268(22), 16321–6. Retrieved from http://www.ncbi.nlm.nih.gov/pubmed/8344919

Lukas, C., Melander, F., Stucki, M., Falck, J., Bekker-Jensen, S., Goldberg, M., Lerenthal, Y., et al. (2004). Mdc1 couples DNA double-strand break recognition by Nbs1 with its H2AX-dependent chromatin retention. *The EMBO journal*, 23(13), 2674–83. doi:10.1038/sj.emboj.7600269

Ma, Y., Pannicke, U., Schwarz, K., & Lieber, M. R. (2002). Hairpin opening and overhang processing by an Artemis/DNA-dependent protein kinase complex in nonhomologous end joining and V(D)J recombination. *Cell*, 108(6), 781–94. Retrieved from http://www.ncbi.nlm.nih.gov/pubmed/11955432

Ma, Y., Schwarz, K., & Lieber, M. R. (2005). The Artemis:DNA-PKcs endonuclease cleaves DNA loops, flaps, and gaps. *DNA repair*, 4(7), 845–51. doi:10.1016/j.dnarep.2005.04.013

Machiels, B. M., Zorenc, A. H., Endert, J. M., Kuijpers, H. J., van Eys, G. J., Ramaekers, F. C., & Broers, J. L. (1996). An alternative splicing product of the lamin A/C gene lacks exon 10. *The Journal of biological chemistry*, 271(16), 9249–53. Retrieved from http://www.ncbi.nlm.nih.gov/pubmed/8621584

Mailand, N., Bekker-Jensen, S., Faustrup, H., Melander, F., Bartek, J., Lukas, C., & Lukas, J. (2007). RNF8 ubiquitylates histones at DNA double-strand breaks and promotes assembly of repair proteins. *Cell*, 131(5), 887–900. doi:10.1016/j.cell.2007.09.040

Mattout, A., Dechat, T., Adam, S. A., Goldman, R. D., & Gruenbaum, Y. (2006). Nuclear lamins, diseases and aging. *Current opinion in cell biology*, 18(3), 335–41. doi:10.1016/j.ceb.2006.03.007

McCabe, N., Turner, N. C., Lord, C. J., Kluzek, K., Bialkowska, A., Swift, S., Giavara, S., et al. (2006). Deficiency in the repair of DNA damage by homologous recombination and sensitivity to poly(ADP-ribose) polymerase inhibition. *Cancer research*, 66(16), 8109–15. doi:10.1158/0008-5472.CAN-06-0140

Miki, Y., Swensen, J., Shattuck-Eidens, D., Futreal, P. A., Harshman, K., Tavtigian, S., Liu, Q., et al. (1994). A strong candidate for the breast and ovarian cancer susceptibility gene BRCA1. *Science (New York, N.Y.)*, 266(5182), 66–71. Retrieved from http://www.ncbi.nlm.nih.gov/pubmed/7545954

Mimitou, E. P., & Symington, L. S. (2009). Nucleases and helicases take center stage in homologous recombination. *Trends in biochemical sciences*, 34(5), 264–72. doi:10.1016/j.tibs.2009.01.010

Morales, J. C., Xia, Z., Lu, T., Aldrich, M. B., Wang, B., Rosales, C., Kellems, R. E., et al. (2003). Role for the BRCA1 C-terminal repeats (BRCT) protein 53BP1 in maintaining

genomic stability. *The Journal of biological chemistry*, 278(17), 14971–7. doi:10.1074/jbc.M212484200

Morris, J. R., Boutell, C., Keppler, M., Densham, R., Weekes, D., Alamshah, A., Butler, L., et al. (2009). The SUMO modification pathway is involved in the BRCA1 response to genotoxic stress. *Nature*, 462(7275), 886–90. doi:10.1038/nature08593

Moshous, D., Callebaut, I., de Chasseval, R., Corneo, B., Cavazzana-Calvo, M., Le Deist, F., Tezcan, I., et al. (2001). Artemis, a novel DNA double-strand break repair/V(D)J recombination protein, is mutated in human severe combined immune deficiency. *Cell*, 105(2), 177–86. Retrieved from http://www.ncbi.nlm.nih.gov/pubmed/11336668

Mounkes, L. C., Kozlov, S., Hernandez, L., Sullivan, T., & Stewart, C. L. (2003). A progeroid syndrome in mice is caused by defects in A-type lamins. *Nature*, 423(6937), 298–301. doi:10.1038/nature01631

Mullan, P. B., Quinn, J. E., & Harkin, D. P. (2006). The role of BRCA1 in transcriptional regulation and cell cycle control. *Oncogene*, 25(43), 5854–63. doi:10.1038/sj.onc.1209872

Nakamura, K., Sakai, W., Kawamoto, T., Bree, R. T., Lowndes, N. F., Takeda, S., & Taniguchi, Y. (2006). Genetic dissection of vertebrate 53BP1: a major role in non-homologous end joining of DNA double strand breaks. *DNA repair*, 5(6), 741–9. doi:10.1016/j.dnarep.2006.03.008

Nanda, R. (2011). "Targeting" triple-negative breast cancer: the lessons learned from BRCA1-associated breast cancers. *Seminars in oncology*, 38(2), 254–62. doi:10.1053/j.seminoncol.2011.01.007

Nick McElhinny, S A, Snowden, C. M., McCarville, J., & Ramsden, D. A. (2000). Ku recruits the XRCC4-ligase IV complex to DNA ends. *Molecular and cellular biology*, 20(9), 2996–3003. Retrieved from http://www.pubmedcentral.nih.gov/articlerender.fcgi?artid=85565&tool=pmcentrez&rendertype=abstract

Nick McElhinny, Stephanie A, & Ramsden, D. A. (2004). Sibling rivalry: competition between Pol X family members in V(D)J recombination and general double strand break repair. *Immunological reviews*, 200, 156–64. doi:10.1111/j.0105-2896.2004.00160.x

Noon, A. T., & Goodarzi, A. A. (2011). 53BP1-mediated DNA double strand break repair: insert bad pun here. *DNA repair*, 10(10), 1071–6. doi:10.1016/j.dnarep.2011.07.012

Panier, S., & Durocher, D. (2009). Regulatory ubiquitylation in response to DNA double-strand breaks. *DNA repair*, 8(4), 436–43. doi:10.1016/j.dnarep.2009.01.013

Paull, T. T., Rogakou, E. P., Yamazaki, V., Kirchgessner, C. U., Gellert, M., & Bonner, W. M. (n.d.). A critical role for histone H2AX in recruitment of repair factors to nuclear foci after

DNA damage. *Current biology : CB*, 10(15), 886–95. Retrieved from http://www.ncbi.nlm.nih.gov/pubmed/10959836

Pendás, A. M., Zhou, Z., Cadiñanos, J., Freije, J. M. P., Wang, J., Hultenby, K., Astudillo, A., et al. (2002). Defective prelamin A processing and muscular and adipocyte alterations in Zmpste24 metalloproteinase-deficient mice. *Nature genetics*, 31(1), 94–9. doi:10.1038/ng871

Prokocimer, M., Davidovich, M., Nissim-Rafinia, M., Wiesel-Motiuk, N., Bar, D. Z., Barkan, R., Meshorer, E., et al. (2009). Nuclear lamins: key regulators of nuclear structure and activities. *Journal of cellular and molecular medicine*, 13(6), 1059–85. doi:10.1111/j.1582-4934.2008.00676.x

Prokocimer, M., Margalit, A., & Gruenbaum, Y. (2006). The nuclear lamina and its proposed roles in tumorigenesis: projection on the hematologic malignancies and future targeted therapy. *Journal of structural biology*, 155(2), 351–60. doi:10.1016/j.jsb.2006.02.016

Rakha, E. A., El-Sayed, M. E., Green, A. R., Lee, A. H. S., Robertson, J. F., & Ellis, I. O. (2007). Prognostic markers in triple-negative breast cancer. *Cancer*, 109(1), 25–32. doi:10.1002/cncr.22381

Rappold, I., Iwabuchi, K., Date, T., & Chen, J. (2001). Tumor suppressor p53 binding protein 1 (53BP1) is involved in DNA damage-signaling pathways. *The Journal of cell biology*, 153(3), 613–20. Retrieved from http://www.pubmedcentral.nih.gov/articlerender.fcgi?artid=2190566&tool=pmcentrez&rendertype=abstract

Redwood, A. B., Perkins, S. M., Vanderwaal, R. P., Feng, Z., Biehl, K. J., Gonzalez-Suarez, I., Morgado-Palacin, L., et al. (2011). A dual role for A-type lamins in DNA double-strand break repair. *Cell cycle (Georgetown, Tex.)*, 10(15), 2549–60. Retrieved from http://www.pubmedcentral.nih.gov/articlerender.fcgi?artid=3180193&tool=pmcentrez&rendertype=abstract

Reis-Filho, J. S., & Tutt, A. N. J. (2008). Triple negative tumours: a critical review. *Histopathology*, 52(1), 108–18. doi:10.1111/j.1365-2559.2007.02889.x

Riballo, E., Kühne, M., Rief, N., Doherty, A., Smith, G. C. M., Recio, M.-J., Reis, C., et al. (2004). A pathway of double-strand break rejoining dependent upon ATM, Artemis, and proteins locating to gamma-H2AX foci. *Molecular cell*, 16(5), 715–24. doi:10.1016/j.molcel.2004.10.029

Riha, K., Heacock, M. L., & Shippen, D. E. (2006). The role of the nonhomologous end-joining DNA double-strand break repair pathway in telomere biology. *Annual review of genetics*, 40, 237–77. doi:10.1146/annurev.genet.39.110304.095755

Rooney, S., Sekiguchi, J., Zhu, C., Cheng, H. L., Manis, J., Whitlow, S., DeVido, J., et al. (2002). Leaky Scid phenotype associated with defective V(D)J coding end processing in Artemis-deficient mice. *Molecular cell*, 10(6), 1379–90. Retrieved from http://www.ncbi.nlm.nih.gov/pubmed/12504013

Roth, W., Deussing, J., Botchkarev, V. A., Pauly-Evers, M., Saftig, P., Hafner, A., Schmidt, P., et al. (2000). Cathepsin L deficiency as molecular defect of furless: hyperproliferation of keratinocytes and pertubation of hair follicle cycling. *FASEB journal : official publication of the Federation of American Societies for Experimental Biology*, 14(13), 2075–86. doi:10.1096/fj.99-0970com

Roy, R., Chun, J., & Powell, S. N. (2012). BRCA1 and BRCA2: different roles in a common pathway of genome protection. *Nature reviews. Cancer*, 12(1), 68–78. doi:10.1038/nrc3181

Röber, R. A., Sauter, H., Weber, K., & Osborn, M. (1990). Cells of the cellular immune and hemopoietic system of the mouse lack lamins A/C: distinction versus other somatic cells. *Journal of cell science*, *95 (Pt 4)*, 587–98. Retrieved from http://www.ncbi.nlm.nih.gov/pubmed/2200797

San Filippo, J., Sung, P., & Klein, H. (2008). Mechanism of eukaryotic homologous recombination. *Annual review of biochemistry*, 77, 229–57. doi:10.1146/annurev.biochem.77.061306.125255

Sartori, A. A., Lukas, C., Coates, J., Mistrik, M., Fu, S., Bartek, J., Baer, R., et al. (2007). Human CtIP promotes DNA end resection. *Nature*, 450(7169), 509–14. doi:10.1038/nature06337

Schultz, L. B., Chehab, N. H., Malikzay, a, & Halazonetis, T. D. (2000). p53 binding protein 1 (53BP1) is an early participant in the cellular response to DNA double-strand breaks. *The Journal of cell biology*, 151(7), 1381–90. Retrieved from http://www.pubmedcentral.nih.gov/articlerender.fcgi?artid=2150674&tool=pmcentrez&rendertype=abstract

Scully, R., Chen, J., Ochs, R. L., Keegan, K., Hoekstra, M., Feunteun, J., & Livingston, D. M. (1997). Dynamic changes of BRCA1 subnuclear location and phosphorylation state are initiated by DNA damage. *Cell*, 90(3), 425–35. Retrieved from http://www.ncbi.nlm.nih.gov/pubmed/9267023

Shukla, V., Coumoul, X., Lahusen, T., Wang, R.-H., Xu, X., Vassilopoulos, A., Xiao, C., et al. (2010). BRCA1 affects global DNA methylation through regulation of DNMT1. *Cell research*, 20(11), 1201–15. doi:10.1038/cr.2010.128

Simsek, D., Brunet, E., Wong, S. Y.-W., Katyal, S., Gao, Y., McKinnon, P. J., Lou, J., et al. (2011). DNA ligase III promotes alternative nonhomologous end-joining during chromosomal translocation formation. *PLoS genetics*, 7(6), e1002080. doi:10.1371/journal.pgen.1002080

Skrzydlewska, E., Sulkowska, M., Koda, M., & Sulkowski, S. (2005). Proteolytic-antiproteolytic balance and its regulation in carcinogenesis. *World journal of gastroenterology : WJG*, 11(9), 1251–66. Retrieved from http://www.ncbi.nlm.nih.gov/pubmed/15761961

So, S., Davis, A. J., & Chen, D. J. (2009). Autophosphorylation at serine 1981 stabilizes ATM at DNA damage sites. *The Journal of cell biology*, 187(7), 977–90. doi:10.1083/jcb.200906064

Sobhian, B., Shao, G., Lilli, D. R., Culhane, A. C., Moreau, L. A., Xia, B., Livingston, D. M., et al. (2007). RAP80 targets BRCA1 to specific ubiquitin structures at DNA damage sites. *Science (New York, N.Y.)*, 316(5828), 1198–202. doi:10.1126/science.1139516

Song, B., & Sung, P. (2000). Functional interactions among yeast Rad51 recombinase, Rad52 mediator, and replication protein A in DNA strand exchange. *The Journal of biological chemistry*, 275(21), 15895–904. doi:10.1074/jbc.M910244199

Sorlie, T., Tibshirani, R., Parker, J., Hastie, T., Marron, J. S., Nobel, A., Deng, S., et al. (2003). Repeated observation of breast tumor subtypes in independent gene expression data sets. *Proceedings of the National Academy of Sciences of the United States of America*, 100(14), 8418–23. doi:10.1073/pnas.0932692100

Stewart, G. S., Panier, S., Townsend, K., Al-Hakim, A. K., Kolas, N. K., Miller, E. S., Nakada, S., et al. (2009). The RIDDLE syndrome protein mediates a ubiquitin-dependent signaling cascade at sites of DNA damage. *Cell*, 136(3), 420–34. doi:10.1016/j.cell.2008.12.042

Stewart, G. S., Wang, B., Bignell, C. R., Taylor, A. M. R., & Elledge, S. J. (2003). MDC1 is a mediator of the mammalian DNA damage checkpoint. *Nature*, 421(6926), 961–6. doi:10.1038/nature01446

Stucki, M., Clapperton, J. A., Mohammad, D., Yaffe, M. B., Smerdon, S. J., & Jackson, S. P. (2005). MDC1 directly binds phosphorylated histone H2AX to regulate cellular responses to DNA double-strand breaks. *Cell*, 123(7), 1213–26. doi:10.1016/j.cell.2005.09.038

Stuurman, N., Heins, S., & Aebi, U. (1998). Nuclear lamins: their structure, assembly, and interactions. *Journal of structural biology*, 122(1-2), 42–66. doi:10.1006/jsbi.1998.3987

Stypmann, J., Gläser, K., Roth, W., Tobin, D. J., Petermann, I., Matthias, R., Mönnig, G., et al. (2002). Dilated cardiomyopathy in mice deficient for the lysosomal cysteine peptidase cathepsin L. *Proceedings of the National Academy of Sciences of the United States of America*, 99(9), 6234–9. doi:10.1073/pnas.092637699

Sullivan, T., Escalante-Alcalde, D., Bhatt, H., Anver, M., Bhat, N., Nagashima, K., Stewart, C. L., et al. (1999). Loss of A-type lamin expression compromises nuclear envelope integrity leading to muscular dystrophy. *The Journal of cell biology*, 147(5), 913–20. Retrieved from http://www.pubmedcentral.nih.gov/articlerender.fcgi?artid=2169344&tool=pmcentrez&rendertype=abstract

Swisher, E. M., Sakai, W., Karlan, B. Y., Wurz, K., Urban, N., & Taniguchi, T. (2008). Secondary BRCA1 mutations in BRCA1-mutated ovarian carcinomas with platinum resistance. *Cancer research*, 68(8), 2581–6. doi:10.1158/0008-5472.CAN-08-0088

Sørlie, T., Perou, C. M., Tibshirani, R., Aas, T., Geisler, S., Johnsen, H., Hastie, T., et al. (2001). Gene expression patterns of breast carcinomas distinguish tumor subclasses with clinical implications. *Proceedings of the National Academy of Sciences of the United States of America*, 98(19), 10869–74. doi:10.1073/pnas.191367098

Thompson, D., & Easton, D. F. (2002). Cancer Incidence in BRCA1 mutation carriers. *Journal of the National Cancer Institute*, 94(18), 1358–65. Retrieved from http://www.ncbi.nlm.nih.gov/pubmed/12237281

Tirkkonen, M., Johannsson, O., Agnarsson, B. A., Olsson, H., Ingvarsson, S., Karhu, R., Tanner, M., et al. (1997). Distinct somatic genetic changes associated with tumor progression in carriers of BRCA1 and BRCA2 germ-line mutations. *Cancer research*, 57(7), 1222–7. Retrieved from http://www.ncbi.nlm.nih.gov/pubmed/9102202

Turk, D., & Guncar, G. (2003). Lysosomal cysteine proteases (cathepsins): promising drug targets. *Acta crystallographica. Section D, Biological crystallography*, 59(Pt 2), 203–13. Retrieved from http://www.ncbi.nlm.nih.gov/pubmed/12554931

Varela, I., Cadiñanos, J., Pendás, A. M., Gutiérrez-Fernández, A., Folgueras, A. R., Sánchez, L. M., Zhou, Z., et al. (2005). Accelerated ageing in mice deficient in Zmpste24 protease is linked to p53 signalling activation. *Nature*, 437(7058), 564–8. doi:10.1038/nature04019

Walker, J. R., Corpina, R. A., & Goldberg, J. (2001). Structure of the Ku heterodimer bound to DNA and its implications for double-strand break repair. *Nature*, 412(6847), 607–14. doi:10.1038/35088000

Wang, B., Matsuoka, S., Ballif, B. A., Zhang, D., Smogorzewska, A., Gygi, S. P., & Elledge, S. J. (2007). Abraxas and RAP80 form a BRCA1 protein complex required for the DNA damage response. *Science (New York, N.Y.)*, 316(5828), 1194–8. doi:10.1126/science.1139476

Wang, W., & Figg, W. D. (2008). Secondary BRCA1 and BRCA2 alterations and acquired chemoresistance. *Cancer biology & therapy*, 7(7), 1004–5. Retrieved from http://www.pubmedcentral.nih.gov/articlerender.fcgi?artid=2731297&tool=pmcentrez&rendertype=abstract

Ward, I. M., Minn, K., van Deursen, J., & Chen, J. (2003). p53 Binding protein 53BP1 is required for DNA damage responses and tumor suppression in mice. *Molecular and cellular biology*, 23(7), 2556–63. Retrieved from http://www.pubmedcentral.nih.gov/articlerender.fcgi?artid=150747&tool=pmcentrez&rendertype=abstract

Weigelt, B, Horlings, H. M., Kreike, B., Hayes, M. M., Hauptmann, M., Wessels, L. F. A., de Jong, D., et al. (2008). Refinement of breast cancer classification by molecular characterization of histological special types. *The Journal of pathology*, 216(2), 141–50. doi:10.1002/path.2407

Weigelt, Britta, Baehner, F. L., & Reis-Filho, J. S. (2010). The contribution of gene expression profiling to breast cancer classification, prognostication and prediction: a retrospective of the last decade. *The Journal of pathology*, 220(2), 263–80. doi:10.1002/path.2648

Weigelt, Britta, & Reis-Filho, J. S. (2009). Histological and molecular types of breast cancer: is there a unifying taxonomy? *Nature reviews. Clinical oncology*, 6(12), 718–30. doi:10.1038/nrclinonc.2009.166

Willis, N. D., Cox, T. R., Rahman-Casañs, S. F., Smits, K., Przyborski, S. A., van den Brandt, P., van Engeland, M., et al. (2008). Lamin A/C is a risk biomarker in colorectal cancer. *PloS one*, 3(8), e2988. doi:10.1371/journal.pone.0002988

Wright, W. W., Smith, L., Kerr, C., & Charron, M. (2003). Mice that express enzymatically inactive cathepsin L exhibit abnormal spermatogenesis. *Biology of reproduction*, 68(2), 680–7. Retrieved from http://www.ncbi.nlm.nih.gov/pubmed/12533435

Wyman, C., & Kanaar, R. (2006). DNA double-strand break repair: all's well that ends well. *Annual review of genetics*, 40, 363–83. doi:10.1146/annurev.genet.40.110405.090451

Xu, B., Kim St, & Kastan, M. B. (2001). Involvement of Brca1 in S-phase and G(2)-phase checkpoints after ionizing irradiation. *Molecular and cellular biology*, 21(10), 3445–50. doi:10.1128/MCB.21.10.3445-3450.2001

Xu, X., Weaver, Z., Linke, S. P., Li, C., Gotay, J., Wang, X. W., Harris, C. C., et al. (1999). Centrosome amplification and a defective G2-M cell cycle checkpoint induce genetic instability in BRCA1 exon 11 isoform-deficient cells. *Molecular cell*, 3(3), 389–95. Retrieved from http://www.ncbi.nlm.nih.gov/pubmed/10198641

Yan, J., Kim, Y.-S., Yang, X.-P., Li, L.-P., Liao, G., Xia, F., & Jetten, A. M. (2007). The ubiquitin-interacting motif containing protein RAP80 interacts with BRCA1 and functions in DNA damage repair response. *Cancer research*, 67(14), 6647–56. doi:10.1158/0008-5472.CAN-07-0924

Yang, H., Li, Q., Fan, J., Holloman, W. K., & Pavletich, N. P. (2005). The BRCA2 homologue Brh2 nucleates RAD51 filament formation at a dsDNA-ssDNA junction. *Nature*, 433(7026), 653–7. doi:10.1038/nature03234

Yang, S. H., Bergo, M. O., Toth, J. I., Qiao, X., Hu, Y., Sandoval, S., Meta, M., et al. (2005). Blocking protein farnesyltransferase improves nuclear blebbing in mouse fibroblasts with a targeted Hutchinson-Gilford progeria syndrome mutation. *Proceedings of the National*

Academy of Sciences of the United States of America, 102(29), 10291–6. doi:10.1073/pnas.0504641102

Yang, S. H., Meta, M., Qiao, X., Frost, D., Bauch, J., Coffinier, C., Majumdar, S., et al. (2006). A farnesyltransferase inhibitor improves disease phenotypes in mice with a Hutchinson-Gilford progeria syndrome mutation. *The Journal of clinical investigation*, 116(8), 2115–21. doi:10.1172/JCI28968

Yarden, R. I., Pardo-Reoyo, S., Sgagias, M., Cowan, K. H., & Brody, L. C. (2002). BRCA1 regulates the G2/M checkpoint by activating Chk1 kinase upon DNA damage. *Nature genetics*, 30(3), 285–9. doi:10.1038/ng837

Yu, X., Wu, L. C., Bowcock, A. M., Aronheim, A., & Baer, R. (1998). The C-terminal (BRCT) domains of BRCA1 interact in vivo with CtIP, a protein implicated in the CtBP pathway of transcriptional repression. *The Journal of biological chemistry*, 273(39), 25388–92. Retrieved from http://www.ncbi.nlm.nih.gov/pubmed/9738006

Yun, M. H., & Hiom, K. (2009). CtIP-BRCA1 modulates the choice of DNA double-strand-break repair pathway throughout the cell cycle. *Nature*, 459(7245), 460–3. doi:10.1038/nature07955

Zhang, F., Ma, J., Wu, J., Ye, L., Cai, H., Xia, B., & Yu, X. (2009). PALB2 links BRCA1 and BRCA2 in the DNA-damage response. *Current biology : CB*, 19(6), 524–9. doi:10.1016/j.cub.2009.02.018

Zhang, Y., & Jasin, M. (2011). An essential role for CtIP in chromosomal translocation formation through an alternative end-joining pathway. *Nature structural & molecular biology*, 18(1), 80–4. doi:10.1038/nsmb.1940

Zhu, Q., Pao, G. M., Huynh, A. M., Suh, H., Tonnu, N., Nederlof, P. M., Gage, F. H., et al. (2011). BRCA1 tumour suppression occurs via heterochromatin-mediated silencing. *Nature*, 477(7363), 179–84. doi:10.1038/nature10371

CHAPTER TWO

BRCA1-deficient cells activate cathepsin L-mediated degradation of 53BP1 to overcome genomic instability and growth arrest

2.1 Abstract

BRCA1-mutated breast cancers, which are most often also characterized as being triple-negative breast cancers (TNBC) are very difficult to treat and have poor prognosis. BRCA1 deficiency is associated with defects in HR, which leads to genomic instability and cell death. Thus, investigators have been trying to determine how BRCA1-deficient tumor cells are able to overcome genomic instability and proliferation defects. Several studies published in 2010 showed that loss of 53BP1 partially rescues the BRCA1-deficient phenotype, including the embryonic lethality in mice expressing a loss-of-function mutant form of BRCA1 (deletion of BRCA1 exon 11) (Bouwman et al. 2010; Bunting et al. 2010; L. Cao et al. 2009). 53BP1 loss also rescued HR and rendered cells resistant to PARP inhibitor treatment, drugs on the forefront of cancer treatment that are effective in cells deficient in HR. The model that was proposed is that when BRCA1 is absent, the presence of 53BP1 at a DNA double strand break blocks DNA end resection and shifts DNA repair to error prone NHEJ while loss of 53BP1 allows end resection and HR. Therefore, it is tempting to speculate that raising levels of 53BP1 in the context of BRCA1 deficiency could shift DNA repair towards NHEJ and render cells sensitive to PARPi and other DNA damaging strategies. However, until studies performed in our laboratory identifying the cysteine protease cathepsin L (CTSL) as a regulator of 53BP1 levels, little was known about the regulation of this DNA repair factor. Here, we show that upon loss of BRCA1, breast cancer cells activate CTSL-mediated degradation of 53BP1 and that CTSL is responsible for the decrease in 53BP1 levels. Activation of this pathway allows BRCA1-deficient cells to overcome genomic instability and growth arrest. Furthermore, inhibition of CTSL with a cathepsin inhibitor or vitamin D rescues levels of 53BP1. Raising 53BP1 levels in BRCA1-deficient cells rescues NHEJ and inhibits HR, thereby causing an increase in genomic instability

following irradiation or PARPi treatment, and compromising proliferation. Thus, inhibiting CTSL via specific inhibitors or vitamin D could represent a novel therapeutic strategy for treatment of breast cancers with the poorest prognosis.

2.2 BRCA1-deficient cells activate CTSL mediated degradation of 53BP1 to overcome growth arrest

Previous studies have demonstrated that loss of 53BP1 rescues the BRCA1-deficient phenotype (Bouwman et al. 2010; Bunting et al. 2010; L. Cao et al. 2009). Here, we investigated whether breast tumor cells are able to downregulate 53BP1 upon loss of BRCA1 in order to restore proliferation and if CTSL could be a mechanism responsible for the depletion of 53BP1. To recapitulate a BRCA1-deficient phenotype, we knocked down BRCA1 via lentiviral transduction using specific short hairpin RNAs (sh RNAs) in MCF7 cells (**Figure 2-1)**. We chose MCF7 cells because they are a human breast cancer cell line that is proficient in BRCA1 and 53BP1 and could therefore be used to monitor the effects of depletion of either protein. MCF7 cells are positive for estrogen receptor and progesterone receptor (Brooks, Locke, and Soule 1973)(Levenson and Jordan 1997). Consistent with previous findings in human fibroblasts (Tu et al. 2011), MCF7

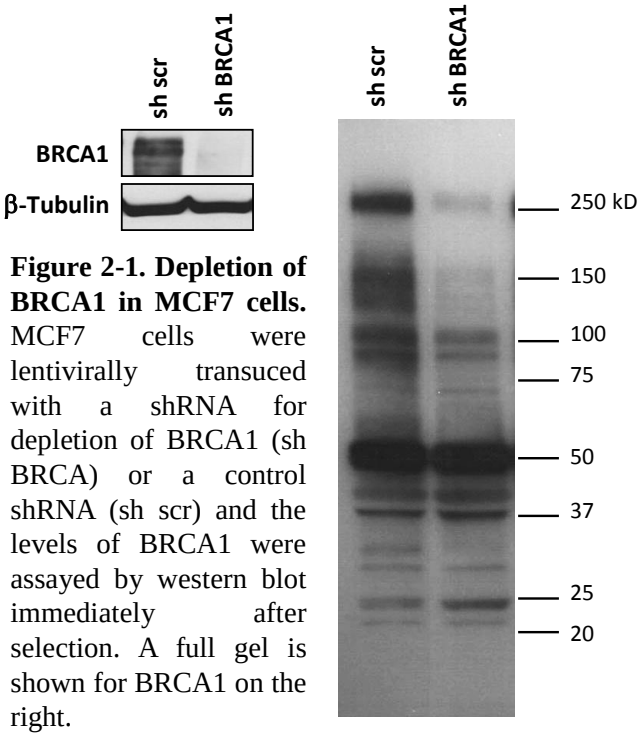

Figure 2-1. Depletion of BRCA1 in MCF7 cells. MCF7 cells were lentivirally transuced with a shRNA for depletion of BRCA1 (sh BRCA) or a control shRNA (sh scr) and the levels of BRCA1 were assayed by western blot immediately after selection. A full gel is shown for BRCA1 on the right.

cells depleted of BRCA1 entered a growth arrest while control short hairpin cells continued to grow exponentially (**Figure 2-2A)**. We monitored levels of 53BP1 and CTSL by western blot while the cells were growth arrested and found no difference in protein levels between controls and BRCA1-depleted cells (**Figure 2-2B**). Interestingly, after approximately two weeks in culture, the BRCA1-deficient cells resumed proliferation, albeit at a slower rate than control cells (**Figure 2-2C**). When we measured the protein levels of CTSL and 53BP1 in these BRCA1-deficient cells that Overcome Growth Arrest (herein referred to as BOGA cells, for clarity), we found decreased 53BP1 and increased CTSL levels (**Figure 2-2D**).

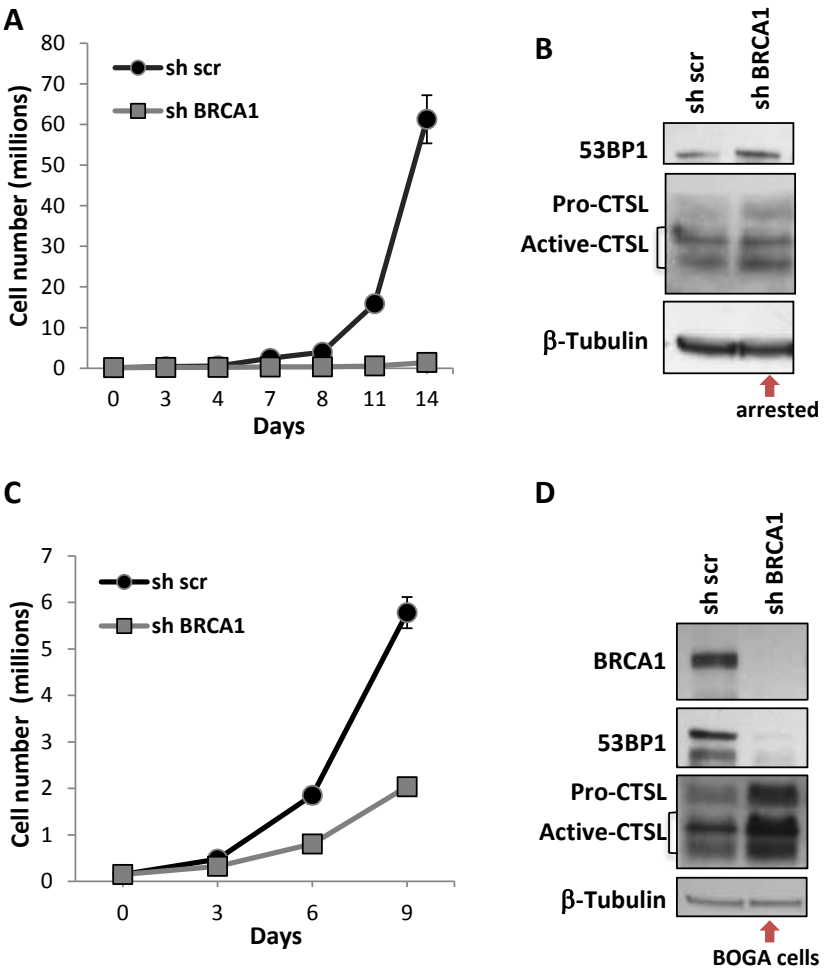

Figure 2-2. Bypass of growth arrest following BRCA1 loss is associated with upregulation of CTSL and degradation of 53BP1. **(A)** Proliferation rate of MCF7 cells shows that depletion of BRCA1 induces a growth arrest for up to 14 days. **(B)** Western blots show 53BP1 and CTSL (Pro-CTSL and Active CTSL) levels in growth-arrested cells. **(C)** Proliferation rate of BRCA1-deficient cells that overcome growth arrest (BOGA cells). **(D)** Western blots show levels of BRCA1, 53BP1, and CTSL in control and BOGA cells (representative experiment of 25 biological repeats).

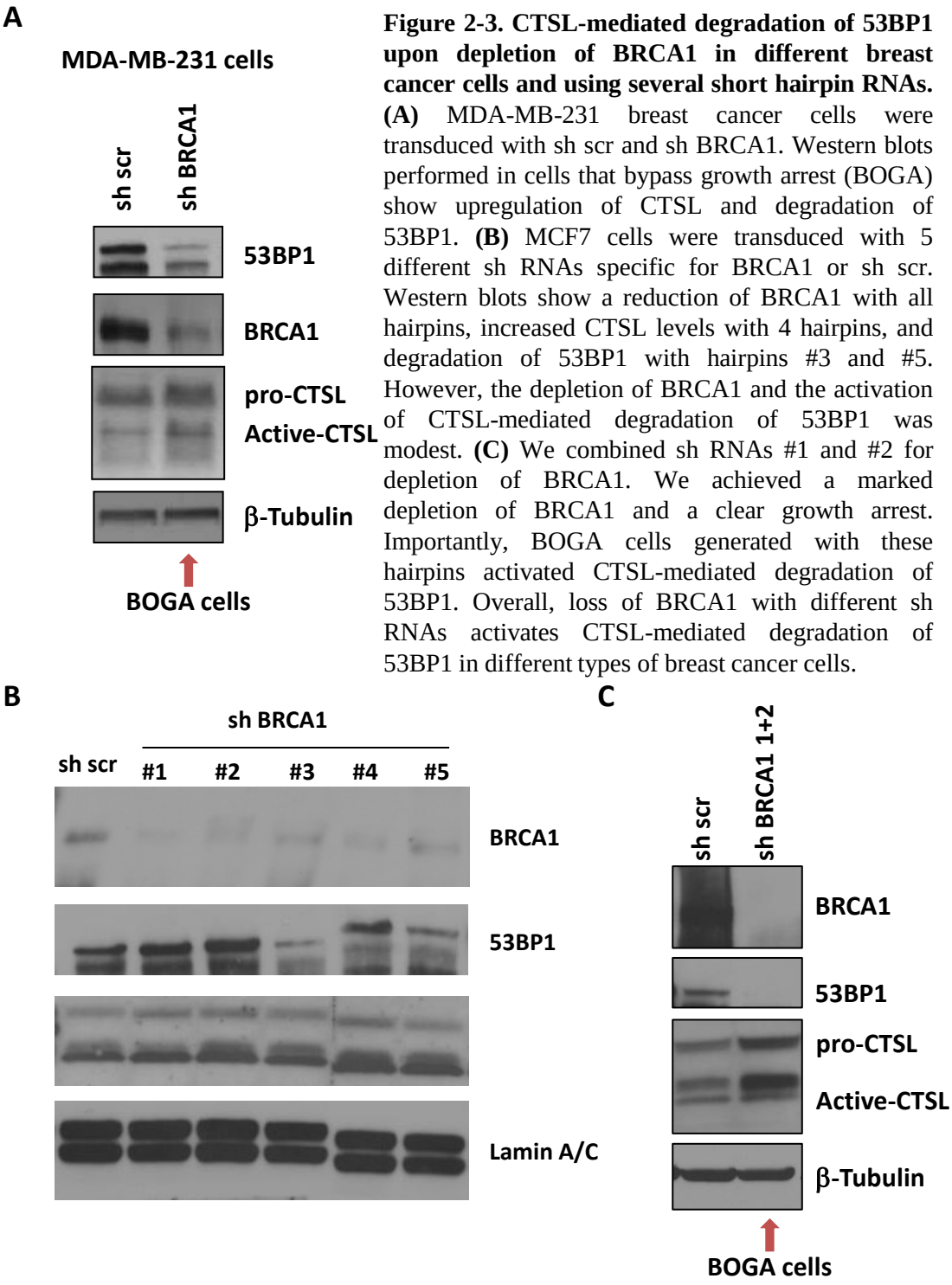

Figure 2-3. CTSL-mediated degradation of 53BP1 upon depletion of BRCA1 in different breast cancer cells and using several short hairpin RNAs. **(A)** MDA-MB-231 breast cancer cells were transduced with sh scr and sh BRCA1. Western blots performed in cells that bypass growth arrest (BOGA) show upregulation of CTSL and degradation of 53BP1. **(B)** MCF7 cells were transduced with 5 different sh RNAs specific for BRCA1 or sh scr. Western blots show a reduction of BRCA1 with all hairpins, increased CTSL levels with 4 hairpins, and degradation of 53BP1 with hairpins #3 and #5. However, the depletion of BRCA1 and the activation of CTSL-mediated degradation of 53BP1 was modest. **(C)** We combined sh RNAs #1 and #2 for depletion of BRCA1. We achieved a marked depletion of BRCA1 and a clear growth arrest. Importantly, BOGA cells generated with these hairpins activated CTSL-mediated degradation of 53BP1. Overall, loss of BRCA1 with different sh RNAs activates CTSL-mediated degradation of 53BP1 in different types of breast cancer cells.

We also observed this signature of low 53BP1 and high CTSL in another breast tumor cell line, MDA-MB-231 (**Figure 2-3A**), as well as with several other sh RNAs for depletion of BRCA1 (**Figure 2-3B**). We next monitored levels of BRCA1, CTSL, and 53BP1 transcripts by qRT-PCR (**Figure 2-4A**). BRCA1 depleted cells exhibited a significant decrease in BRCA1 while CTSL transcripts levels were significantly increased. Interestingly, there was no significant change in 53BP1 transcripts levels, indicating a posttranslational effect on 53BP1 protein stability. To confirm that BRCA1 loss leads to the decrease in 53BP1 levels, we overexpressed BRCA1 via transient transfection in BOGA cells and in the human BRCA1-deficient breast tumor line HCC1937. We monitored levels of 53BP1 and found that BRCA1 reconstitution stabilizes 53BP1 levels in both cell lines (**Figure 2-4B)**, indicating a novel function for BRCA1 in regulating 53BP1 levels.

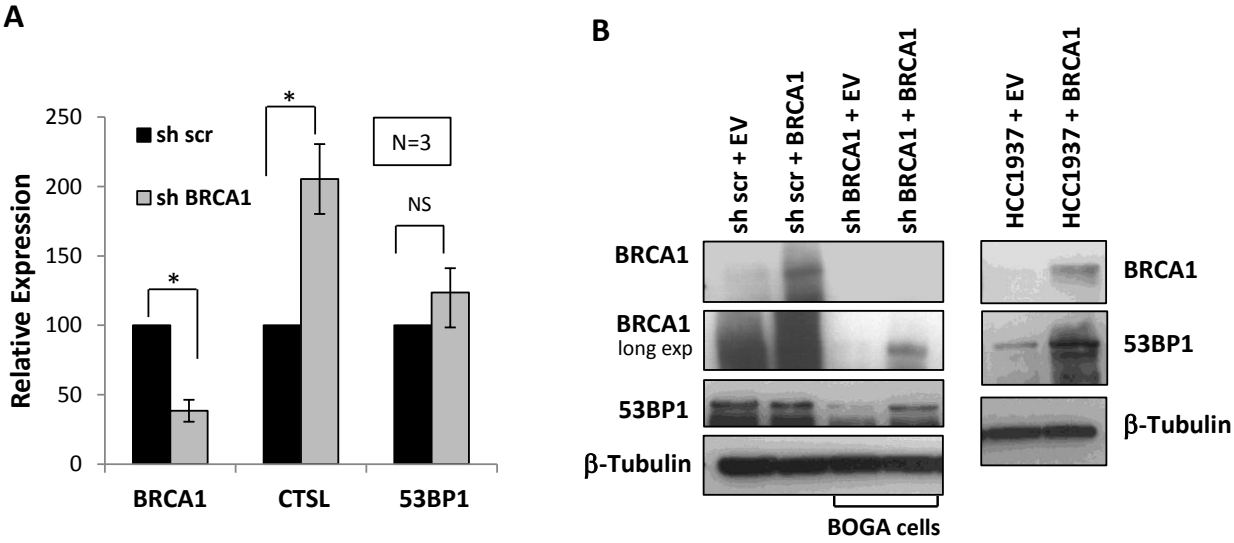

Figure 2-4. Transcripts levels upon BRCA1 depletion and western blot after BRCA1 reconstitution in BRCA1-deficient cells (A) Relative expression of BRCA1, CTSL, and 53BP1 in control and BOGA cells as determined by qRT-PCR. The average ± standard deviation of 3 independent experiments is shown. * p-value of statistical significance ($p \leq 0.05$). NS, no statistically significant differences. **(B)** Western blots show BRCA1 and 53BP1 levels upon reconstitution of BRCA1 by transient transfection into BRCA1-deficient cells lines – BOGA cells (left panel) and HCC1937 cells (right panel). Transfection of an empty vector (EV) was used as control. B-tubulin was used as loading control.

Given that loss of 53BP1 in a BRCA1-deficient context allows cells to proliferate, we wanted to determine if depletion of 53BP1 prior to BRCA1 depletion leads to a bypass of the growth arrest. We were able to obtain a marked decrease in both 53BP1 and BRCA1 using specific sh RNAs (**Figure 2-5A**). Importantly, cells depleted of 53BP1 prior to BRCA1 continued to proliferate and did not exhibit the characteristic growth arrest upon BRCA1 depletion, although these cells proliferated slower than controls (**Figure 2-5B)**. Interestingly, cells that were depleted of 53BP1 prior to depletion of BRCA1 still upregulated CTSL (**Figure 2-5C**), indicating the upregulation of CTSL is independent of 53BP1 levels.

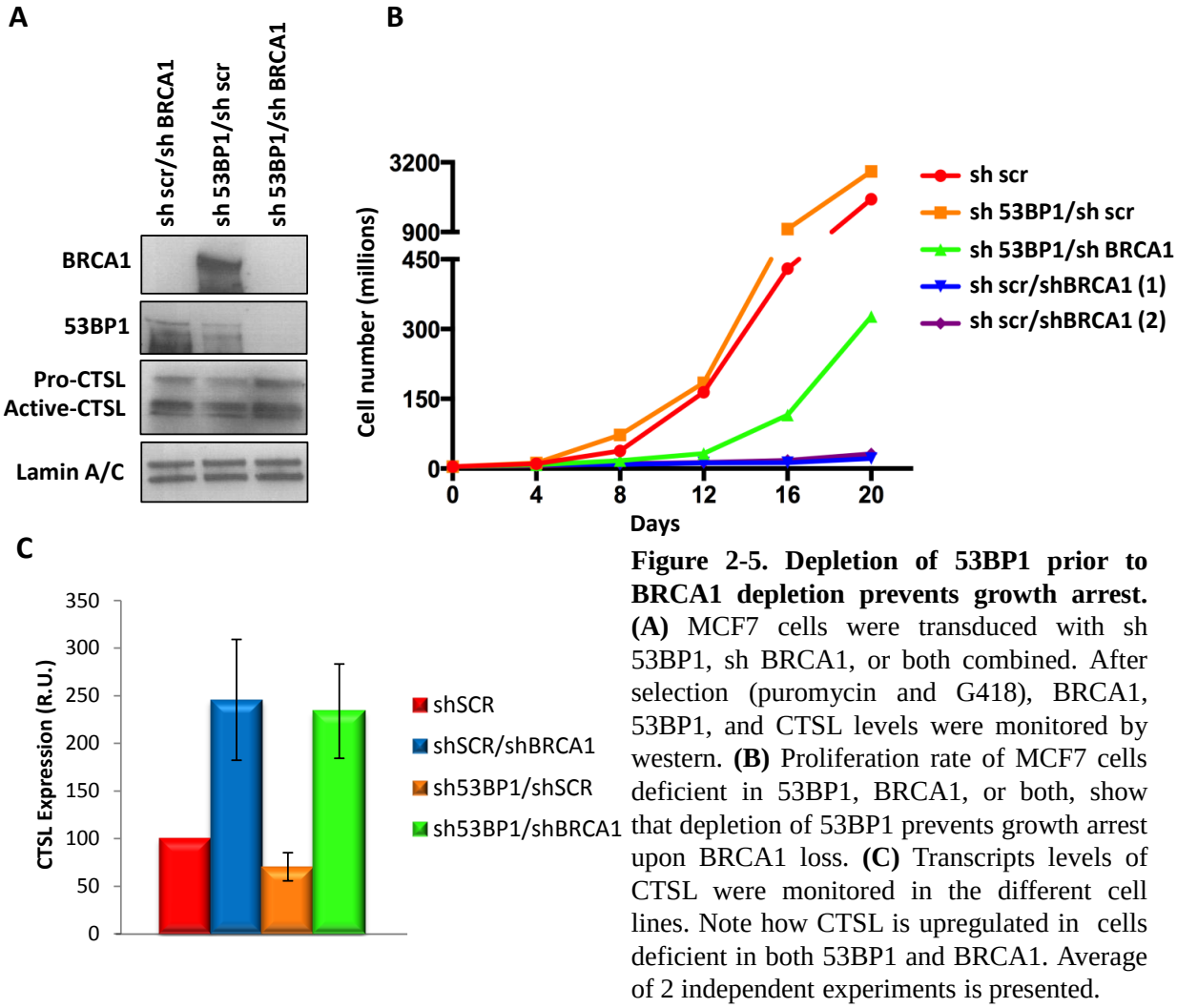

Figure 2-5. Depletion of 53BP1 prior to BRCA1 depletion prevents growth arrest. **(A)** MCF7 cells were transduced with sh 53BP1, sh BRCA1, or both combined. After selection (puromycin and G418), BRCA1, 53BP1, and CTSL levels were monitored by western. **(B)** Proliferation rate of MCF7 cells deficient in 53BP1, BRCA1, or both, show that depletion of 53BP1 prevents growth arrest upon BRCA1 loss. **(C)** Transcripts levels of CTSL were monitored in the different cell lines. Note how CTSL is upregulated in cells deficient in both 53BP1 and BRCA1. Average of 2 independent experiments is presented.

We next tested if CTSL is responsible for the decrease in 53BP1 protein levels in BRCA1-deficient cells by depleting CTSL in control and BOGA cells. Importantly, depletion of CTSL in BOGA cells rescued levels of 53BP1 protein to the same level as control cells (**Figure 2-6A)** without having an effect on BRCA1 transcripts levels (**Figure 2-6B**). We also observed a slight increase in BRCA1 protein levels in BOGA cells depleted of CTSL, suggesting a possible feedback mechanism of CTSL on BRCA1 protein levels.

To confirm that CTSL is responsible for the decrease in 53BP1 in BRCA1-deficient cells, we treated BOGA cells with CTSL inhibitors. Previous studies in colon cancer cells had shown that vitamin D inhibits the activity of cathepsins (Alvarez-Díaz et al. 2009). The mechanism involves the upregulation by vitamin D receptor (VDR) of cystatin D, an endogenous inhibitor of cathepsins, including CTSL. We also previously showed that vitamin D inhibits CTSL activity and stabilizes 53BP1 protein levels in MEFs (Gonzalez-Suarez et al. 2011). Thus, we determined whether vitamin D treatment could stabilize 53BP1 protein levels in BRCA1-deficient cells. We show that treatment of BOGA cells with vitamin D (1α,25-dihydroxyvitamin D_3) for 24 hours stabilizes the levels of 53BP1 (**Figure 2-6C**). In addition, vitamin D stabilizes levels of p107, an Rb family member that is a known target of CTSL-mediated degradation (Redwood, Gonzalez-suarez, and Gonzalo 2011). Similarly, treatment of BOGA cells with the cathepsin inhibitor E-64 increased 53BP1 protein levels (**Figure 2-6D**). Overall, these data demonstrate that growth arrested BRCA1-deficient cells activate CTSL mediated degradation of 53BP1 to bypass the growth arrest. Furthermore, depletion or inhibition of CTSL increases 53BP1 levels in BRCA1-deficient cells with potential therapeutic effects.

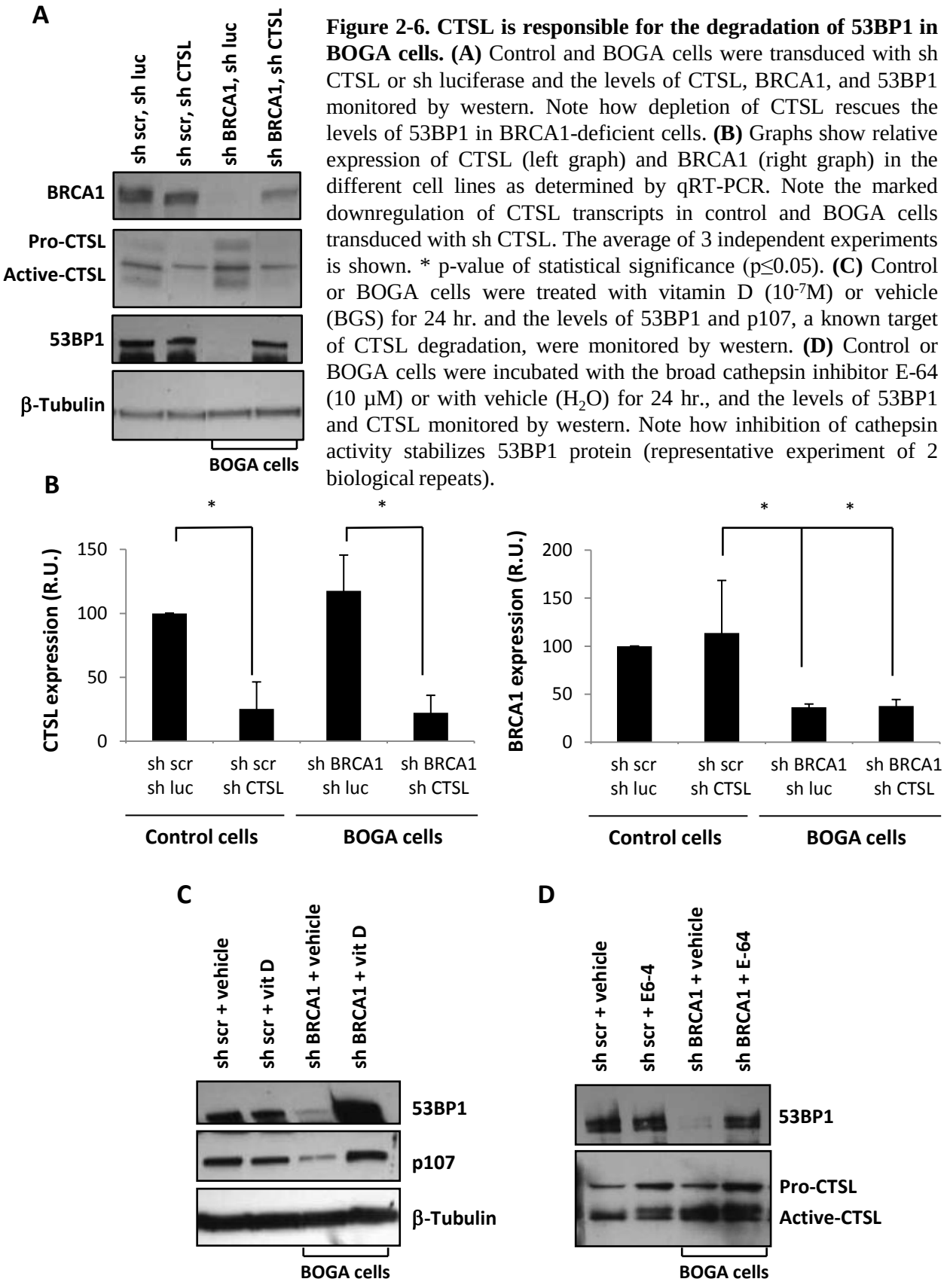

Figure 2-6. CTSL is responsible for the degradation of 53BP1 in BOGA cells. (A) Control and BOGA cells were transduced with sh CTSL or sh luciferase and the levels of CTSL, BRCA1, and 53BP1 monitored by western. Note how depletion of CTSL rescues the levels of 53BP1 in BRCA1-deficient cells. **(B)** Graphs show relative expression of CTSL (left graph) and BRCA1 (right graph) in the different cell lines as determined by qRT-PCR. Note the marked downregulation of CTSL transcripts in control and BOGA cells transduced with sh CTSL. The average of 3 independent experiments is shown. * p-value of statistical significance ($p \leq 0.05$). **(C)** Control or BOGA cells were treated with vitamin D (10^{-7}M) or vehicle (BGS) for 24 hr. and the levels of 53BP1 and p107, a known target of CTSL degradation, were monitored by western. **(D)** Control or BOGA cells were incubated with the broad cathepsin inhibitor E-64 (10 μM) or with vehicle (H_2O) for 24 hr., and the levels of 53BP1 and CTSL monitored by western. Note how inhibition of cathepsin activity stabilizes 53BP1 protein (representative experiment of 2 biological repeats).

2.3 CTSL-mediated degradation of 53BP1 rescues HR defects in BRCA1-deficient cells

BRCA1 plays a key role in DNA double strand break repair by HR and is involved in facilitating end resection at breaks and formation of RAD51 coated filaments that are necessary for HR to occur (Bhattacharyya et al. 2000; Moynahan et al. 1999; Brian P Schlegel, Jodelka, and Nunez 2006; Scully, J Chen, Plug, et al. 1997; Scully, J Chen, Ochs, et al. 1997; Snouwaert et al. 1999; Sung et al. 2003). Interestingly, a previous study had demonstrated that loss of 53BP1 in BRCA1-deficient cells partially rescues HR and recruitment of RAD51 at ionizing radiation-induced foci (IRIF) (Bunting et al. 2010). Here, we determined how CTSL mediated degradation of 53BP1 impacts on 53BP1 and RAD51 foci formation in BRCA1-deficient cells. We used the presence or absence of 53BP1 or RAD51 IRIF as readout of NHEJ or HR proficiency, respectively. Growth arrested MCF7 cells following BRCA1 depletion are able to form 53BP1 IRIF (**Figure 2-7A**), consistent with normal protein levels of 53BP1 in growth arrested cells (**Figure 2-2B**). As we expected, BOGA cells were unable to form 53BP1 IRIF (**Figure 2-7B**), consistent with the decrease in 53BP1 protein levels (**Figure 2-2D**). Given that CTSL inhibition rescues 53BP1 protein levels, we sought to determine if treatment of BOGA cells would rescue 53BP1 IRIF formation. Indeed, BOGA cells treated with vehicle were unable to form 53BP1 foci formation while treatment with vitamin D for 24 hours rescued the formation of 53BP1 foci (**Figure 2-7C**), which is quantitated in **Figure 2-7D,** indicating a possible shift towards NHEJ upon CTSL inhibition.

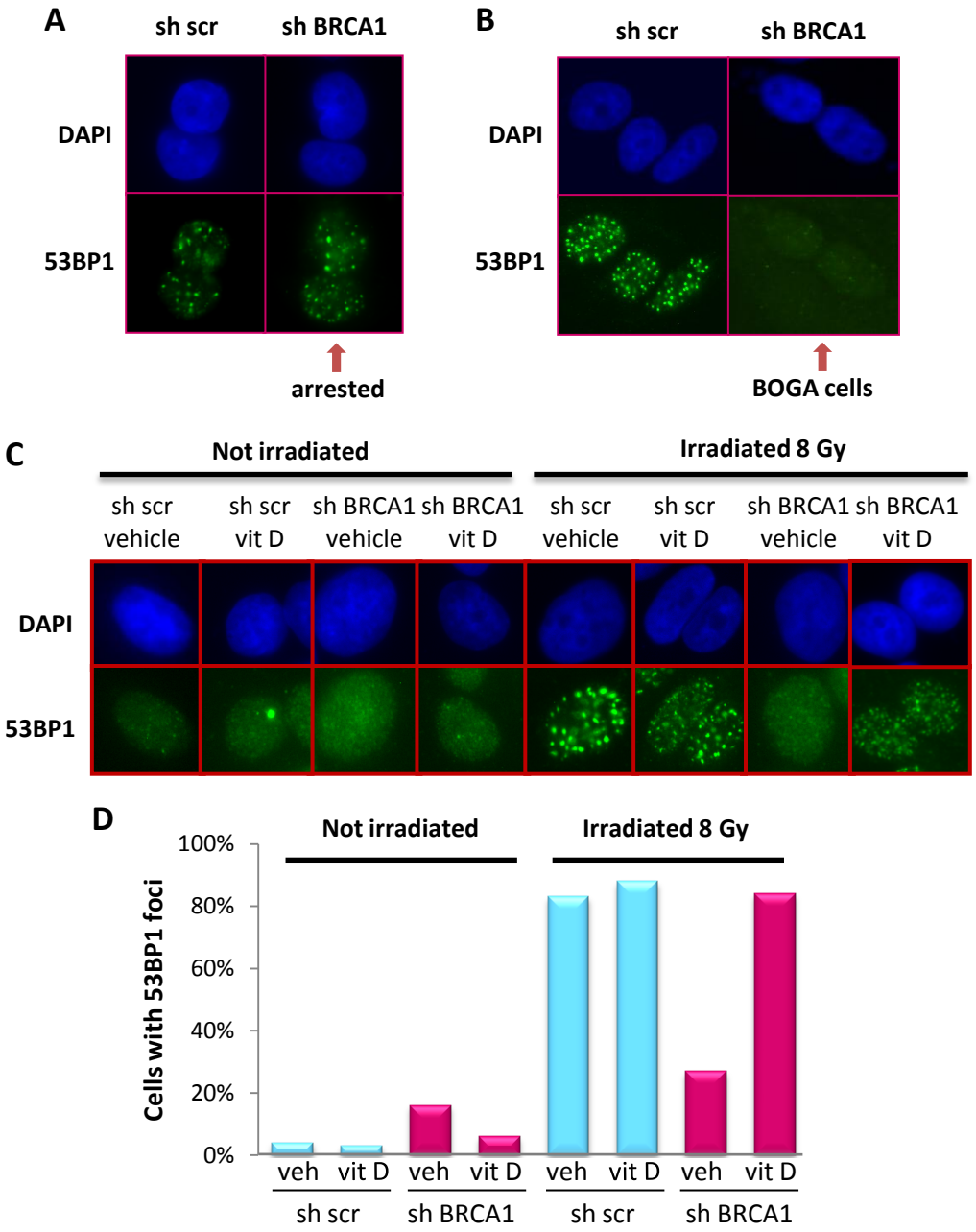

Figure 2-7. Regulation of 53BP1 IRIF in BOGA cells by vitamin D treatment. (A) Immunofluorescence to detect 53BP1 IRIF in control (sh scr) and growth-arrested BRCA1-depleted cells (sh BRCA1) 1 hr. after 8 Gy of IR. **(B)** The same assay was performed as in (A), but after bypass of growth arrest (BOGA cells). **(C)** Immunofluorescence performed in control and BOGA cells treated with vitamin D or vehicle 24 hr. prior to IR. Note how treatment with vitamin D restores 53BP1 IRIF in BOGA cells. **(D)** Graph shows the percentage of cells that form 53BP1 IRIF in the presence of vitamin D or vehicle. Cells with >10 53BP1 IRIF were considered positive. At least 1000 cells were analyzed per condition.

In contrast to 53BP1, RAD51 recruitment to IRIF was inhibited in growth arrested cells shortly after BRCA1 depletion (**Figure 2-8**). However, once the BRCA1-deficient cells resumed proliferation, RAD51 IRIF formation was rescued at 1 hour post irradiation (**Figure 2-9A**). This rescue was not due to an increase in BRCA1 levels, as BOGA cells were unable to form BRCA1 labeled IRIF (**Figure 2-10**). We next tested whether CTSL mediated degradation of 53BP1 was responsible for rescuing RAD51 IRIF formation in BOGA cells. First, we showed that stabilization of 53BP1 in BOGA cells by treatment with vitamin D inhibited RAD51 IRIF formation (**Figure 2-9B**), revealing an unprecedented role for vitamin D in modulating HR. Similarly, depletion of CTSL reduces the ability of BOGA cells to recruit RAD51 to double-strand breaks (**Figure 2-9C**). Intriguingly, while control cells formed RAD51 foci for up to 6 hours post irradiation, the percentage of BOGA cells positive for RAD51 IRIF decreased significantly over time (**Figure 2-11**), indicating that 53BP1 loss in BOGA cells does not completely compensate for the depletion of BRCA1. It is unclear what the cause of this gradual decrease in RAD51 foci over time is, but we speculate that it could be due to an inability to recruit RAD51 to foci or an inability to retain RAD51 at the double-strand break in the absence of BRCA1.

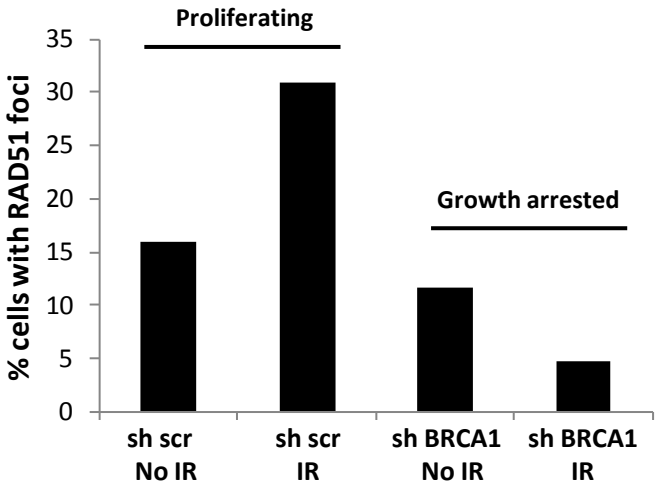

Figure 2-8. Growth arrested BRCA1-deficient cells show defects in RAD51 foci formation. MCF7 cells lentivirally transduced with sh scr or sh BRCA1 were irradiated with 8 Gy and subjected to immunofluorescence with RAD51 antibody following arrest of BRCA1-deficient cells. Note how growth arrested cells are deficient in RAD51 IRIF.

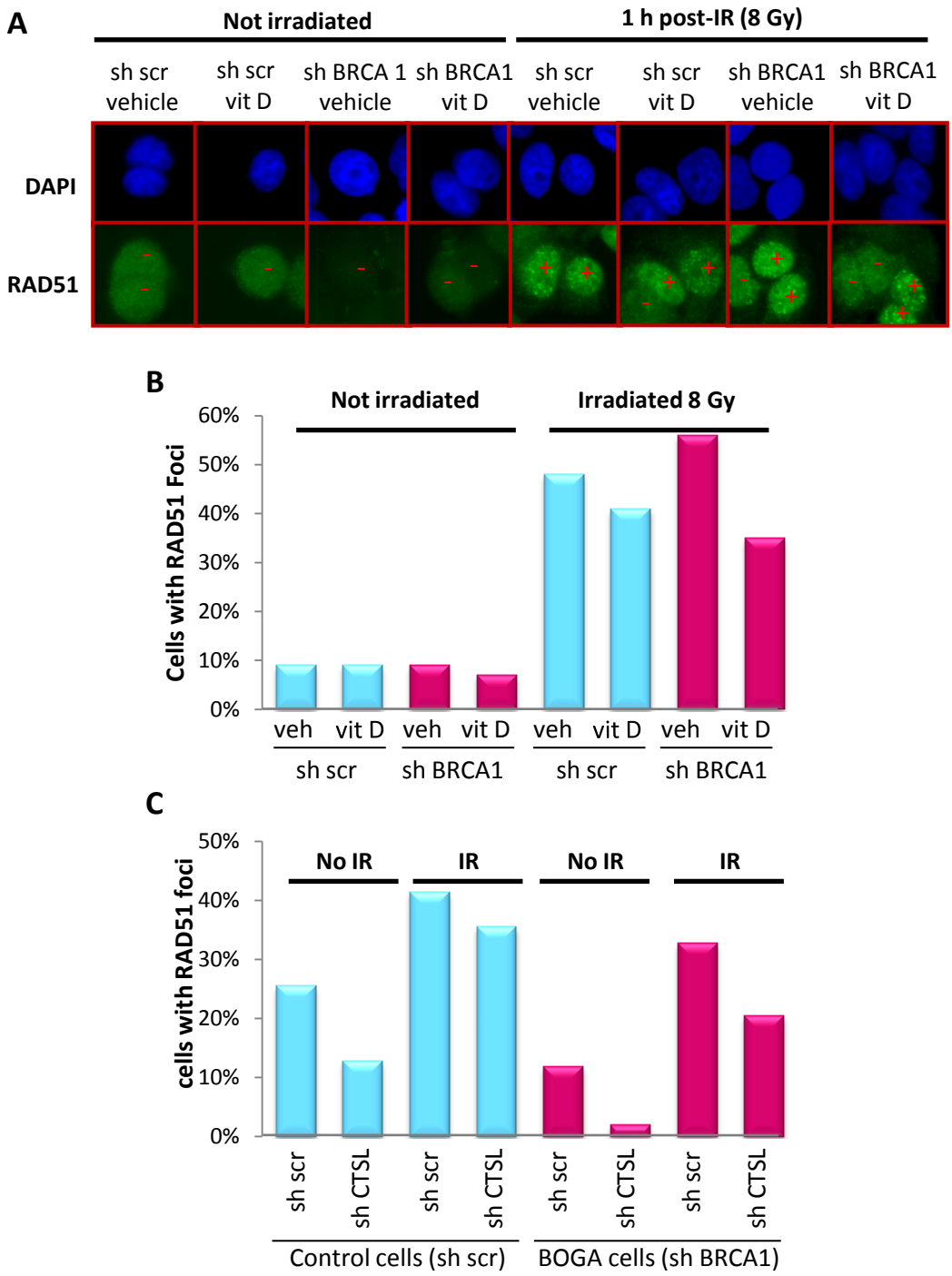

Figure 2-9. Regulation of RAD51 IRIF in BOGA cells by CTSL and vitamin D. (A) Immunofluorescence to detect RAD51 IRIF after 8 Gy of IR in control and BOGA cells following treatment with vitamin D or vehicle. (+) denotes positive cells (>10 IRIF) and (–) negative cells. **(B)** Graph shows the percentage of cells that form RAD51 IRIF 1 hr. post-IR in the presence of vitamin D or vehicle. Approximately 1000 cells were analyzed per condition. **(C)** Quantitation of RAD51 IRIF in control or BOGA cells proficient or deficient in CTSL showing reduced number of positive cells in CTSL-depleted BOGA cells. At least 200 cells were analyzed per condition.

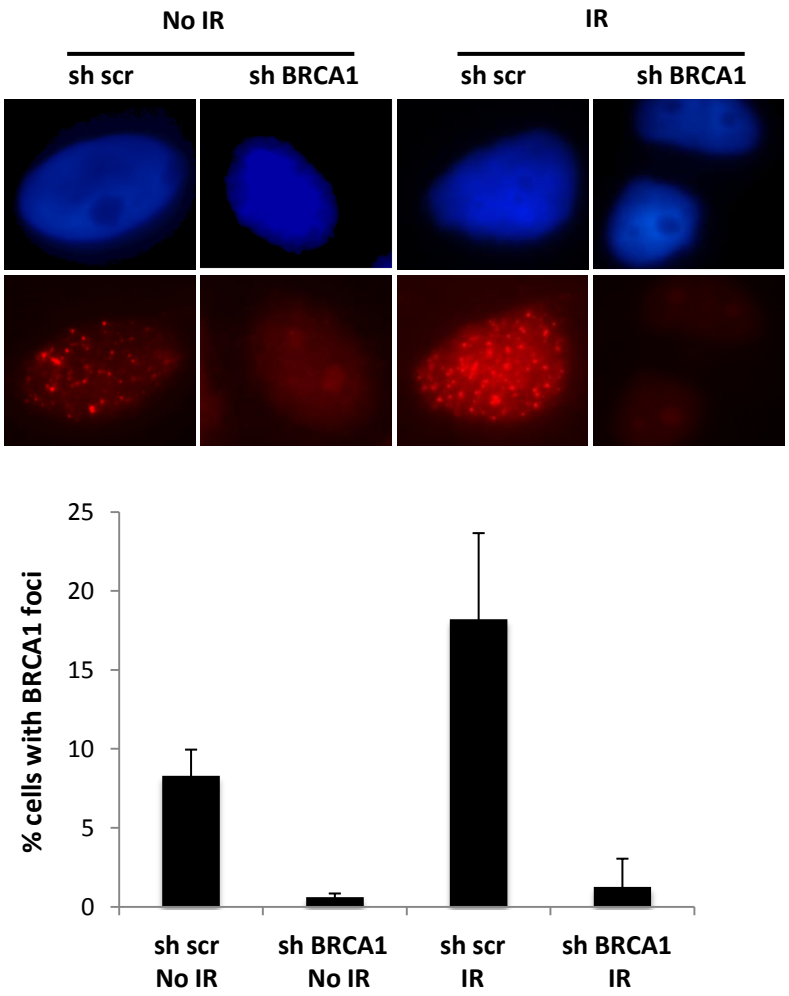

Figure 2-10. BOGA cells do not form BRCA1 foci. Control and BOGA cells were subjected to immunofluorescence with BRCA1 antibody after irradiation with 8 Gy. Upper panels show the lack of staining in BOGA cells. Graph shows the quantitation of percentage of cells positive for BRCA1 IRIF. Note how BOGA cells are unable to form BRCA1 IRIF.

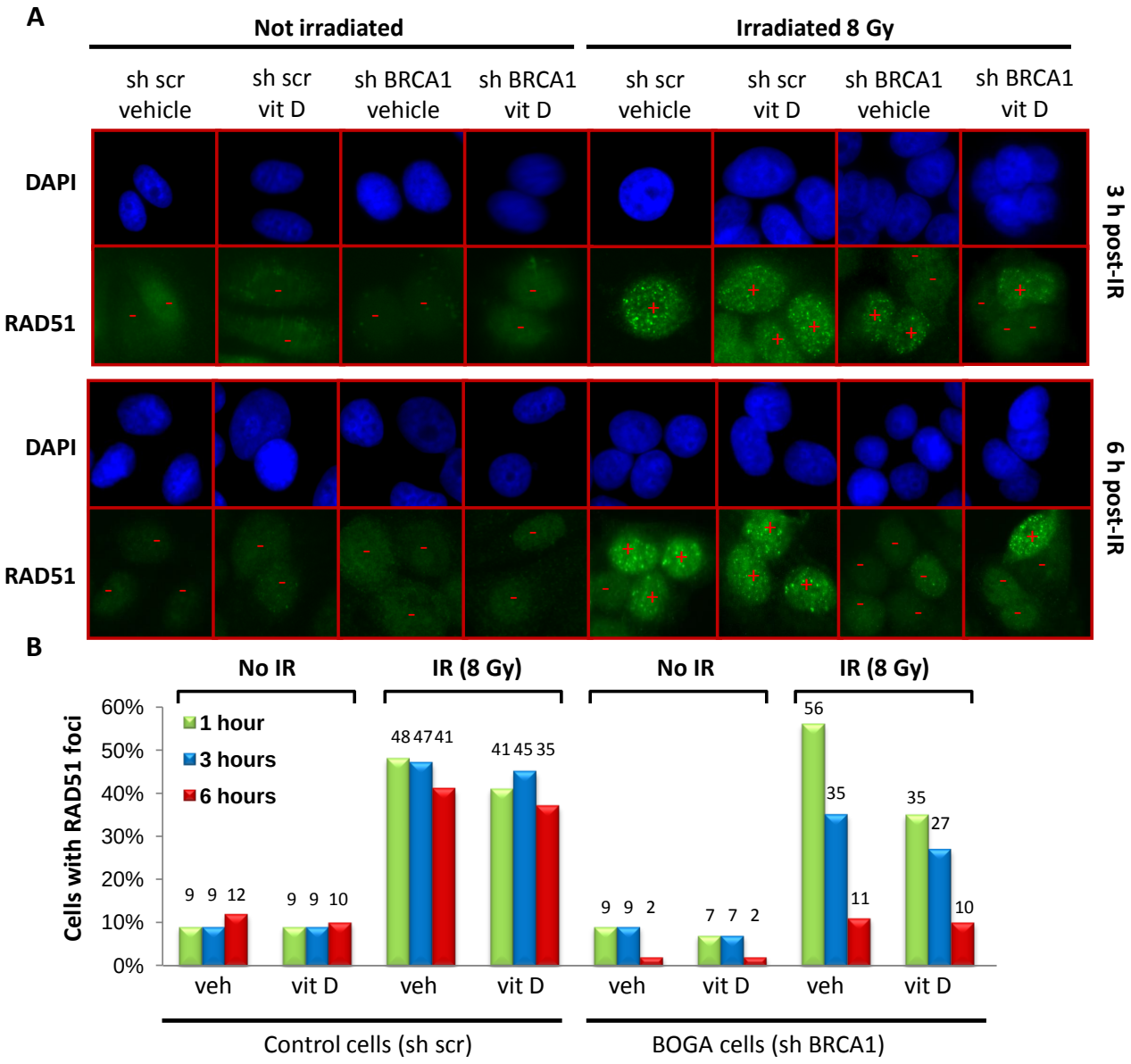

Figure 2-11. Formation of RAD51 IRIF over time. (A) Immunofluorescence images showing the formation of RAD51 IRIF in control and BOGA cells at 3 hours and 6 hours post irradiation with 8 Gy. Each cell line was treated with vitamin D or vehicle 24 hours prior to irradiation. Note the decrease in RAD51 foci formation at 3 and 6 hours post IR. **(B)** Graph shows quantitation of percentage of control and BOGA cells positive for RAD51 IRIF 1, 3, and 6 hours post IR. **(C)** Quantitation of percentage of cells positive for RAD51 foci at different times post IR and upon treatment with vitamin D or vehicle.

These studies demonstrate that CTSL mediated degradation of 53BP1 in BOGA cells rescues HR defects exhibited by BRCA1-deficient cells, promoting survival. Furthermore, CTSL inhibition and the stabilization of 53BP1 in BRCA1-deficient cells could be utilized as a novel strategy to inhibit HR and cause genomic instability.

2.4 Consequences of CTSL mediated degradation of 53BP1 for DNA repair and genomic stability

To determine the functional consequences of CTSL mediated degradation of 53BP1, we evaluated the kinetics of DNA double strand break repair by performing comet assays under neutral, non denaturing conditions (Olive, Banáth, and Durand 2012). In the comet assay, cells irradiated with 8Gy are collected at 30 minutes intervals post IR and fixed in agarose. Single cell gel electrophoresis is performed, DNA is stained with ethidium bromide, and pictures are taken on a microscope. Fragmented DNA migrates in the agarose and appears as a comet, and a quantitative score known as olive moment is calculated based on the intensity and lengths of comet tails. When olive moments are graphed, a characteristic biphasic curve emerges where a fast phase of DNA repair occurs in the first 30 minutes post irradiation, followed by a slow phase of repair. The fast phase of DNA double strand break repair has been attributed to classical or DNA-PK dependent NHEJ, as depletion of factors required for this pathway significantly slows the fast kinetics of repair (Iliakis et al. 2004). In contrast, the slow phase of repair has been attributed to alternative or backup NHEJ or HR. **Figure 2-12** shows that BOGA cells exhibit defects in the fast phase of repair, indicating a defect in classical NHEJ. This result is consistent with our previous finding that upregulation of CTSL in MEFs leads to defects in the fast phase of repair due to degradation of 53BP1 (Gonzalez-Suarez et al. 2011). Furthermore, by inhibiting

CTSL via vitamin D treatment and stabilizing 53BP1 levels (**Figure 2-6C**), DNA double-strand break repair kinetics are rescued and mirror those of control cells (**Figure 2-12**). These results suggest that CTSL mediated degradation of 53BP1 hinders NHEJ in BRCA1-deficient cells. However, these cells are still able to repair DNA double-strand breaks, albeit at a lower rate, suggesting that repair by HR or alternative NHEJ might remain relatively intact. This is consistent with the ability for RAD51 foci to form at early times post irradiation.

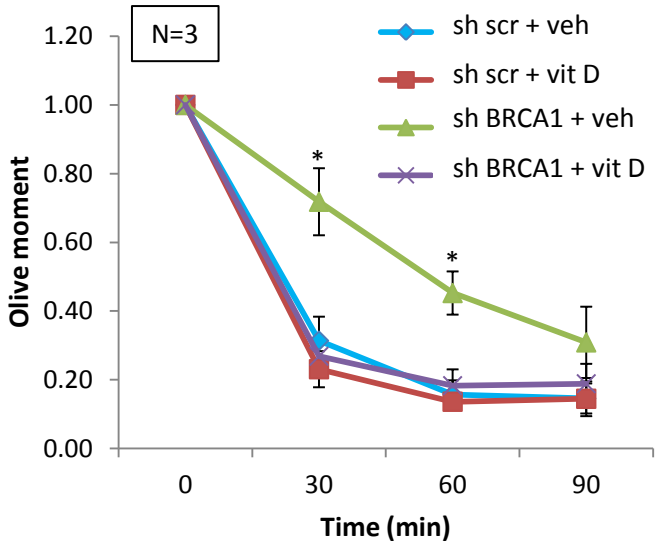

Figure 2-12. Effect of CTSL inhibition on DNA repair kinetics. Neutral comet assays after 8 Gy of IR show higher olive moments, and thus defects in the fast-phase of DNA repair in BOGA cells. Inhibition of CTSL activity by treatment with vitamin D (10^{-7} M) 24 hr. pre-IR rescues defects in DNA DSBs repair.

Cells deficient in HR become dependent on alternative pathways of DNA double strand break repair, which often leads to complex chromosomal aberrations that trigger cell cycle arrest or death. It has been shown that loss of 53BP1 is sufficient to reduce the extent of aberrant chromosomal structures in BRCA1-deficient cells (Bunting et al. 2010). Given that BOGA cells are defective in NHEJ and stabilization of 53BP1 levels rescues this error-prone DNA double-strand break repair pathway, we determined if CTSL inhibition increases genomic instability after irradiation by analyzing metaphase spreads. We did not find a profound increase in chromosome aberrations after irradiation in BOGA cells (**Figure 2-13A**), consistent with the deficiency in BRCA1 and 53BP1.

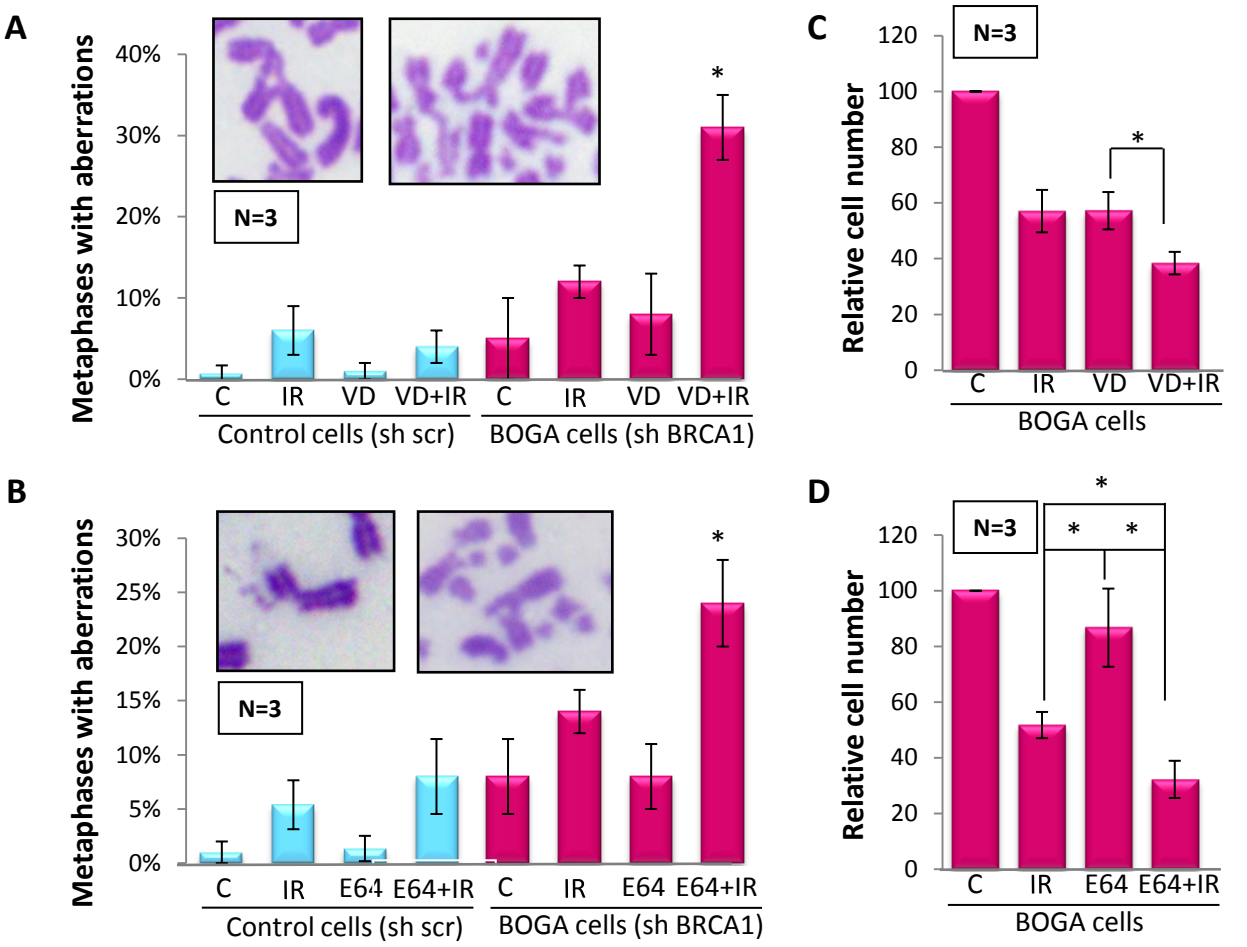

Figure 2-13. Effect of CTSL inhibition on genomic stability in BOGA cells. (A) Control and BOGA cells were incubated with vehicle control (C) or vitamin D (VD) for 24 hr. prior to irradiation with 2 Gy (IR). Cells collected 24 hr. post-IR were analyzed for genomic instability by quantitating the percentage of metaphases presenting with chromosomal aberrations, as shown in the images. N, number of independent experiments (50 metaphases analyzed per condition in each experiment). **(B)** Control and BOGA cells were incubated with the cathepsin inhibitor (E-64) or vehicle control (C) for 24 hr. prior to IR, and the extent of genomic instability assessed as in (A). **(C)** Graph shows relative numbers of BOGA cells 4 days after treatment with IR, vitamin D, or the combination of both. Treatment protocol as in (A). **(D)** Graph shows relative numbers of BOGA cells 4 days after treatment with IR, E-64, or the combination of both. Treatment performed as in (B). All values expressed as mean ± SEM. N, number of independent experiments; *p value of statistical significance (*p≤0.05).

However, stabilization of 53BP1 by vitamin D treatment significantly increased the percentage of metaphases exhibiting aberrant chromosomes after irradiation (**Figure 2-13A**). Similarly, stabilization of 53BP1 in BOGA cells by treatment with the cathepsin inhibitor E-64 markedly increased genomic instability after irradiation (**Figure 2-13B**). To determine if the increase in genomic instability caused by 53BP1 stabilization in BOGA cells has a negative effect on proliferation, we monitored the cells' ability to recover from irradiation after treatment with vitamin D or E-64. Indeed, irradiated cells treated with vitamin D (**Figure 2-13C)** or E-64 (**Figure 2-13D)** exhibited decreased proliferation compared to controls. Thus, CTSL inhibition could represent a novel strategy to induce radiosensitivity in specific types of breast tumors.

To confirm that inhibition of CTSL mediated degradation of 53BP1 is responsible for the increase in chromosomal aberrations after irradiation, we analyzed metaphase spreads for genomic instability in BOGA cells depleted of CTSL. Similarly to cells in which CTSL is inhibited, CTSL depleted BOGA cells showed a marked increase in chromosomal aberrations after irradiation when compared to cells depleted of either BRCA1 or CTSL alone (**Figure 2-14A**). Furthermore, we determined if the effect of vitamin D increasing genomic instability after irradiation in BOGA cells is mediated by 53BP1 by monitoring chromosomal aberrations in cells doubly depleted of BRCA1 and 53BP1. If stabilization of 53BP1 is responsible for the increase in genomic instability after vitamin D treatment, we would expect that loss of 53BP1 blocks vitamin D's effect on inducing genomic instability. In 53BP1/BRCA1 doubly depleted cells the combination of vitamin D and ionizing radiation does not result in such profound genomic instability (**Figure 2-14B**) as that observed when BOGA cells are treated with vitamin D (**Figure 2-13A**).

A

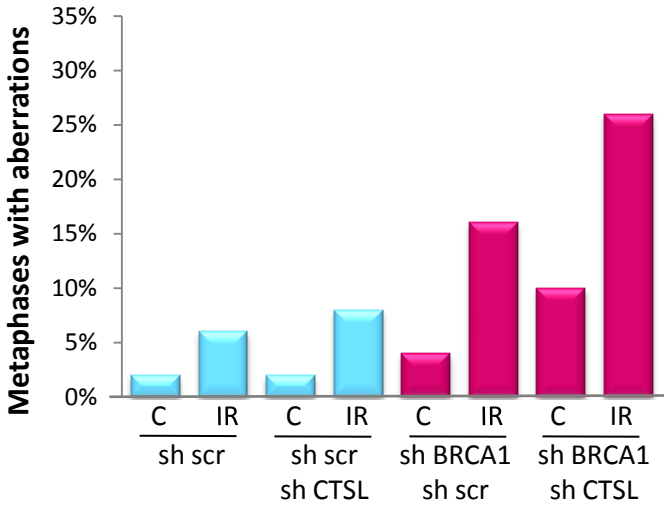

B

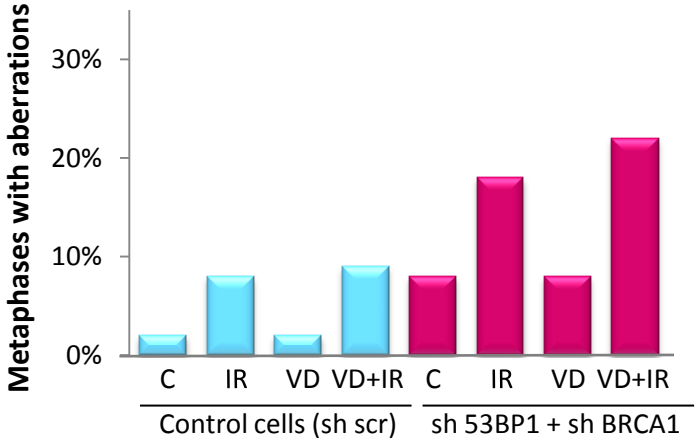

Figure 2-14. Chromosomal aberrations in response to IR. **(A)** BOGA cells transduced with a shRNA control (sh scr) or a sh RNA for CTSL were irradiated with 2 Gy and the percentage of cells with aberrant metaphases was quantified 24 hr. post-IR. A total of 400 metaphases were analyzed (50 per condition). **(B)** MCF7 cells depleted of 53BP1 and BRCA1 (sh 53BP1 + sh BRCA1) were treated with vitamin D or vehicle 24 hr. prior to IR, and the percentage of metaphases with aberrant chromosomes were quantitated. A total of 400 metaphases were analyzed (50 per condition).

These results demonstrate that vitamin D exerts its effect in part by stabilizing 53BP1levels and that the extent of CTSL mediated degradation of 53BP1 is a key determinant of the ability of BRCA1-deficient cells to deal with the DNA damage generated by irradiation and putatively other genotoxic agents.

Cells deficient in HR, such as BRCA1-deficient or mutated cells, are exquisitely sensitive to PARP inhibitors (Bryant et al. 2005; Drew et al. 2011; Farmer et al. 2005). PARP inhibitors block a key step in repair of single stranded DNA breaks. When single strand breaks are unrepaired they become double strand breaks, which are repaired by HR. Importantly, previous studies demonstrated that loss of 53BP1 allows cells to overcome the BRCA1-deficient phenotype and that these cells are resistant to PARP inhibitor treatment (Aly and Ganesan 2011; Bunting et al. 2010). We assessed whether stabilization of 53BP1 in BOGA cells would increase the extent of genomic instability induced by the PARP inhibitor EB-47. **Figure 2-15** shows that treatment of BOGA cells with the PARP inhibitor does not result in genomic instability, in agreement with the resistance of cells double deficient in 53BP1 and BRCA1 to this treatment. Interestingly, stabilization of 53BP1 via CTSL inhibition by vitamin D increases the extent of chromosomal aberrations in response to the PARP inhibitor. These data suggest that inhibition of CTSL mediated

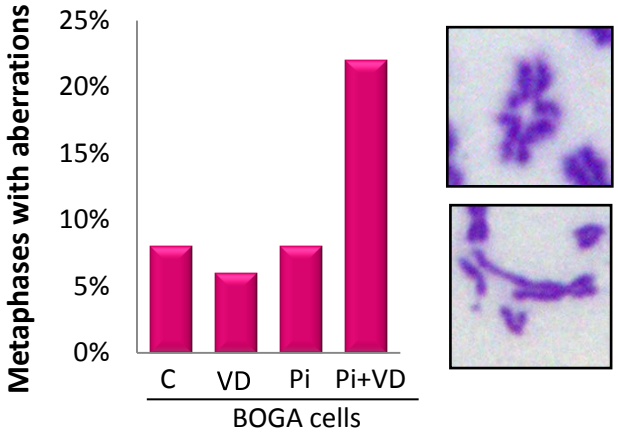

Figure 2-15. Chromosomal aberrations in response to PARP inhibitors. BOGA cells were treated with vitamin D (10^{-7} M) 24 hr. prior to treatment with the PARPi EB-47 (Pi, 1.2 µg/mL) for an additional 48 hr. Graph shows the percentage of metaphases with chromosomal aberrations. Images show the types of chromosomal aberrations observed. A total of 400 metaphases were analyzed (100 per condition).

degradation of 53BP1 could induce PARP inhibitor sensitivity.

2.5 Discussion and future experiments

Triple-negative and BRCA1-mutated cancers are among the most aggressive and difficult to treat. Given that these tumors often exhibit defects in HR, exploiting the lack of HR capabilities through treatment with DNA damaging agents such as PARP inhibitors, has emerged as a promising treatment strategy for these cancers (Foulkes, I. E. Smith, and Reis-Filho 2010). However, many of these tumors become mutated to gain HR functionality or acquire it through other means (Ashworth 2008; Swisher et al. 2008). Recent studies have shown that 53BP1 loss allows BRCA1-deficient cells to re-gain HR functionality and render the cells resistant to PARPi and other DNA damaging strategies (Bouwman et al. 2010; Bunting et al. 2010; L. Cao et al. 2009). Thus, stabilizing 53BP1 levels represents a promising new strategy for treatment of these cancers. However, prior to this study, no information was available about how 53BP1 levels are downregulated in breast cancer cells.

Here, we show that CTSL is upregulated following BRCA1 loss in human breast cancer cells, and that CTSL is responsible for lowering 53BP1 protein levels, which in turn allows the bypass of the characteristic growth arrest upon loss of BRCA1 function. Since previous studies in our laboratory have implicated the proteasome in degradation of 53BP1 (Gonzalez-Suarez et al. 2011), it is possible that other mechanisms contribute to the loss of 53BP1 in BRCA1-deficient cells. In addition, a previous study had shown that 53BP1 mRNA levels are downregulated in BRCA1-associated tumors and TNBC, which could represent another mechanism for 53BP1 regulation (Bouwman et al. 2010). Here, we provide clear evidence that depletion or inhibition of CTSL activity stabilizes 53BP1 protein levels and induces genomic

instability in BRCA1-deficient cancer cells after treatment with IR or PARPi. Thus, inhibition of this pathway via treatment with vitamin D or cathepsin inhibitors could provide a new therapeutic strategy for breast cancer.

CTSL upregulation upon loss of BRCA1

In this study, we show that CTSL is transcriptionally upregulated upon loss of BRCA1 to raise 53BP1 levels and overcome the growth arrest. Given that BRCA1 has been implicated in a whole host of cellular processes including transcriptional regulation, maintenance of heterochromatin, regulation of DNA methylation, and miRNA biogenesis, and that little is known about how CTSL is regulated in the cell, many questions remain to be answered about how BRCA1 loss leads to CTSL upregulation. BRCA1 has been copurified with the RNA polymerase II holoenzyme complex (Anderson et al. 1998), indicating that BRCA1 is a component of the core transcriptional machinery. BRCA1 has also been shown to associate with and stimulate p53 transcription (H. Zhang et al. 1998) which has implications for regulating the cell cycle and DNA repair.

However, in our study the activation of CTSL upon loss of BRCA1 can take upwards of two weeks to occur, indicating that CTSL is not likely to be a direct transcriptional target of BRCA1. Rather, we speculate that loss of BRCA1 might result in alterations in chromatin structure that make the CTSL gene more permissive to transcriptional activation over time. BRCA1 has been shown to interact with the histone deacetylases HDAC1 and HDAC2 (Yarden and Brody 1999) and with the BRG1 subunit of the chromatin remodeling SWI/SNF complex (Bochar et al. 2000). Other studies have shown that BRCA1 maintains heterochromatin structure through ubiquitylation of histone H2A (Zhu et al. 2011) and that loss of BRCA1 function leads

to global DNA hypomethylation and an open chromatin configuration through its regulation of DNMT1 (Shukla et al. 2010). All of these studies suggest that alterations of BRCA1 levels could have an effect on the chromatin structure of the CTSL gene promoter. Chromatin immunoprecipitation (ChIP) analyses need to be performed on the CTSL promoter to identify changes in chromatin marks or to detect binding of chromatin-modifying factors that could explain the transcriptional upregulation of the gene. The effect that loss of BRCA1 has on CTSL promoter activity can also be measured using a luciferase reporter construct (Bakhshi et al. 2001) and promoter mutants can be made to determine which domains of the CTSL promoter are important for its upregulation.

Currently, there is very little information about how the levels of CTSL are regulated in the cell. There is ample evidence, however, that activation of Ras leads to increased expression of cysteine proteases of the cathepsin family, including CTSL. This has been shown *in vitro* in mouse fibroblasts (Chambers et al. 1992; Denhardt et al. 1987), mouse melanocytes (Donatien et al. 1996), and human breast epithelial cells (Lah et al. 1995). As Ras is frequently mutated in human cancers, it is no surprise that increased cathepsin L levels are often observed in cancer (Chauhan, Goldstein, and Gottesman 1991; Collette et al. 2004). Experiments can be performed to determine if Ras or any of its downstream effectors are activated upon loss of BRCA1 in breast tumor cells and if overexpression of Ras activates CTSL mediated degradation of 53BP1, which would reveal a novel role for Ras in the regulation of a key DNA repair factor. Experiments can also be performed to determine if inhibition of Ras using farnesyltransferase inhibitors can block CTSL mediated degradation of 53BP1. There is also evidence that the transcription factor STAT3 regulates CTSL mRNA and protein levels (Kreuzaler et al. 2011), an avenue that can also be studied. Lastly, it remains to be determined whether CTSL-mediated

degradation of 53BP1 is activated in different subtypes of breast cancer.

Another interesting question that arises from this study relates to the similar phenotypes observed upon loss of BRCA1 as with loss of A-type lamins. When BRCA1 or A-type lamins are depleted, CTSL is transcriptionally upregulated, leading to degradation of 53BP1. Interestingly, our previous studies demonstrated that loss of A-type lamins results in downregulation of BRCA1 at the transcriptional level. Thus, it is possible that downregulation of BRCA1 is behind the activation of CTSL-mediated degradation of 53BP1 in lamins-deficient cells, a hypothesis that remains to be tested. If this were the case, we would expect that downregulation of 53BP1 and BRCA1 via depletion of A-type lamins would contribute to bypass the growth arrest that accompanies the loss of BRCA1. In addition, reconstitution of BRCA1 into lamins-deficient cells could restore the levels of 53BP1, demonstrating a novel functional interplay between DNA repair factors and lamins. Characterizing the relationship between these proteins could have a great impact on our understanding of molecular mechanisms of cancer and laminopathies.

Vitamin D and cathepsin inhibitors can modulate DNA repair pathway choice

In this study, we uncover an unprecedented role for vitamin D and cathepsin inhibitors in the regulation of DNA double strand break repair pathway choice. By stabilizing 53BP1 levels in BRCA1-deficient cells, we show that DNA repair is shifted towards NHEJ and HR is inhibited, leading to genomic instability and reduced proliferation when cells are challenged with DNA damaging agents such as irradiation or PARP inhibitors. We believe that the upregulation of CTSL upon loss of BRCA1 leads to an increase in nuclear CTSL similar to the increase in nuclear CTSL observed upon loss of A-type lamins (Gonzalez-Suarez et al. 2011). However, it is

unclear whether this nuclear CTSL is degrading 53BP1 in the nucleus or is somehow targeting the protein for nuclear export to be degraded in the cytoplasm.

Detecting an increase in nuclear CTSL levels in BOGA cells has been an active area of research in the laboratory. We have recently had success in detecting nuclear cathepsin L by performing immunohistochemistry in MCF7 cells embedded in paraffin blocks. **Figure 2-16** shows that BOGA cells have more nuclei stained with cathepsin L and that the staining is more intense compared to control cells. As expected, 53BP1 levels are clearly reduced in BOGA cells.

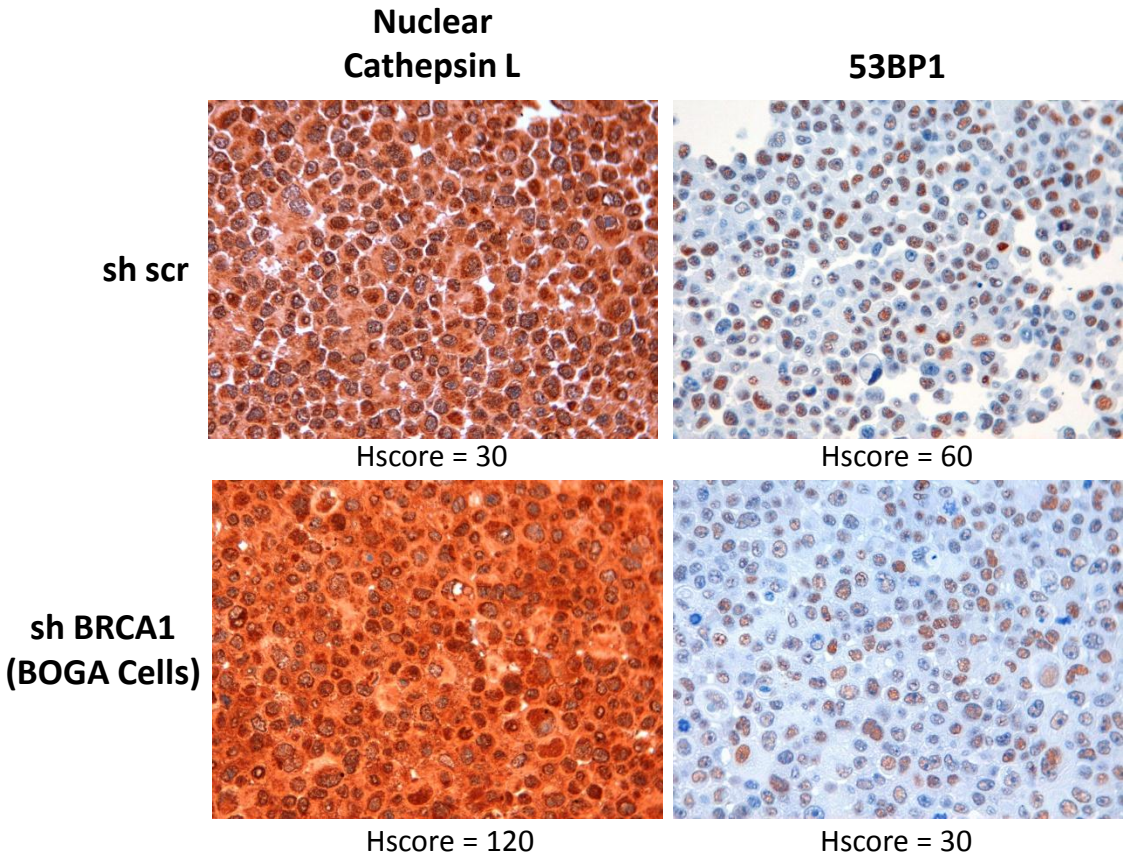

Figure 2-16. High nuclear CTSL and low 53BP1 in BOGA cells. Immunohistochemistry of control (sh scr) and BRCA1 depleted (sh BRCA1) MCF7 cells embedded in paraffin blocks was performed using antibodies recognizing CTSL and 53BP1. Note that BOGA cells have increased nuclear CTSL staining and lower 53BP1. Histochemical scores (Hscore) are indicated below each micrograph.

The histochemical scores (Hscore), which are a semi-quantitative measurement of immunohistochemical staining that takes into account the percentage of positive cells and intensity of the stain, are indicated below each micrograph. We have also shown that nuclear CTSL is upregulated in triple-negative and BRCA1-mutated tumors by immunohistochemistry (see Chapter 3). We have also attempted subcellular fractionation experiments to measure CTSL in the nucleus by western blot, but these experiments have been unsuccessful, possibly due to the levels being too low to be detected in these cells. We have also attempted to construct a cathepsin L species lacking the signal peptide which excludes it from the endoplasmic reticulum and that has been previously shown to be targeted to the nucleus (Goulet et al. 2004), but following transduction of the plasmid the cells died, possibly due to toxicity from too much CTSL in the nucleus.

Altogether, the ability to impact on the choice of DNA repair pathway could have profound consequences for cancer therapy. In tumor cells that activate CTSL-mediated degradation of 53BP1 as a means to ensure survival, cathepsin inhibition could stabilize 53BP1, increase genomic instability, and induce growth arrest and/or cell death, especially in combination with irradiation or PARPi. Thus, treatment with vitamin D or CTSL inhibitors could represent a new therapeutic strategy for specific types of breast cancer.

CTSL regulation of BRCA1 and 53BP1 levels during the cell cycle

This study shows that in cells that are growth arrested by depletion of BRCA1, CTSL levels are upregulated to degrade 53BP1. We were interested in determining if cells that are growth arrested by other means also activate cathepsin L-mediated degradation of 53BP1. We found that growth arresting MCF7 cells in G0/G1 by serum deprivation leads to decreased levels

of BRCA1, upregulation of CTSL, and downregulation of 53BP1 (**Figure 2-17)**.

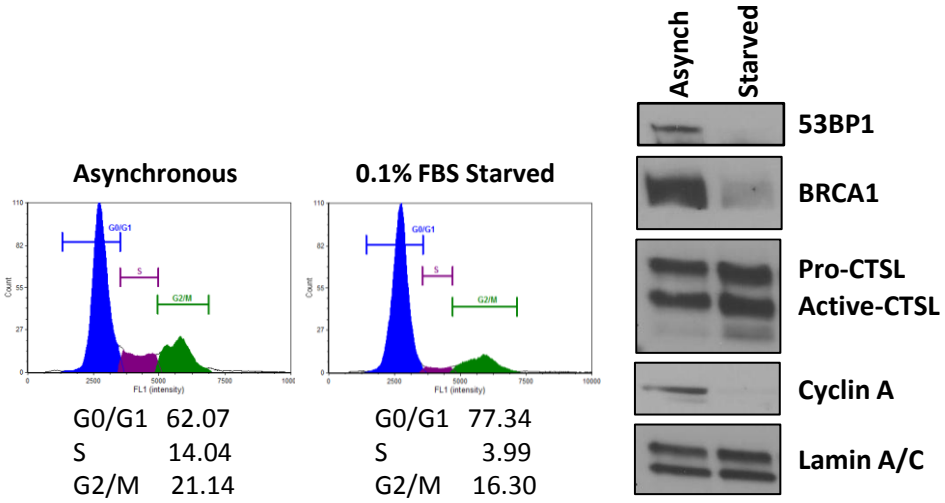

Figure 2-17. Growth arrest by serum starvation leads to increased CTSL and decreased 53BP1 and BRCA1 levels. The cell cycle profiles of MCF7 cells growing asynchronously or growth arrested for 48 hours by serum deprivation were analyzed by propidium iodide staining (left panels). Western blots show increased CTSL levels and decreased 53BP1 and BRCA1 levels (right panel). (Representative experiment of three biological repeats).

While it is known that BRCA1 levels are low during the G0/G1 phases of the cell cycle (W. Liu et al. 2010), we show here that levels of 53BP1 are also low in growth arrested cells. These data suggest a functional relationship during the cell cycle where BRCA1 might regulate CTSL mediated degradation of 53BP1, and that the growth arrest induced by BRCA1 depletion itself could contribute to the activation of CTSL-mediated degradation of 53BP1. Future experiments involving growth arrest by different means and depletion or inhibition of cathepsin L during growth arrest will be necessary to determine if CTSL regulates 53BP1 and BRCA1 during the cell cycle. Intriguingly, we also have preliminary evidence that upregulation of cathepsin L could trigger a feedback mechanism that lowers BRCA1 protein levels (experiments are ongoing). This

is supported by studies showing that BRCA1 is a target for degradation by cathepsins, though the specific cathepsin was not identified (Blagosklonny et al. 1999).

2.6 References

Alvarez-Díaz, Silvia et al. 2009. "Cystatin D is a candidate tumor suppressor gene induced by vitamin D in human colon cancer cells." *The Journal of clinical investigation* 119(8):2343–58. Retrieved October 22, 2012 (http://www.pubmedcentral.nih.gov/articlerender.fcgi?artid=2719930&tool=pmcentrez&rendertype=abstract).

Aly, Amal, and Shridar Ganesan. 2011. "BRCA1, PARP, and 53BP1: conditional synthetic lethality and synthetic viability." *Journal of molecular cell biology* 3(1):66–74. Retrieved July 26, 2012 (http://www.pubmedcentral.nih.gov/articlerender.fcgi?artid=3030974&tool=pmcentrez&rendertype=abstract).

Anderson, S F, B P Schlegel, T Nakajima, E S Wolpin, and J D Parvin. 1998. "BRCA1 protein is linked to the RNA polymerase II holoenzyme complex via RNA helicase A." *Nature genetics* 19(3):254–6. Retrieved November 20, 2012 (http://www.ncbi.nlm.nih.gov/pubmed/9662397).

Ashworth, Alan. 2008. "Drug resistance caused by reversion mutation." *Cancer research* 68(24):10021–3. Retrieved November 14, 2012 (http://www.ncbi.nlm.nih.gov/pubmed/19074863).

Bakhshi, R, A Goel, P Seth, P Chhikara, and S S Chauhan. 2001. "Cloning and characterization of human cathepsin L promoter." *Gene* 275(1):93–101. Retrieved November 20, 2012 (http://www.ncbi.nlm.nih.gov/pubmed/11574156).

Bhattacharyya, A, U S Ear, B H Koller, R R Weichselbaum, and D K Bishop. 2000. "The breast cancer susceptibility gene BRCA1 is required for subnuclear assembly of Rad51 and survival following treatment with the DNA cross-linking agent cisplatin." *The Journal of biological chemistry* 275(31):23899–903. Retrieved October 18, 2012 (http://www.ncbi.nlm.nih.gov/pubmed/10843985).

Blagosklonny, M V et al. 1999. "Regulation of BRCA1 by protein degradation." *Oncogene* 18(47):6460–8. Retrieved (http://www.ncbi.nlm.nih.gov/pubmed/10597248).

Bochar, D A et al. 2000. "BRCA1 is associated with a human SWI/SNF-related complex: linking chromatin remodeling to breast cancer." *Cell* 102(2):257–65. Retrieved November 20, 2012 (http://www.ncbi.nlm.nih.gov/pubmed/10943845).

Bouwman, Peter et al. 2010. "53BP1 loss rescues BRCA1 deficiency and is associated with triple-negative and BRCA-mutated breast cancers." *Nature structural & molecular biology* 17(6):688–95. Retrieved July 31, 2012 (http://www.pubmedcentral.nih.gov/articlerender.fcgi?artid=2912507&tool=pmcentrez&rendertype=abstract).

Brooks, S C, E R Locke, and H D Soule. 1973. “Estrogen receptor in a human cell line (MCF-7) from breast carcinoma.” *The Journal of biological chemistry* 248(17):6251–3. Retrieved October 18, 2012 (http://www.ncbi.nlm.nih.gov/pubmed/4353636).

Bryant, Helen E et al. 2005. “Specific killing of BRCA2-deficient tumours with inhibitors of poly(ADP-ribose) polymerase.” *Nature* 434(7035):913–7. Retrieved October 19, 2012 (http://www.ncbi.nlm.nih.gov/pubmed/15829966).

Bunting, Samuel F et al. 2010. “53BP1 inhibits homologous recombination in Brca1-deficient cells by blocking resection of DNA breaks.” *Cell* 141(2):243–54. Retrieved July 12, 2012 (http://www.pubmedcentral.nih.gov/articlerender.fcgi?artid=2857570&tool=pmcentrez&rendertype=abstract).

Cao, Liu et al. 2009. “A selective requirement for 53BP1 in the biological response to genomic instability induced by Brca1 deficiency.” *Molecular cell* 35(4):534–41. Retrieved October 18, 2012 (http://www.pubmedcentral.nih.gov/articlerender.fcgi?artid=3392030&tool=pmcentrez&rendertype=abstract).

Chambers, A F, R Colella, D T Denhardt, and S M Wilson. 1992. “Increased expression of cathepsins L and B and decreased activity of their inhibitors in metastatic, ras-transformed NIH 3T3 cells.” *Molecular carcinogenesis* 5(3):238–45. Retrieved November 20, 2012 (http://www.ncbi.nlm.nih.gov/pubmed/1586450).

Chauhan, S S, L J Goldstein, and M M Gottesman. 1991. “Expression of cathepsin L in human tumors.” *Cancer research* 51(5):1478–81. Retrieved November 20, 2012 (http://www.ncbi.nlm.nih.gov/pubmed/1997186).

Collette, John, Aylin S Ulku, Channing J Der, Anta’Sha Jones, and Ann H Erickson. 2004. “Enhanced cathepsin L expression is mediated by different Ras effector pathways in fibroblasts and epithelial cells.” *International journal of cancer. Journal international du cancer* 112(2):190–9. Retrieved November 20, 2012 (http://www.ncbi.nlm.nih.gov/pubmed/15352030).

Denhardt, D T, A H Greenberg, S E Egan, R T Hamilton, and J A Wright. 1987. “Cysteine proteinase cathepsin L expression correlates closely with the metastatic potential of H-ras-transformed murine fibroblasts.” *Oncogene* 2(1):55–9. Retrieved November 20, 2012 (http://www.ncbi.nlm.nih.gov/pubmed/3438085).

Donatien, P D, S L Diment, R E Boissy, and S J Orlow. 1996. “Melanosomal and lysosomal alterations in murine melanocytes following transfection with the v-rasHa oncogene.” *International journal of cancer. Journal international du cancer* 66(4):557–63. Retrieved November 20, 2012 (http://www.ncbi.nlm.nih.gov/pubmed/8635874).

Drew, Yvette et al. 2011. “Therapeutic potential of poly(ADP-ribose) polymerase inhibitor AG014699 in human cancers with mutated or methylated BRCA1 or BRCA2.” *Journal of*

the National Cancer Institute 103(4):334–46. Retrieved October 6, 2012 (http://www.ncbi.nlm.nih.gov/pubmed/21183737).

Farmer, Hannah et al. 2005. "Targeting the DNA repair defect in BRCA mutant cells as a therapeutic strategy." *Nature* 434(7035):917–21. Retrieved (http://www.ncbi.nlm.nih.gov/pubmed/15829967).

Foulkes, William D, Ian E Smith, and Jorge S Reis-Filho. 2010. "Triple-negative breast cancer." *The New England journal of medicine* 363(20):1938–48. Retrieved November 20, 2012 (http://www.ncbi.nlm.nih.gov/pubmed/21067385).

Gonzalez-Suarez, Ignacio et al. 2011. "A new pathway that regulates 53BP1 stability implicates cathepsin L and vitamin D in DNA repair." *The EMBO journal* 30(16):3383–96. Retrieved July 13, 2012 (http://www.ncbi.nlm.nih.gov/pubmed/21750527).

Goulet, Brigitte et al. 2004. "A cathepsin L isoform that is devoid of a signal peptide localizes to the nucleus in S phase and processes the CDP/Cux transcription factor." *Molecular cell* 14(2):207–19. Retrieved (http://www.ncbi.nlm.nih.gov/pubmed/15099520).

Iliakis, G et al. 2004. "Mechanisms of DNA double strand break repair and chromosome aberration formation." *Cytogenetic and genome research* 104(1-4):14–20. Retrieved October 19, 2012 (http://www.ncbi.nlm.nih.gov/pubmed/15162010).

Kreuzaler, Peter A et al. 2011. "Stat3 controls lysosomal-mediated cell death in vivo." *Nature cell biology* 13(3):303–9. Retrieved November 20, 2012 (http://www.ncbi.nlm.nih.gov/pubmed/21336304).

Lah, T T et al. 1995. "Cathepsins D, B and L in breast carcinoma and in transformed human breast epithelial cells (HBEC)." *Biological chemistry Hoppe-Seyler* 376(6):357–63. Retrieved November 20, 2012 (http://www.ncbi.nlm.nih.gov/pubmed/7576229).

Levenson, Anait S, and V Craig Jordan. 1997. "MCF-7 : The First Hormone-responsive Breast Cancer Cell Line MCF-7 : The First Hormone-responsive Breast Cancer Cell Line ’." 3071–3078.

Liu, Weijun et al. 2010. "Turnover of BRCA1 involves in radiation-induced apoptosis." *PloS one* 5(12):e14484. Retrieved November 20, 2012 (http://www.pubmedcentral.nih.gov/articlerender.fcgi?artid=3013096&tool=pmcentrez&rendertype=abstract).

Moynahan, M E, J W Chiu, B H Koller, and M Jasin. 1999. "Brca1 controls homology-directed DNA repair." *Molecular cell* 4(4):511–8. Retrieved October 18, 2012 (http://www.ncbi.nlm.nih.gov/pubmed/10549283).

Olive, Peggy L, Judit P Banáth, and Ralph E Durand. 2012. "Heterogeneity in radiation-induced DNA damage and repair in tumor and normal cells measured using the ‘comet’ assay.

1990.” *Radiation research* 178(2):AV35–42. Retrieved October 19, 2012 (http://www.ncbi.nlm.nih.gov/pubmed/22870978).

Redwood, Abena B, Ignacio Gonzalez-suarez, and Susana Gonzalo. 2011. “Regulating the levels of key factors in cell cycle and DNA repair: New pathways revealed by lamins.” 10(21):3652–3657.

Schlegel, Brian P, Francine M Jodelka, and Rafael Nunez. 2006. “BRCA1 promotes induction of ssDNA by ionizing radiation.” *Cancer research* 66(10):5181–9. Retrieved October 18, 2012 (http://www.ncbi.nlm.nih.gov/pubmed/16707442).

Scully, R, J Chen, A Plug, et al. 1997. “Association of BRCA1 with Rad51 in mitotic and meiotic cells.” *Cell* 88(2):265–75. Retrieved October 18, 2012 (http://www.ncbi.nlm.nih.gov/pubmed/9008167).

Scully, R, J Chen, R L Ochs, et al. 1997. “Dynamic changes of BRCA1 subnuclear location and phosphorylation state are initiated by DNA damage.” *Cell* 90(3):425–35. Retrieved October 18, 2012 (http://www.ncbi.nlm.nih.gov/pubmed/9267023).

Shukla, Vivek et al. 2010. “BRCA1 affects global DNA methylation through regulation of DNMT1.” *Cell research* 20(11):1201–15. Retrieved November 12, 2012 (http://www.ncbi.nlm.nih.gov/pubmed/20820192).

Snouwaert, J N et al. 1999. “BRCA1 deficient embryonic stem cells display a decreased homologous recombination frequency and an increased frequency of non-homologous recombination that is corrected by expression of a brca1 transgene.” *Oncogene* 18(55):7900–7. Retrieved October 18, 2012 (http://www.ncbi.nlm.nih.gov/pubmed/10630642).

Sung, Patrick, Lumir Krejci, Stephen Van Komen, and Michael G Sehorn. 2003. “Rad51 recombinase and recombination mediators.” *The Journal of biological chemistry* 278(44):42729–32. Retrieved October 18, 2012 (http://www.ncbi.nlm.nih.gov/pubmed/12912992).

Swisher, Elizabeth M et al. 2008. “Secondary BRCA1 mutations in BRCA1-mutated ovarian carcinomas with platinum resistance.” *Cancer research* 68(8):2581–6. Retrieved November 14, 2012 (http://www.pubmedcentral.nih.gov/articlerender.fcgi?artid=2674369&tool=pmcentrez&rendertype=abstract).

Tu, Zhigang et al. 2011. “Oncogenic RAS regulates BRIP1 expression to induce dissociation of BRCA1 from chromatin, inhibit DNA repair, and promote senescence.” *Developmental cell* 21(6):1077–91. Retrieved October 8, 2012 (http://www.ncbi.nlm.nih.gov/pubmed/22137763).

Yarden, R I, and L C Brody. 1999. “BRCA1 interacts with components of the histone deacetylase complex.” *Proceedings of the National Academy of Sciences of the United States of America* 96(9):4983–8. Retrieved November 20, 2012 (http://www.pubmedcentral.nih.gov/articlerender.fcgi?artid=21803&tool=pmcentrez&rendertype=abstract).

Zhang, H et al. 1998. “BRCA1 physically associates with p53 and stimulates its transcriptional activity.” *Oncogene* 16(13):1713–21. Retrieved November 20, 2012 (http://www.ncbi.nlm.nih.gov/pubmed/9582019).

Zhu, Quan et al. 2011. “BRCA1 tumour suppression occurs via heterochromatin-mediated silencing.” *Nature* 477(7363):179–84. Retrieved July 19, 2012 (http://www.pubmedcentral.nih.gov/articlerender.fcgi?artid=3240576&tool=pmcentrez&rendertype=abstract).

CHAPTER THREE

Discovery of nuclear CTSL, vitamin D receptor, and 53BP1 as a novel triple biomarker for triple-negative breast cancer and BRCA1-mutated tumors

3.1 Abstract

Triple-negative breast cancers (TNBC) are classified immunohistochemically by the absence of estrogen receptor, progesterone receptor, and HER2. This classification alone is not sufficient to determine the proper treatment course for women with this type of breast cancer, as there is evidence of great heterogeneity between triple-negative tumors and the efficacy of chemotherapy treatment varies widely between women with these kinds of tumors. Therefore, it is important to identify new markers for TNBC to stratify women into groups to determine a course of treatment that would be most beneficial. A previous study identified low levels of 53BP1 in TNBC (Bouwman et al., 2010). Loss of 53BP1 also renders BRCA1-deficient cells synthetically viable, and most BRCA1-mutated tumors are triple-negative. Given that we found that cathepsin L-mediated degradation of 53BP1 rescues genomic instability and growth arrest in BRCA1-deficient cells, we determined whether high CTSL could be a biomarker for sporadic TNBC and for breast tumors from patients carrying germline mutations in BRCA1, along with low levels of 53BP1. Indeed, we identify nuclear CTSL as a novel biomarker for TNBC and BRCA1-related tumors, which correlates inversely with 53BP1. Furthermore, since vitamin D inhibits CTSL and stabilizes 53BP1 *in vitro*, we determined the status of vitamin D receptor (VDR), which mediates most of vitamin D's functions in the cell. We found low nuclear levels of vitamin D receptor with low 53BP1 and high nuclear CTSL to be the most common signature in TNBC and BRCA1-mutated tumors, thus revealing a novel triple biomarker. Based on our *in* vitro data, we hypothesize that these patients could be treated with vitamin D or cathepsin inhibitors to raise 53BP1 levels and render tumors susceptible to PARPi treatment or other DNA damaging strategies. We also show that vitamin D treatment has an anti-proliferative effect on triple-negative breast tumor cells implanted in mice.

To note, the immunohistochemistry was carried out by Anna Novell and the statistical analysis was performed by Montserrat Martinez-Alonso in the laboratory of Xavier Matias-Guiu at the University of Lleida in Spain under the guidance of me, Adriana Dusso, and Susana Gonzalo. They did wonderful work and I am greatly thankful for their contributions to my thesis.

3.2 Increased levels of nuclear CTSL in TNBC and tumors from patients with BRCA1-germline mutations

We have uncovered that BRCA1-deficient cells upregulate CTSL to degrade 53BP1 and overcome genomic instability and growth arrest in human breast cancer cells in culture. Similarly to the BOGA cells, BRCA1-mutated and triple-negative tumors are able to proliferate and overcome genomic instability. Recent studies have demonstrated that loss of 53BP1 is more frequent in BRCA1-mutated and triple-negative tumors (Bouwman et al., 2010). Given our findings *in vitro*, we determined whether CTSL-mediated degradation of 53BP1 is activated in BRCA1-mutated and triple-negative tumors from human patients. Specifically, given that others have found CTSL to be present in the nucleus (Duncan et al., 2008; Goulet et al., 2004) and studies in our laboratory shown that upregulation of nuclear CTSL leads to the degradation of 53BP1 (Gonzalez-Suarez et al., 2011), we investigated whether high nuclear CTSL would correlate with low 53BP1 in triple-negative and BRCA-mutated tumors. In addition, given the inhibitory effect of vitamin D on this pathway, we monitored levels of nuclear VDR in these types of tumors.

We performed immunohistochemical (IHC) analyses of multitumor tissue microarrays (TMA) constructed with tissue from 249 patients with sporadic breast cancer (**Figure 3-1**) classified into four molecular subtypes: Luminal A, Luminal B, HER2, and triple-negative.

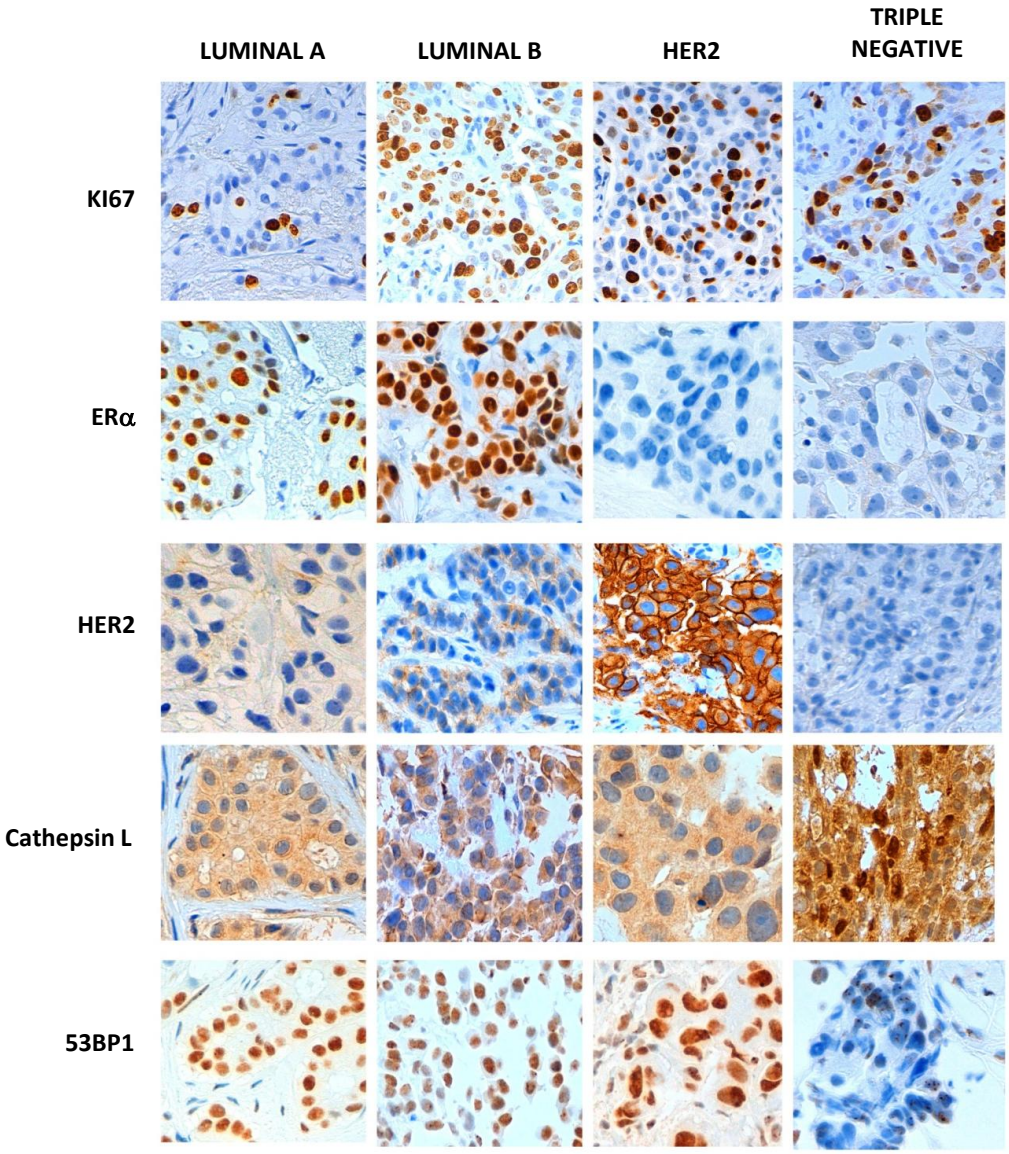

Figure 3-1. A new signature for subsets of TNBC patients. Immunohistochemical analysis was performed in breast tumor tissue microarrays from 249 patients which included four molecular subtypes: Luminal A, luminal B, HER2, and triple-negative. Representative images of IHC labeling with Ki67, ERα, HER2, CTSL, and 53BP1 are shown. Note that while cytoplasmic CTSL is observed in all tumor subtypes, nuclear CTSL is markedly upregulated in a subset of TNBC. In addition, TNBC tumors exhibit a marked decrease in 53BP1.

Luminal A tumors tend to be estrogen receptor positive and progesterone receptor positive, HER2/neu negative, and have the best prognosis out of the four molecular subtypes (Carey et al., 2006). Luminal B tumors tend to be positive for estrogen receptor, progesterone receptor, and Ki67. Luminal B tumors are usually diagnosed at a younger age than luminal A tumors, and have a slightly poorer prognosis than luminal A (Arvold et al., 2011; Voduc et al., 2010). HER2 tumors are positive for HER2/neu and negative for estrogen receptor and progesterone receptor. HER2 tumors have a poor prognosis and are prone to recurrence and metastasis (Arvold et al., 2011; Carey et al., 2006; Voduc et al., 2010). Triple-negative tumors have very poor prognosis and are characterized by the lack of estrogen receptor, progesterone receptor, and HER2/neu and most BRCA1-mutated tumors are triple-negative (Atchley et al., 2008; Carey et al., 2006; Hartman et al., 2012; Millar et al., 2009; Voduc et al., 2010).

Immunohistochemical scores (Hscores) for Ki67, ER, CTSL, 53BP1, and VDR provided and semi-quantitative measurement of their expression for each tumor subtype (Goulding et al., 1995; Pallares et al., 2009). Scores are generated by adding together 3 x % of strongly stained cells, 2 x % of moderately stained cells, and 1 x % of weakly stained cells, giving a possible range of 0 to 300. As shown in Figure, CTSL staining was both cytoplasmic and nuclear while 53BP1 staining was only nuclear. The immunohistochemical results are summarized in **Table 3-1**. Whereas cytoplasmic CTSL Hscores were similar in all tumor subtypes, nuclear CTSL Hscores were markedly enhanced in triple-negative tumors.

Proteins	Molecular Type	H score			Kruskal-Wallis test p-value
		Mean(SD)	Median [P25, P75]	Min-Max	
Cytoplasmic Cathepsin L	Luminal A	137 (36.6)	135 [110,160]	50-205	0.50
	Luminal B	134 (35.2)	130 [110,155]	75-230	
	Erbb2 $_{(-1)}$	141 (43.1)	135 [110,171]	50-230	
	Triple Negative $_{(-1)}$	145 (35.2)	140 [120,175]	80-200	
Nuclear Cathepsin L	Luminal A	8 (18.0)	0 [0, 0]	0-90	**<.0001**
	Luminal B	8 (14.9)	0 [0, 15]	0-75	
	Erbb2 $_{(-1)}$	9 (18.3)	0 [0, 5]	0-75	
	Triple Negative $_{(-1)}$	**42 (44.3)**	**30 [0, 83]**	**0-125**	
53BP1	Luminal A	155 (56.5)	160 [120, 200]	0-270	**0.0002**
	Luminal B	150 (45.8)	150 [120, 170]	40-280	
	Erbb2 $_{(-4)}$	154 (58.1)	150 [110, 200]	20-300	
	Triple Negative	**112 (44.4)**	**105 [80, 143]**	**0-190**	
Cytoplasmic VDR	Luminal A $_{(-4)}$	50 (50.9)	50 [0, 90]	0-185	0.22
	Luminal B $_{(-4)}$	52 (50.8)	50 [0, 80]	0-190	
	Erbb2 $_{(-2)}$	53 (48.8)	50 [0, 95]	0-160	
	Triple Negative $_{(-3)}$	69 (50.6)	50 [20, 110]	0-170	
Nuclear VDR	Luminal A $_{(-4)}$	121 (68.2)	110 [100, 170]	0-300	0.78
	Luminal B $_{(-4)}$	125 (65.2)	130 [90, 160]	0-300	
	Erbb2 $_{(-2)}$	122 (73.3)	125 [95, 160]	0-300	
	Triple Negative $_{(-3)}$	114 (62.3)	110 [80, 150]	0-270	

Table 3-1. Immunohistochemical analysis of CTSL, 53BP1 and VDR expression in sporadic human breast cancers. Values are Mean and Median Hscores for nuclear and/or cytosolic CTSL, 53BP1 and VDR per tumor molecular types. Dispersion is assessed by standard deviation (SD) and percentiles 25 and 75 ([P25,P75]); Min-Max denotes Minimal and Maximal Values within the tumor subtype. (-X) represents X missing values in antigen expression per molecular type due to insufficient specimen. Bolded Hscore values highlight the molecular subtype responsible for the statistical significant difference identified with the Kruskal-Wallis Test that compares all molecular types (highlighted by a bold p value in case of any significant difference among them).

In agreement with the *in vitro* findings, these high nuclear CTSL Hscores correspond with lower 53BP1 Hscores in TNBC compared to all other tumor types. Furthermore, we used the median nuclear Hscores for CTSL and 53BP1 of 0 and 150, respectively, as cut-off points with identical statistical power to confirm these significant differences in CTSL and 53BP1 expression among tumor types. Again, statistically significant differences were obtained, and TNBC emerged from this analysis as a remarkably different tumor subtype. **Table 3-2** shows that 60% of triple-negative tumors elicited Hscores of nuclear CTSL greater than 0, a frequency more than 2-fold higher than for any other molecular type (p=0.0013). Also, 75% of triple-negative tumors expressed 53BP1 Hscores below 150 compared to 40% of luminal A, 49% of luminal B, and

Proteins	Molecular Type	n (%)	Fisher exact test p-value
Nuclear Cathepsin L > 0	Luminal A	23 (23.2)	**0.0013**
	Luminal B	22 (31.9)	
	Erbb2 $_{(-1)}$	12 (27.3)	
	Triple Negative $_{(-1)}$	**21 (60.0)**	
53BP1 < 150	Luminal A	59 (59.6)	**0.0049**
	Luminal B	35 (50.7)	
	Erbb2 $_{(-4)}$	21 (51.2)	
	Triple Negative	**9 (25.0)**	
Nuclear VDR < 120	Luminal A	46 (48.4)	0.34
	Luminal B	40 (61.5)	
	Erbb2 $_{(-4)}$	25 (58.1)	
	Triple Negative	16 (48.5)	

Table 3-2. Frequency of CTSL, 53BP1 and VDR expression within molecular subtype relative to the median values in sporadic human breast cancers. Values denote the absolute (n) and the relative (%) frequencies of tumors with Hscore values above (nuclear CTSL) or below (nuclear 53BP1 and VDR) the median Hscore values for each protein in the overall population of sporadic breast cancer. Bolded Hscore values highlight the molecular subtype responsible for the statistical significant difference identified with the Fisher Exact Test that compares all molecular types (highlighted by a bold p value in case of any significant difference among them).

39% of HER2 tumors (p=0.0049). These data clearly show that higher expression of nuclear CTSL as well as lower 53BP1 is significantly more associated with TNBC than any other molecular subtype of breast cancer. Thus, we have identified nuclear CTSL as a novel biomarker for subsets of TNBC patients. Importantly, this new signature (high nuclear CTSL and low 53BP1) could serve to stratify TNBC patients.

Next, we analyzed breast tumors from patients with germline mutations in BRCA1 (n=18) or BRCA2 (n=14) for levels of nuclear CTSL and 53BP1 by IHC (**Table 3-3**). In concurrence with the subsample of sporadic TNBC, tumors from patients with BRCA1 germline mutations elicited the same high Hscores for nuclear CTSL (p=0.95) and low Hscores for 53BP1 (p=1). In contrast, tumors from patients with BRCA2 germline mutations had nuclear CTSL Hscores similar to those in all molecular subtypes of sporadic tumors and significantly lower than BRCA1 germline tumors. Accordingly, 53BP1 Hscores were higher in tumors from patients with BRCA2 germline mutations than in BRCA1-mutated tumors or all molecular subtypes of sporadic tumors. These results support our *in vitro* data for a role of CTSL in the degradation of 53BP1 in BRCA1-deficient cells. **Table 3-4** shows that a very high frequency of BRCA1-mutated tumors exhibit high nuclear CTSL, low 53BP1, and low nuclear VDR. Importantly, **Figure 3-2A** shows a statistically significant inverse linear correlation between Hscores for nuclear CTSL and 53BP1 in all tumor subtypes with a positive nuclear CTSL expression. However, a coefficient of determination of only 6.6% indicates that there is 93.4% of the variability in 53BP1 Hscores that cannot be accounted for by increases in nuclear CTSL. These results suggest that additional factors might contribute to CTSL-mediated degradation of 53BP1 in these tumors. Identifying these factors could help to discriminate subsets of patients in which this pathway is activated.

Proteins	Mutation Type	H score			M-W Test p-value (vs. Sporadics)	M-W Test p-value (BRCA1 vs. BRCA2)
		Mean (SD)	Median [P25, P75]	Min-Max		
Cytoplasmic Cathepsin L	BRCA1 mutation $_{(-4)}$	119 (34.2)	110 [100, 138]	60-190	0.0563	0.88
	BRCA2 mutation $_{(-1)}$	118 (46.2)	120 [100, 120]	100-150	**0.0437**	
Nuclear Cathepsin L	BRCA1 mutation $_{(-4)}$	38 (45.2)	30 [15, 45]	0-180	**0.0001**	**0.0494**
	BRCA2 mutation $_{(-1)}$	15 (22.7)	4 [0, 15]	0-75	0.19	
53BP1	BRCA1 mutation $_{(-1)}$	111 (28.4)	115 [100, 125]	70-175	**0.0016**	**0.0001**
	BRCA2 mutation $_{(-1)}$	198 (43.6)	210 [185, 220]	110-270	**0.0008**	
Cytoplasmic VDR	BRCA1 mutation	86 (38.5)	100 [50, 100]	0-150	**0.0048**	**0.0011**
	BRCA2 mutation $_{(-3)}$	145 (36.7)	150 [115, 165]	100-200	**<.0001**	
Nuclear VDR	BRCA1 mutation	66 (52.9)	53 [27, 100]	0-180	**0.0010**	**0.0001**
	BRCA2 mutation $_{(-3)}$	175 (57.8)	170 [135, 193]	110-300	**0.0074**	

Table 3-3. Immunohistochemical analysis of CTSL, 53BP1 and VDR expression in tumors from patients with BRCA1 or BRCA2 germline mutations. (A) Values are Mean and Median Hscores for nuclear and/or cytosolic CTSL, 53BP1 and VDR in tumors with BRCA1 or BRCA2 germline mutations. Dispersion is assessed by standard deviation (SD) and percentiles 25 and 75 ([P25,P75]); Min-Max denotes Minimal and Maximal Values within the tumor subtype. (-X) represents X missing values in antigen expression per molecular type due to insufficient specimen. Bolded Hscore values highlight the statistical significance of differences measured by Mann-Whitney test (M-W) between each tumor mutation subtype vs. the overall population of sporadic breast cancer (sporadics) or between tumors with BRCA1 vs. BRCA2 germline mutations (BRCA1 vs. 2). Significant differences are highlighted with bold p value.

Proteins	Mutation Type	n (%)	Fisher exact test p-value (vs. Sporadics)	Fisher exact test p-value (BRCA1 vs. BRCA2)
Nuclear Cathepsin L > 0	BRCA1 mutation $_{(-4)}$	12 (85.7)	**0.0001**	0.10
	BRCA2 mutation $_{(-1)}$	7 (53.8)	0.13	
53BP1 < 150	BRCA1 mutation $_{(-1)}$	2 (11.8)	**0.0019**	**0.0001**
	BRCA2 mutation $_{(-1)}$	11 (84.6)	**0.0210**	
Nuclear VDR < 120	BRCA1 mutation $_{(-1)}$	3 (16.7)	**0.0027**	**0.0051**
	BRCA2 mutation $_{(-1)}$	8 (72.7)	0.35	

Table 3-4. Frequency of nuclear CTSL, 53BP1 and VDR expression within BRCA1 and BRCA2-mutated tumors. Values denote the absolute (n) and the relative (%) frequencies of tumors with Hscore values above (nuclear CTSL) or below (nuclear 53BP1 and VDR) the median Hscore values for each protein in tumors with BRCA1 or BRCA2 germline mutations. Bolded Hscore values highlight the statistical significant difference measured by the bold p value from Fisher exact test comparing a molecular subtype with either the overall population of sporadic breast cancer (sporadics) or between tumors with BRCA1 vs. BRCA2 germline mutations (BRCA1 vs. 2).

Previous studies in human colon cancer cells showed a correlation between expression of vitamin D receptor and cystatin D, an inhibitor of several cathepsins including CTSL (Alvarez-Díaz et al., 2009), and upregulation of cystatin D by vitamin D. In addition, our *in vitro* data show that vitamin D inhibits CTSL-mediated degradation of 53BP1. Vitamin D requires a functional vitamin D receptor to exert its actions (Dusso, Brown, & Slatopolsky, 2005). Because VDR levels are reduced in several human cancers and the loss of BRCA1 causes defective VDR translocation to the nucleus in osteosarcoma cells (Deng et al., 2009), we hypothesized that there might be a threshold for nuclear VDR required to inhibit CTSL-mediated degradation of 53BP1, which in turn could explain the signature of tumors with high Hscores for both nuclear CTSL and 53BP1.

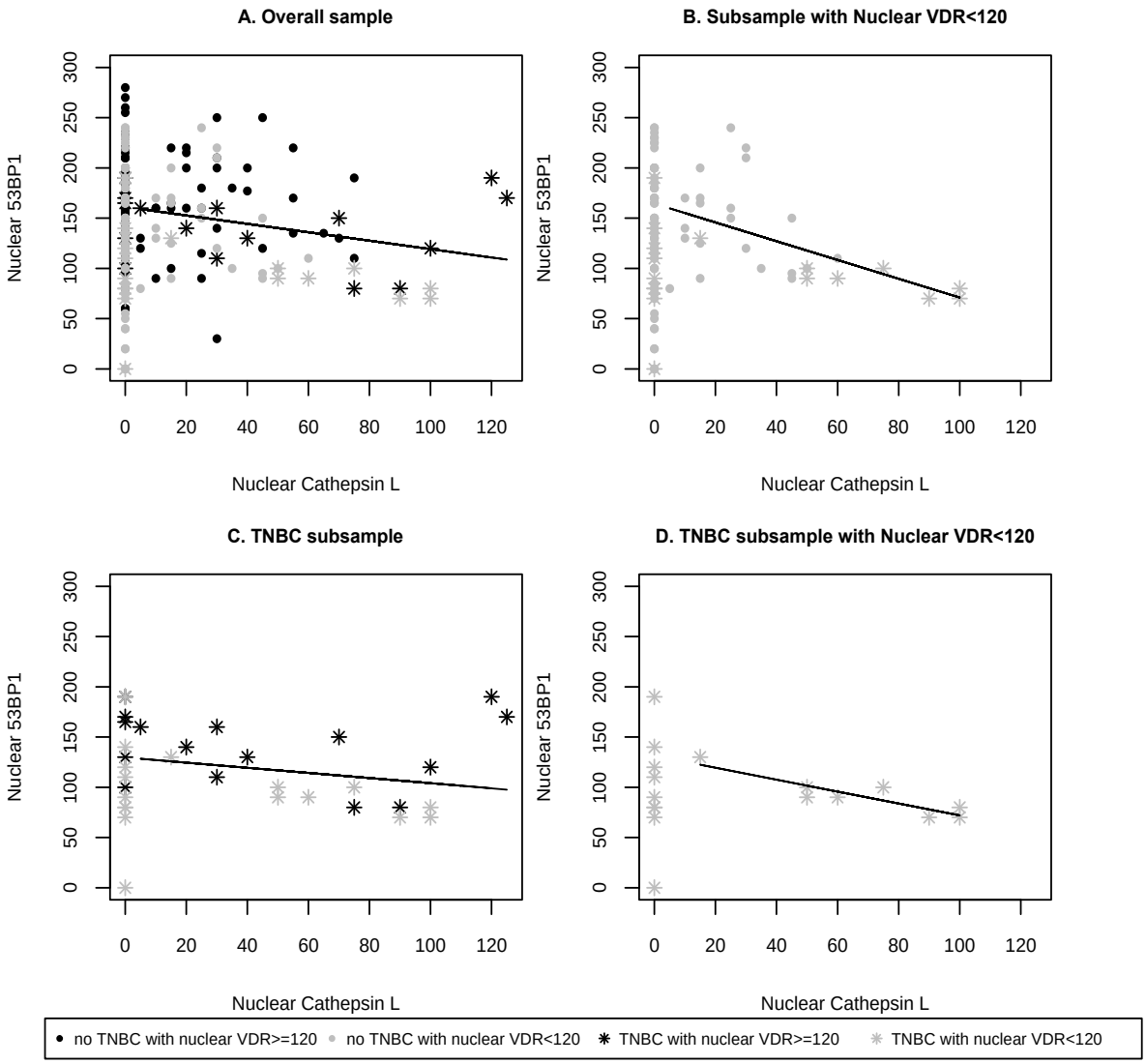

Figure 3-2. Nuclear 53BP1 expression correlates inversely with nuclear CTSL expression in sporadic human breast cancers. (A-D) Linear regression analysis between Hscores for nuclear 53BP1 and CTSL in sporadic breast cancer samples with Hscores for CTSL>0. Note the high variability in nuclear 53BP1 Hscores in tumors without nuclear CTSL. The linear regression analysis of the association between nuclear 53BP1 and CTSL depicted in panels **A** (Linear regression coefficient (r)= -0.42; p=0.02; coefficient of determination (r^2)= 6.6%) and **B** (r= -0.93 ; p=0.0025 ; r^2=29.2%) include Hscores from both TNBC and no TNBC tumors, while panels **C** (r= -0.255 ; p=0.294; r^2= 5.8) and **D** (r=-0.89; p=0.0027; r^2= 80.2%) depict TNBC only. Note the marked increase in % of the variability in nuclear 53BP1 levels that can be explained by changes in nuclear CTSL parameters of Panels B and D when only tumors with nuclear VDR Hscores < 120 are included in the regression analysis.

Our hypothesis is supported by the findings of a direct linear correlation between nuclear levels of VDR and 53BP1 for all 249 tumor types (Pearson Correlation r=0.238; p=0.0002). Analyzing the linear relationship for those tumors with nuclear VDR expression below the median Hscore of 120 obtained in the 249 sporadic tumors (**Figure 3-2B**), we find an increase in the slope of the linear regression of nuclear CTSL and 53BP1 Hscores (from -0.41 to -0.93) as well as an increased coefficient of determination (from 6.6% to 29.2%). Furthermore, when the correlation between 53BP1 and CTSL was examined exclusively in TNBC, the non-significant correlation depicted in **Figure 3-2C** becomes highly significant when only tumors with VDR less than 120 are examined ($p<0.0027$), as seen in **Figure 3-2D**, with a coefficient of determination of 80.2%. Indeed, the outliers in **Figure 3-2C** correspond to patients with VDR Hscores far above 120, which maintain high Hscores for nuclear 53BP1 despite Hscores for nuclear CTSL above 100 (**Figure 3-3**, top panels). **Figure 3-3** (lower panels) shows the most common biomarker signature found in TNBC and BRCA-mutated tumors. Furthermore, average nuclear Hscores for VDR are lower in tumors from patients with germline BRCA1 mutations compared to TNBC (66 vs. 114, with $p<0.009$) (**Tables 3-3 and 3-1**), suggesting that loss of BRCA1 may also impair VDR translocation to the nucleus in breast cancer. The cytosolic and nuclear VDR Hscores in BRCA2 germline mutations depicted in **Table 3-3** suggest that only BRCA1 mutations hinder VDR translocation to the nucleus allowing CTSL-mediated degradation of 53BP1.

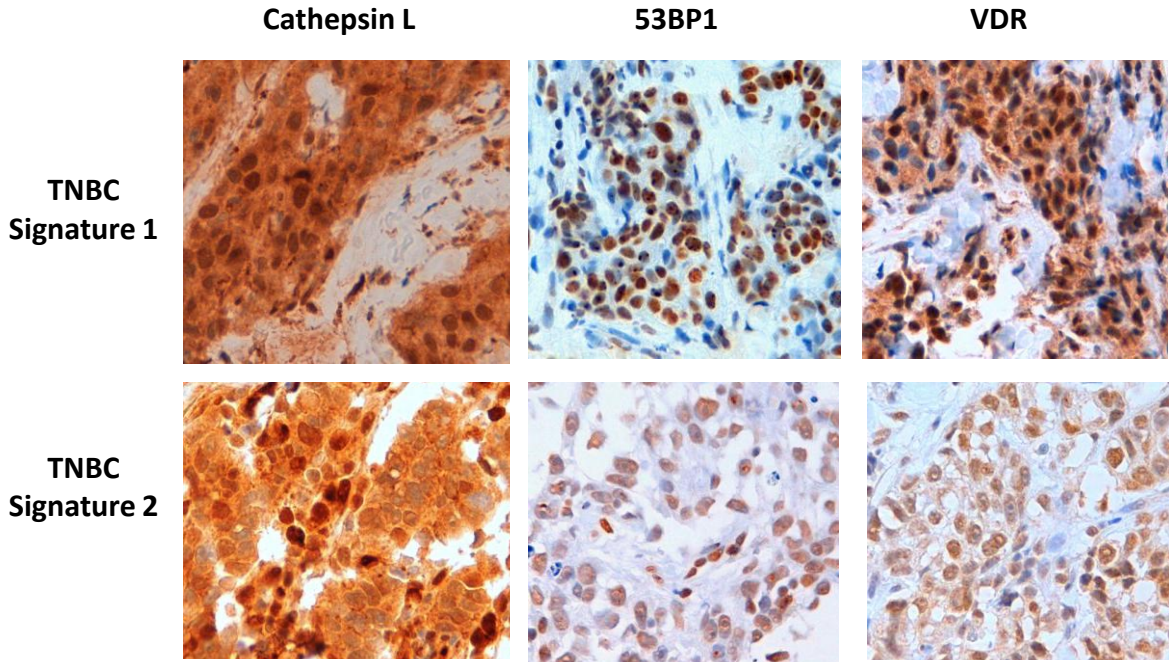

Figure 3-3. Common immunohistochemical signatures in TNBC. Images of immunohistochemical analysis results in TNBC patients. Two different signatures were observed in these patients (as well as in patients with BRCA1 germline mutations). Top panels show the signature of a few TNBC patients -high nuclear CTSL, 53BP1 and VDR-. Bottom panels show the most common signature in TNBC patients –high nuclear CTSL, low 53BP1 and low nuclear VDR-.

In summary, this study reveals a new triple biomarker signature – levels of nuclear VDR, CTSL, and 53BP1- for stratification of patients with TNBC (in which BRCA1 is frequently somatically altered) and tumors from patients with BRCA1 germline mutations. Based on our *in vitro* data, this signature could potentially be used as a predictor of the response of these specific tumors to DNA damaging therapeutic strategies such as radiation, crosslinking agents, and PARP inhibitors.

3.3 Vitamin D inhibits breast tumor cell growth *in vivo*

A main future goal for this study is to determine if this pathway can be exploited with therapeutic purposes using preclinical models. Triple-negative or BRCA1-deficient or mutated tumors can be implanted into mice and treated with vitamin D or cathepsin inhibitors to putatively reduce tumor growth by stabilizing 53BP1 levels. Vitamin D or cathepsin inhibitors can also be combined with radiation therapy or PARPi to increase sensitivity to the treatments. We have performed preliminary experiments both in culture and in mice using the 4T1 murine breast tumor cell line. The 4T1 cell line, isolated from a BALB/c mammary tumor, is highly malignant and can metastasize to lung, liver, lymph nodes, and brain (Aslakson & Miller, 1992; Miller, Miller, & Heppner, 1983). Importantly, 4T1 cells are similar to a triple-negative breast cancer cell line as they have low levels of estrogen receptor, progesterone receptor, and HER2 (Kau et al., 2012) and they also have high cathepsin activity (Ren et al., 2011) which could lead to low endogenous 53BP1 levels. Despite obtaining inconclusive results regarding the effect of vitamin D treatment on 53BP1 levels by

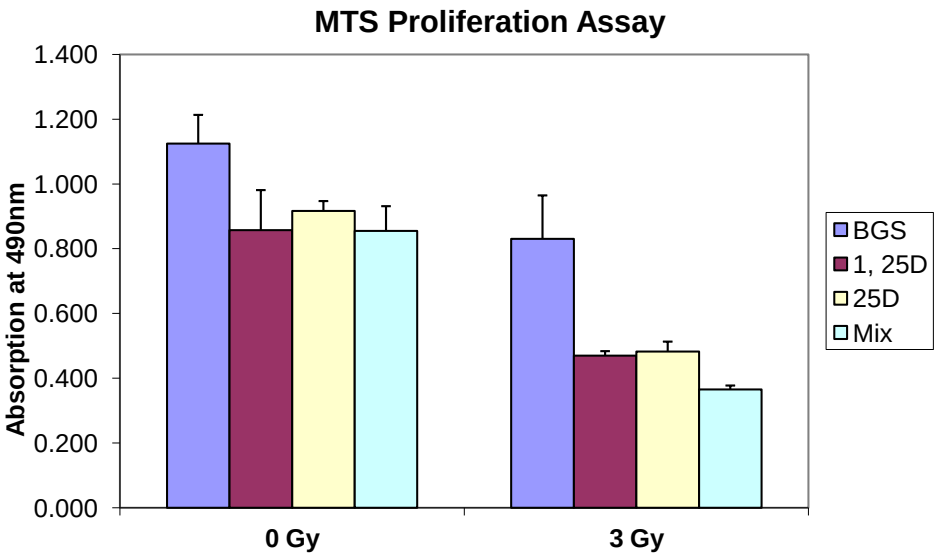

Figure 3-4. Vitamin D radiosensitizes 4T1 cells. Representative MTS assay showing proliferation of 4T1 cells after treatment with 3 modalities of vitamin D or a combination of vitamin D with ionizing radiation. Vitamin D alone has an antiproliferative effect that is exacerbated following irradiation indicating radiosensitization.

western blot in these cells (data not shown), we show that vitamin D treatment in culture has an antiproliferative effect (**Figure 3-4**). When cells are treated with 3 different forms of vitamin D, the active 1,25-dihydroxyvitamin D_3, the vitamin D precursor 25-hydroxyvitamin D, or a combination of both, proliferation is reduced as measured by MTS assay. Furthermore, when the 3 different vitamin D treatments are combined with ionizing radiation, the antiproliferative effect is enhanced (**Figure 3-4**), indicating that vitamin D is inducing radiosensitization in 4T1 cells.

To test if vitamin D can reduce tumor growth in mice, we injected 4T1 cells into the mammary fat pads of BALB/c mice. The mice were treated by intraperitoneal injection of either vehicle or a combination of active vitamin D and the precursor and tumor growth was monitored by caliper measurements. **Figure 3-5** shows that vitamin D treatment reduced tumor growth compared to mice treated with vehicle. These preliminary results provide a promising basis for future *in vivo* experiments to test if vitamin D and cathepsin inhibitors can be used to inhibit tumor growth as well as increase sensitivity to DNA damaging therapeutic strategies.

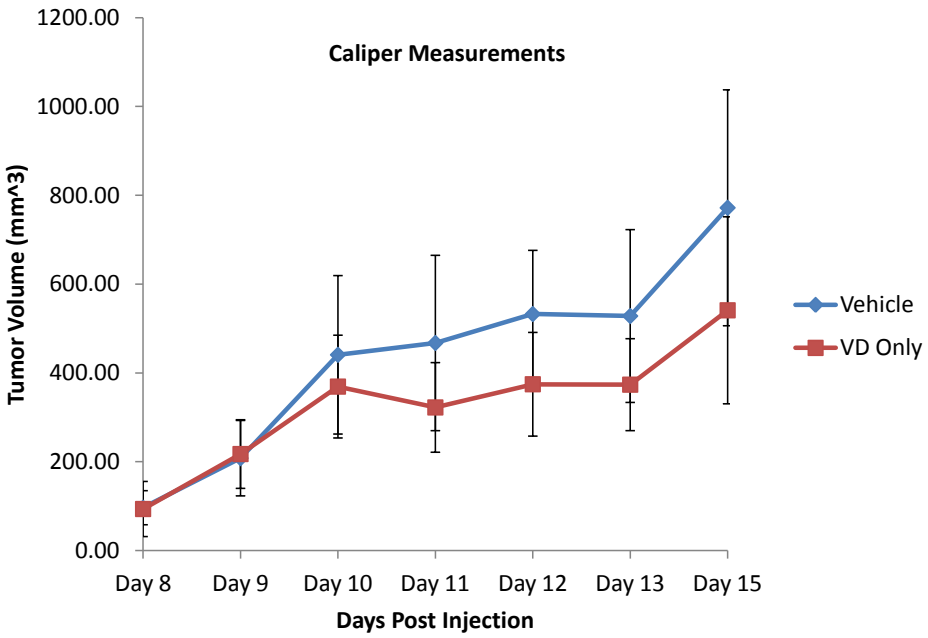

Figure 3-5. Vitamin D treatment reduces tumor growth *in vivo*. 4T1 cells were injected in to mammary fat pads of BALB/c mice and tumor growth was measured using calipers in mice that were treated or untreated with vitamin D.

3.4 Discussion and future experiments

The need to identify new biomarkers for diagnosis and predictive therapeutic outcome for cancer is of great importance. Tumors are grouped into categories based on immunohistochemical staining properties that are similar between a subset of tumors; however there is still great heterogeneity between individual tumors. Triple-negative breast cancers are defined by the lack of immunohistochemical staining of estrogen receptor, progesterone receptor, and HER2, but there are many other molecular mechanisms that affect the growth of these tumors and their response to treatment (Constantinidou, Jones, & Reis-Filho, 2010). BRCA1-related cancers are commonly triple-negative, and while these aggressive tumors have shown some positive response to new treatments such as PARP inhibitors, these strategies are not effective in all women. In this study, we identify novel biomarkers for sporadic TNBC and tumors from patients carrying germline mutations in BRCA1.

The analysis of breast tumor tissue microarrays (TMA) indicates that levels of nuclear CTSL represent a new positive biomarker for subsets of tumors, including TNBC and tumors arising in association with germline mutations in BRCA-1. Similarly, we find that nuclear VDR levels correlate linearly with 53BP1 content in all tumor subtypes, and the lowest nuclear VDR levels correspond to TNBC and tumors from patients with BRCA1 germline mutations. The finding of the strong negative correlation between reductions in nuclear 53BP1 with increases in nuclear CTSL levels (80% coefficient of determination) in TNBC with nuclear VDR<120 is very interesting, as TNBC is associated with severe vitamin D deficiency (Peppone et al., 2011). Furthermore, previous studies had shown a role for VDR in the upregulation of cathepsin inhibitors (Alvarez-Díaz et al., 2009). Thus, it is tempting to speculate that vitamin D

interventions could lead to VDR-induced expression of cystatins and the attenuation of CTSL-mediated degradation of 53BP1. Future studies testing this hypothesis might lead to new strategies of targeted therapy.

The combination of low nuclear VDR or high nuclear CTSL with low 53BP1 levels offers great potential for the stratification of BRCA1-deficient and TNBC patients into different subgroups and as a predictive biomarker for the response of these patients to current therapies. In particular, the use of PARPi as single agents or in combination with radiation or chemotherapy is a leading strategy for breast cancer management, especially for HR-deficient tumors (Drew et al., 2011; Farmer et al., 2005; Fong et al., 2009). However, a significant fraction of these cancers acquire resistance to PARPi. Recent studies in cell culture and mouse models demonstrated that loss of 53BP1 reduces the sensitivity of BRCA1-deficient cells to PARPi (Bunting et al., 2010).

Our study suggests that BRCA1-deficient and TNBC patients that exhibit low nuclear VDR, high nuclear CTSL and low 53BP1 levels are likely to be proficient in HR and resistant to PARPi. Therefore, these patients will not benefit from this specific treatment unless levels of 53BP1 are stabilized. For these patients, treatment with vitamin D or CTSL inhibitors to stabilize 53BP1 levels in combination with PARPi might result in the most effective therapy.

Future studies in the lab will focus on determining if vitamin D or cathepsin L inhibitor treatment is effective in preventing tumor growth. A preliminary study has indicated that vitamin D is able to slow the growth of 4T1 tumors. Vitamin D is known to have an antiproliferative effect, and while tumor inhibition with vitamin D treatment will always be a positive outcome, it will be important to use CTSL inhibitors to determine if the growth reduction is due to inhibition of CTSL-mediated degradation of 53BP1. Cathepsin inhibition would also be supplemented with

either PARP inhibitor treatment or irradiation. All tumors would be collected and subjected to immunohistochemistry to measure levels of nuclear CTSL, VDR, and 53BP1 to determine if the treatment outcome coincides with our hypothesis based on the tumor tissue microarray data and *in vitro* findings. There are several mouse models of tumorigenesis that can be used. An orthotopic model of breast cancer in mice can be used by injecting BOGA cells into mammary fat pads and monitoring tumor progression following different treatments. This model would be difficult with MCF7 cells, however, as they do not grow well in mice. The cell line MDA-MB-231, which is triple-negative and activates cathepsin L mediated degradation of 53BP1, would be a better candidate cell line for implantation into mice. Another mouse model of tumorigenesis that could be utilized to study the effect of vitamin D and cathepsin L inhibitors on tumor growth is the human-in-mouse model, in which pieces of tumors from patients are grown in mouse mammary fat pads (Kuperwasser et al., 2004). In this model, mammary fat pads of NOD/SCID mice are humanized by removing the mammary epithelium from the fat pads and replacing it with a mixture of irradiated and non-irradiated telomerase immortalized human mammary stromal fibroblasts. Two weeks later, human breast epithelial organoids and primary fibroblasts are injected into the humanized site to establish the tumor model. This model has already proved successful using triple-negative tumors (Ma et al., 2012).

Since BRCA1 knockout mice are embryonic lethal, BRCA1 conditional knockout mice have been used extensively to study tumorigenesis upon loss of BRCA1 in the mouse and are available for purchase (Xu et al., 1999). Conditional BRCA1 knockout mice that develop tumors can be treated with vitamin D or cathepsin L inhibitors to evaluate their efficacy in treatment. Finally, a BRCA1 conditional knockout mouse could be crossed to a cathepsin L knockout mouse to determine if complete loss of CTSL can prevent or slow tumor formation and

progression.

3.5 References

Alvarez-Díaz, S., Valle, N., García, J. M., Peña, C., Freije, J. M. P., Quesada, V., Astudillo, A., et al. (2009). Cystatin D is a candidate tumor suppressor gene induced by vitamin D in human colon cancer cells. *The Journal of clinical investigation*, *119*(8), 2343–58. Retrieved from http://www.pubmedcentral.nih.gov/articlerender.fcgi?artid=2719930&tool=pmcentrez&rendertype=abstract

Arvold, N. D., Taghian, A. G., Niemierko, A., Abi Raad, R. F., Sreedhara, M., Nguyen, P. L., Bellon, J. R., et al. (2011). Age, breast cancer subtype approximation, and local recurrence after breast-conserving therapy. *Journal of clinical oncology : official journal of the American Society of Clinical Oncology*, *29*(29), 3885–91. doi:10.1200/JCO.2011.36.1105

Aslakson, C. J., & Miller, F. R. (1992). Selective events in the metastatic process defined by analysis of the sequential dissemination of subpopulations of a mouse mammary tumor. *Cancer research*, *52*(6), 1399–405. Retrieved from http://www.ncbi.nlm.nih.gov/pubmed/1540948

Atchley, D. P., Albarracin, C. T., Lopez, A., Valero, V., Amos, C. I., Gonzalez-Angulo, A. M., Hortobagyi, G. N., et al. (2008). Clinical and pathologic characteristics of patients with BRCA-positive and BRCA-negative breast cancer. *Journal of clinical oncology : official journal of the American Society of Clinical Oncology*, *26*(26), 4282–8. doi:10.1200/JCO.2008.16.6231

Bouwman, P., Aly, A., Escandell, J. M., Pieterse, M., Bartkova, J., Van der Gulden, H., Hiddingh, S., et al. (2010). 53BP1 loss rescues BRCA1 deficiency and is associated with triple-negative and BRCA-mutated breast cancers. *Nature structural & molecular biology*, *17*(6), 688–95. doi:10.1038/nsmb.1831

Carey, L. A., Perou, C. M., Livasy, C. A., Dressler, L. G., Cowan, D., Conway, K., Karaca, G., et al. (2006). Race, breast cancer subtypes, and survival in the Carolina Breast Cancer Study. *JAMA : the journal of the American Medical Association*, *295*(21), 2492–502. doi:10.1001/jama.295.21.2492

Constantinidou, A., Jones, R. L., & Reis-Filho, J. S. (2010). Beyond triple-negative breast cancer: the need to define new subtypes. *Expert review of anticancer therapy*, *10*(8), 1197–213. doi:10.1586/era.10.50

Deng, C., Ueda, E., Chen, K. E., Bula, C., Norman, A. W., Luben, R. A., & Walker, A. M. (2009). Prolactin blocks nuclear translocation of VDR by regulating its interaction with BRCA1 in osteosarcoma cells. *Molecular endocrinology (Baltimore, Md.)*, *23*(2), 226–36. doi:10.1210/me.2008-0075

Drew, Y., Mulligan, E. a, Vong, W.-T., Thomas, H. D., Kahn, S., Kyle, S., Mukhopadhyay, A., et al. (2011). Therapeutic potential of poly(ADP-ribose) polymerase inhibitor AG014699 in

human cancers with mutated or methylated BRCA1 or BRCA2. *Journal of the National Cancer Institute*, *103*(4), 334–46. doi:10.1093/jnci/djq509

Duncan, E. M., Muratore-Schroeder, T. L., Cook, R. G., Garcia, B. a, Shabanowitz, J., Hunt, D. F., & Allis, C. D. (2008). Cathepsin L proteolytically processes histone H3 during mouse embryonic stem cell differentiation. *Cell*, *135*(2), 284–94. doi:10.1016/j.cell.2008.09.055

Dusso, A. S., Brown, A. J., & Slatopolsky, E. (2005). Vitamin D. *American journal of physiology. Renal physiology*, *289*(1), F8–28. doi:10.1152/ajprenal.00336.2004

Farmer, H., McCabe, N., Lord, C. J., Tutt, A. N. J., Johnson, D. a, Richardson, T. B., Santarosa, M., et al. (2005). Targeting the DNA repair defect in BRCA mutant cells as a therapeutic strategy. *Nature*, *434*(7035), 917–21. doi:10.1038/nature03445

Fong, P. C., Boss, D. S., Yap, T. A., Tutt, A., Wu, P., Mergui-Roelvink, M., Mortimer, P., et al. (2009). Inhibition of poly(ADP-ribose) polymerase in tumors from BRCA mutation carriers. *The New England journal of medicine*, *361*(2), 123–34. doi:10.1056/NEJMoa0900212

Gonzalez-Suarez, I., Redwood, A. B., Grotsky, D. a, Neumann, M. a, Cheng, E. H.-Y., Stewart, C. L., Dusso, A., et al. (2011). A new pathway that regulates 53BP1 stability implicates cathepsin L and vitamin D in DNA repair. *The EMBO journal*, *30*(16), 3383–96. doi:10.1038/emboj.2011.225

Goulding, H., Pinder, S., Cannon, P., Pearson, D., Nicholson, R., Snead, D., Bell, J., et al. (1995). A new immunohistochemical antibody for the assessment of estrogen receptor status on routine formalin-fixed tissue samples. *Human pathology*, *26*(3), 291–4. Retrieved from http://www.ncbi.nlm.nih.gov/pubmed/7890280

Goulet, B., Baruch, A., Moon, N.-S., Poirier, M., Sansregret, L. L., Erickson, A., Bogyo, M., et al. (2004). A cathepsin L isoform that is devoid of a signal peptide localizes to the nucleus in S phase and processes the CDP/Cux transcription factor. *Molecular cell*, *14*(2), 207–19. Retrieved from http://www.ncbi.nlm.nih.gov/pubmed/15099520

Hartman, A.-R., Kaldate, R. R., Sailer, L. M., Painter, L., Grier, C. E., Endsley, R. R., Griffin, M., et al. (2012). Prevalence of BRCA mutations in an unselected population of triple-negative breast cancer. *Cancer*, *118*(11), 2787–95. doi:10.1002/cncr.26576

Kau, P., Nagaraja, G. M., Zheng, H., Gizachew, D., Galukande, M., Krishnan, S., & Asea, A. (2012). A mouse model for triple-negative breast cancer tumor-initiating cells (TNBC-TICs) exhibits similar aggressive phenotype to the human disease. *BMC cancer*, *12*, 120. doi:10.1186/1471-2407-12-120

Kuperwasser, C., Chavarria, T., Wu, M., Magrane, G., Gray, J. W., Carey, L., Richardson, A., et al. (2004). Reconstruction of functionally normal and malignant human breast tissues in

mice. *Proceedings of the National Academy of Sciences of the United States of America*, *101*(14), 4966–71. doi:10.1073/pnas.0401064101

Ma, C. X., Cai, S., Li, S., Ryan, C. E., Guo, Z., Schaiff, W. T., Lin, L., et al. (2012). Targeting Chk1 in p53-deficient triple-negative breast cancer is therapeutically beneficial in human-in-mouse tumor models. *The Journal of clinical investigation*, *122*(4), 1541–52. doi:10.1172/JCI58765

Millar, E. K. A., Graham, P. H., O'Toole, S. A., McNeil, C. M., Browne, L., Morey, A. L., Eggleton, S., et al. (2009). Prediction of local recurrence, distant metastases, and death after breast-conserving therapy in early-stage invasive breast cancer using a five-biomarker panel. *Journal of clinical oncology : official journal of the American Society of Clinical Oncology*, *27*(28), 4701–8. doi:10.1200/JCO.2008.21.7075

Miller, F. R., Miller, B. E., & Heppner, G. H. (1983). Characterization of metastatic heterogeneity among subpopulations of a single mouse mammary tumor: heterogeneity in phenotypic stability. *Invasion & metastasis*, *3*(1), 22–31. Retrieved from http://www.ncbi.nlm.nih.gov/pubmed/6677618

Pallares, J., Santacana, M., Puente, S., Lopez, S., Yeramian, A., Eritja, N., Sorolla, A., et al. (2009). A review of the applications of tissue microarray technology in understanding the molecular features of endometrial carcinoma. *Analytical and quantitative cytology and histology / the International Academy of Cytology [and] American Society of Cytology*, *31*(4), 217–26. Retrieved from http://www.ncbi.nlm.nih.gov/pubmed/19736869

Peppone, L. J., Huston, A. J., Reid, M. E., Rosier, R. N., Zakharia, Y., Trump, D. L., Mustian, K. M., et al. (2011). The effect of various vitamin D supplementation regimens in breast cancer patients. *Breast cancer research and treatment*, *127*(1), 171–7. doi:10.1007/s10549-011-1415-4

Ren, G., Blum, G., Verdoes, M., Liu, H., Syed, S., Edgington, L. E., Gheysens, O., et al. (2011). Non-invasive imaging of cysteine cathepsin activity in solid tumors using a 64Cu-labeled activity-based probe. *PloS one*, *6*(11), e28029. doi:10.1371/journal.pone.0028029

Voduc, K. D., Cheang, M. C. U., Tyldesley, S., Gelmon, K., Nielsen, T. O., & Kennecke, H. (2010). Breast cancer subtypes and the risk of local and regional relapse. *Journal of clinical oncology : official journal of the American Society of Clinical Oncology*, *28*(10), 1684–91. doi:10.1200/JCO.2009.24.9284

Xu, X., Wagner, K. U., Larson, D., Weaver, Z., Li, C., Ried, T., Hennighausen, L., et al. (1999). Conditional mutation of Brca1 in mammary epithelial cells results in blunted ductal morphogenesis and tumour formation. *Nature genetics*, *22*(1), 37–43. doi:10.1038/8743

CHAPTER FOUR

Telomere defects and genomic stability in a premature aging laminopathy

4.1 Abstract

Expression of mutant forms of A-type lamins is associated with human diseases known as laminopathies, which include a variety of degenerative diseases and premature aging syndromes such as Hutchinson Gilford Progeria Syndrome (HGPS). In addition, changes in the expression of A-type lamins have been linked to tumorigenesis. Recent studies suggest that increased genomic instability could contribute to the pathogenesis of lamins-related diseases, however the cellular mechanisms that lead to these diseases remain poorly defined. Research in our laboratory has found that loss of A-type lamins leads to defects in telomere homeostasis and increased genomic instability, and implicates loss of 53BP1 as a possible mechanism behind these phenotypes. Here, we sought to determine if similar phenotypes are observed in a mouse model of progeria. We used mouse embryonic fibroblasts (MEFs) and mouse adult fibroblasts (MAFs) from mice that express low levels of a mutant form of A-type lamins that lacks exon 9 to investigate if telomere defects, heterochromatin abnormalities, and genomic instability contribute to progeroid syndrome pathogenesis. We find that the Δexon9Lmna mouse model exhibits telomere shortening and alterations of telomeric and centromeric heterochromatin, but not an increase in genomic instability as assessed by the frequency of chromosome and chromatid breaks or the extent of unrepaired DNA damage. Interestingly, the levels of 53BP1 are maintained in cells from these mice. These results demonstrate that different lamins mutations present with varying genomic instability phenotypes and suggest that 53BP1 status could be an important determinant for maintenance of genomic stability in lamins-related diseases.

4.2 Telomere shortening in Δexon9Lmna mice

Previous studies in our laboratory have demonstrated that loss of A-type lamins leads to telomere shortening, defects in telomeric heterochromatin, and increased genomic instability (Gonzalez-Suarez et al., 2009). Furthermore, studies have shown that cells from patients with HGPS undergo faster telomere attrition than normal counterparts (Allsopp et al., 1992; Decker, Chavez, Vulto, & Lansdorp, 2009; Huang, Risques, Martin, Rabinovitch, & Oshima, 2008). Here, we characterized the phenotype of the mouse model of progeria, Δexon9Lmna, in order to compare it with other A-type lamins mutants and determine if defects in telomere biology and overall genomic instability could contribute to pathogenesis in this mouse model.

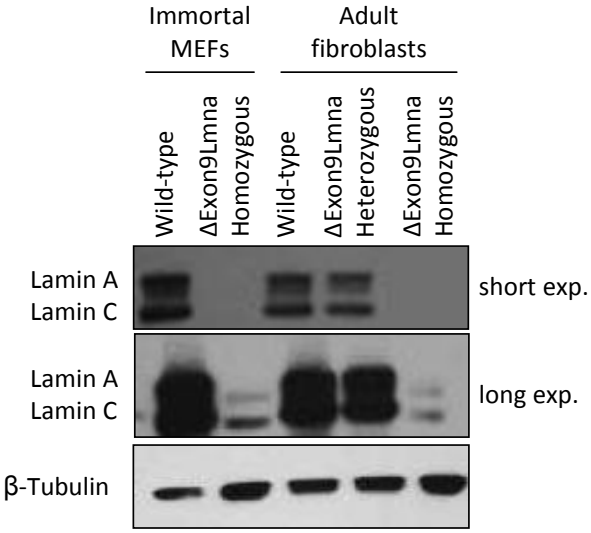

Figure 4-1. Δexon9Lmna cells have decreased levels of A-type lamins. Western blots showing a marked decrease in protein levels of lamin A and lamin C in Δexon9Lmna immortal mouse embyonic fibroblasts (MEFs) and adult fibroblasts.

We first monitored the global levels of mutant lamin A/C proteins in both mouse embryonic and mouse adult fibroblasts (MEFs and MAFs, respectively) isolated from Δexon9Lmna mice. Previous studies had shown that the lamin A/C transcripts are not stable in these cells (Mounkes, Kozlov, Hernandez, Sullivan, & Stewart, 2003). As shown in **Figure 4-1**, cells heterozygous for the mutation exhibit decreased levels of A-type lamins, a defect that is greatly exacerbated in homozygous mutant cells.

Next, we determined if telomere shortening could be a factor contributing to the

phenotype of the Δexon9Lmna mice. Telomere length was measured in embryonic fibroblasts by both telomere restriction fragment analysis (TRF) and quantitative fluorescence *in-situ* hybridization (Q-FISH), and in adult fibroblasts by Q-FISH. Briefly, the TRF is conducted by embedding cells in agarose plugs, permeabilizing, and incubating cells with a restriction endonuclease to fragment genomic DNA, leaving the long telomeric tracks intact. The plugs are then subjected to pulsed-field gel electrophoresis and the gel is transferred to a membrane. Next, a southern blot is performed using a telomere specific probe to determine the distance the telomeres traveled in the gel. Shorter telomeres migrate further in the gel than longer telomeres, providing a rough estimate of telomere length in a cell population. In Q-FISH, cells are arrested in metaphase by treatment with colcemid and fixed in methanol-acetic acid. Metaphases are dropped onto slides and hybridized with a telomere specific PNA probe. Fluorescent images are acquired and intensity of fluorescence is measured using a computer program, TFL-Telo. The intensity of fluorescence is correlated with Kb of telomere tracts, providing quantitative measurement of telomere length in a cell population.

Mouse embryonic fibroblasts show a faster migration of telomeres by TRF in the mutant cells compared to wild type, indicative of shorter telomeres (**Figure 4-2A**). These results were confirmed by three independent Q-FISH assays in Δexon9Lmna embryonic fibroblasts, which show an average telomere length approximately 6 Kb shorter than the telomeres of wild type cells (**Figure 4-2B**). Statistical analysis shows that these differences in telomere length between genotypes is significant ($p=0.0181$). Adult fibroblasts from Δexon9Lmna mice also exhibit telomere shortening (**Figure 4-2B**). Accordingly, a higher percentage of shorter telomeres (≤20 Kb) and a lower percentage of longer telomeres (≥65 Kb) were observed in the mutant embryonic and adult fibroblasts compared to wild type.

A

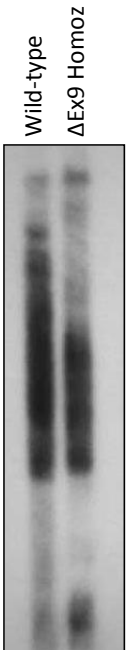

B

Q-FISH	Genotype	# of metaph	# of telom	Average tel length	Tel <20Kb	Tel >65Kb
Exp.1	Wild-Type MEFs	20	3486	**40.36 ± 23.44**	18.50%	14.37%
	ΔEx9 Homoz MEFs	20	4592	**34.05 ± 17.82**	22.85%	5.01%
Exp. 2	Wild-Type MEFs	30	8404	**39.44 ± 20.17**	14.65%	11.21%
	ΔEx9 Homoz MEFs	30	7800	**35.99 ± 18.45**	20.21%	6.61%
Exp. 3	Wild-Type MEFs	30	8032	**44.63 ± 25.13**	14.59%	19.78%
	ΔEx9 Homoz MEFs	30	7571	**32.57 ± 17.37**	25.57%	4.44%
Exp. 4	Wild-Type MAFs	30	7323	**38.79 ± 16.25**	12.70%	5.94%
	ΔEx9 Homoz MAFs	30	6970	**33.96 ± 14.60**	17.62%	2.57%

p = 0.0181

Figure 4-2. Telomere shortening in Δexon9Lmna MEFs and MAFs. (A) TRF analysis showing telomere shortening in Δexon9Lmna MEFs. **(B)** Four independent Q-FISH analyses of telomere length in wild-type and Δexon9Lmna MEFs and MAFs are shown, as indicated. Telomere length of at least 20 metaphases was measured. Note the decreases in average telomere length in all mutant fibroblasts carrying the homozygous Δexon9Lmna mutation (grey column). p value shows statistical significance ($p \leq 0.05$).

These data demonstrate that low levels of expression of the Δexon9Lmna mutant form of A-type lamins leads to defects in the maintenance of telomere length homeostasis, supporting the notion that A-type lamins play a role in the control of telomere length.

4.3 Telomere heterochromatin is altered in Δexon9Lmna fibroblasts

Telomeres have epigenetic marks, such as trimethylation of histone H3 at lysine 9 (H3K9me3) and trimethylation of histone H4 at lysine 20 (H4K20me3), that are characteristic of heterochromatin (Blasco, 2007). Defects in chromatin modifying activities that are responsible for the maintenance of these heterochromatic marks lead to telomere elongation in the presence of A-type lamins (Benetti et al., 2007; García-Cao, O'Sullivan, Peters, Jenuwein, & Blasco, 2004; Gonzalo et al., 2005). Previous studies in our laboratory demonstrated that complete loss of A-type lamins impacts on the epigenetic status of telomeric chromatin. Specifically, loss of A-type lamins led to decreased levels of H4K20me3 (Gonzalez-Suarez et al., 2009). The fact that

this epigenetic defect is accompanied by telomere shortening in the *LMNA* null model suggests that A-type lamins might be necessary for telomere elongation in the context of H4K20me3 deficiency. To determine if fibroblasts from the Δexon9Lmna exhibit alterations in the structure of telomeric heterochromatin, we performed chromatin immunoprecipitation (ChIP) assays with antibodies recognizing H3K9me3 and H4K20me3 marks (**Figure 4-3A**). Quanitification of at least three independent experiments show a 40% decrease in the levels of both heterochromatic marks in the Δexon9Lmna mutant cells (**Figure 4-3B**). These results demonstrate that different alterations of A-type lamins affect the status of telomeric chromatin differently. While complete loss of A-type lamins leads only to decreased levels of H4K20me3 at telomeres, the Δexon9Lmna mutant results in decreased levels of both H4K20me3 and H3K9me3. Collectively, these data support a role for A-type lamins in the maintenance of telomere chromatin structure.

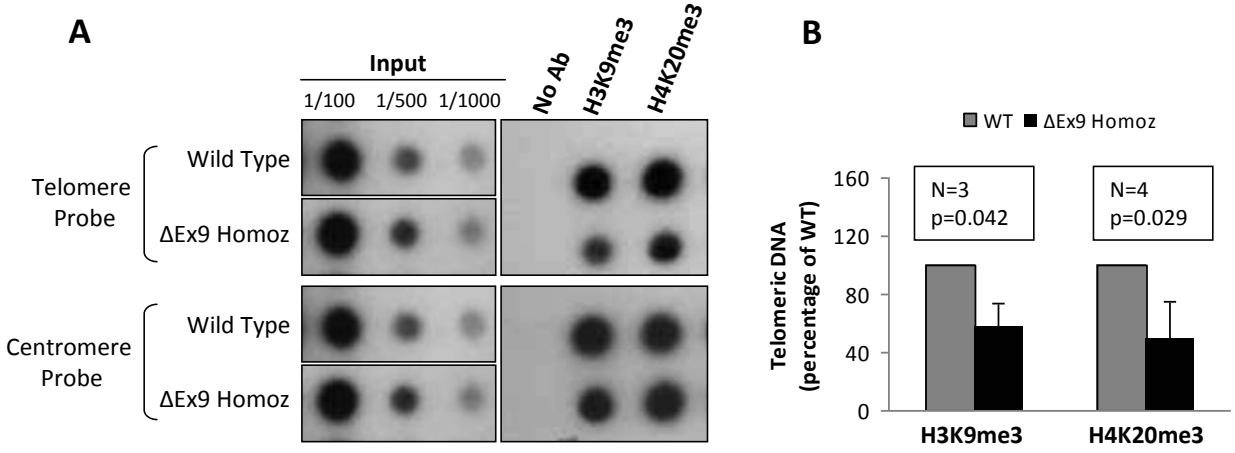

Figure 4-3. Heterochromatin defects at telomeres and centromeres in Δexon9Lmna MEFs. (A) Chromatin immunoprecipitation (ChIP) analysis performed on wild type and Δexon9Lmna MEFs with antibodies recognizing H3K9me3 and H4K20me3. Immunoprecipitated DNA was dot blotted and hybridized to a telomere probe, stripped, and rehybridized to a centromere probe (major satellite). **(B)** Graph showing the quantitation of immunoprecipitated telomeric DNA after normalization to input signals in three independent experiments for H3K9me3 and four independent experiments for H4K20me3. Bars represent standard deviation. p value shows statistical significance ($p \leq 0.05$).

Alterations of telomeric chromatin are often phenocopied by pericentric heterochromatin. Such is the case in *LMNA* null fibroblasts which show reduced levels of H4K20me3 at both the telomeric and pericentric domains (Gonzalez-Suarez et al., 2009). To determine the levels of H3K9me3 and H4K20me3 at pericentric domains, the immunoblots that were hybridized with a telomeric probe were stripped and rehybridized with a probe recognizing major satellite sequences. Interestingly, we found that the levels of H3K9me3 at pericentric chromatin were also reduced in the Δexon9Lmna mutant cells, though to a lower extent than at telomeric chromatin (**Figure 4-3A)**. In contrast, the levels of H4K20me3 were maintained in the mutant cells at these domains. These results indicate a certain specificity with respect to epigenetic changes at telomeric versus pericentric chromatin in Δexon9Lmna fibroblasts.

Mutations in the *LMNA* gene and reduced expression of A-type lamins are associated with loss of heterochromatin from the nuclear periphery (Parnaik, 2008; Reddy, Zullo, Bertolino, & Singh, 2008). In mouse cells, heterochromatic domains, especially pericentric regions, are easily visualized by DAPI staining during interphase. In normal fibroblasts, pericentric domains appear as DAPI-positive clusters called chromocenters that are enriched in H3K9me3 and H4K20me3 marks (Probst & Almouzni, 2008). We performed immunofluorescence studies to test if the Δexon9Lmna mutation impacts on the structure and distribution of heterochromatin domains in the nucleus **(Figure 4-4)**. We found that in mutant cells, DAPI staining is distributed throughout the nucleoplasm exhibiting only a few areas of compacted pericentric chromatin. Labeling with antibodies for H3K9me3 and H4K20me3 mirrored the DAPI distribution. The heterochromatic marks in mutant cells were found to be either distributed more diffusely throughout the nucleus or forming a few big aggregates. Overall, these studies indicate that expression of the Δexon9Lmna mutant protein leads to a decrease in heterochromatic marks at

telomeres and an overall disorganization of pericentric chromatin domains. These results support a role for A-type lamins in the nuclear compartmentalization of heterochromatin in mouse cells.

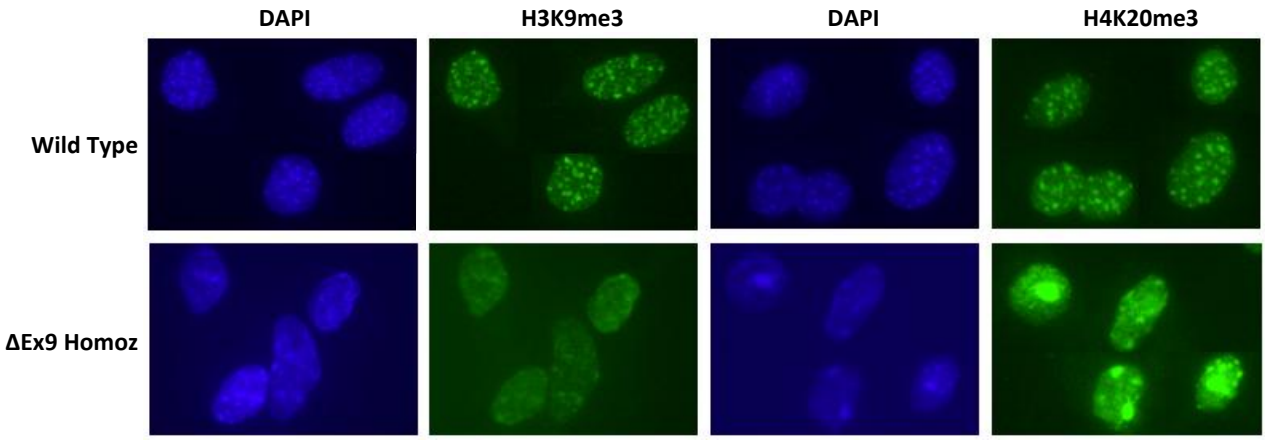

Figure 4-4. Heterochromatin disorganization in Δexon9Lmna MEFs. Immunofluorescence performed in wild type and Δexon9Lmna MEFs with antibodies recognizing H3K9me3 and H4K20me3 (green). DAPI is shown in blue. Note the diffuse and irregular distribution of heterochromatin domains in the mutant cells.

4.4 Fibroblasts from Δexon9Lmna mice do not exhibit high levels of genomic instability

Telomere loss can lead to chromosome end-to-end fusions and other chromosomal aberrations that have serious detrimental effects for the integrity of the genome. *LMNA* null fibroblasts exhibit loss of telomere sequences (signal-free ends), an increased frequency in chromosome and chromatid breaks, and increased basal levels of unrepaired DNA damage. In addition, we observed decreased levels of 53BP1 in *LMNA* null cells (Gonzalez-Suarez et al., 2009). We tested whether Δexon9Lmna mutant fibroblasts phenocopy any of these defects. FISH analysis performed with a telomere PNA probe shows that mutant embryonic fibroblasts have only a modest increase in telomere losses (telomere loss in 24% of metaphases versus 10% in

Genomic instability	# of metaph	Total STL	metaph STL	chrom breaks	metaph breaks
Wild-type MEFs	100	13	10%	0	0%
ΔEx9 Homoz MEFs	100	46	24%	2	2%
Wild-type MAFs	100	27	16%	12	7%
ΔEx9 Homoz MAFs	100	28	13%	5	3%

Table 4-1. Δexon9Lmna MEFs do not have profound genomic instability . Genomic instability was measured in wild type and Δexon9Lmna MEFs and MAFs by counting sister telomere losses (STL) and chromosome and chromatid breaks in metaphase spreads.

wild type) (**Table 4-1**). Similarly, there was no evidence of increase in frequency of signal free ends in adult fibroblasts from Δexon9Lmna mice (**Table 4-1**). These studies indicate that the Δexon9Lmna mutation hinder telomere length maintenance while the mechanisms preventing terminal deletions remain largely intact. Furthermore, no significant increases in chromosome and chromatid breaks or chromosome end-to-end fusions were observed in the mutant cells (**Table 4-1**). To confirm that the Δexon9Lmna fibroblasts were able to maintain chromosome stability, we monitored the presence of γH2AX foci by immunofluorescence. We did not find any evidence of basal levels of unrepaired DNA in these cells (data not shown). In addition, we found that mutant Δexon9Lmna fibroblasts do not exhibit decreased levels of 53BP1 (**Figure 4-5**). Thus, in contrast to other mouse models of laminopathies, the Δexon9Lmna mutation does not lead to telomere deletions, destabilization of 53BP1, or profound genomic instability. This mutation

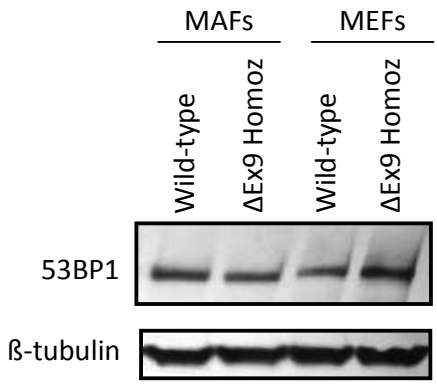

Figure 4-5. Δexon9Lmna cells maintain 53BP1 levels. Western blot with an antibody recognizing 53BP1 shows that the levels of this protein remain stable in Δexon9Lmna MEFs and MAFs.

does lead, however, to telomere shortening and defects in telomeric and pericentric heterochromatin.

4.5 Discussion and future experiments

Although the main function of A-type lamins is to give structure and support to a cell's nucleus, the wide range of diseases that are caused by mutation of the *LMNA* gene or changes in expression reveals a more complex role for these proteins in cellular processes. Much work is being done to elucidate how alterations of A-type lamins lead to disease. There is evidence that lamin-related diseases are associated with genomic instability and that improper maintenance of telomeres is an important factor in the pathophysiology of these diseases (Gonzalez-Suarez et al., 2009; Liu et al., 2005; Liu & Zhou, 2008). However, the data supporting this notion remains scarce. Our previous studies showed that *LMNA* null fibroblasts exhibit defects in telomere structure, length and function, increased chromosome and chromatid breaks, a high degree of unrepaired DNA damage, and an increase in aneuploidy (Gonzalez-Suarez et al., 2009). These cells also exhibited destabilization of 53BP1, a key factor in the DNA damage response pathway. The decrease in 53BP1 provides a putative mechanism by which loss of A-type lamins promotes genomic instability. This study provides evidence that a mutation of *LMNA* that causes a progeroid syndrome in mice leads to different effects on chromatin structure, telomere biology, and genomic stability than seen in other models.

Defects in chromatin structure

Previous studies in HGPS cells revealed epigenetic changes that led to alterations of heterochromatic marks (Shumaker et al., 2006). Mutant cells exhibited decreased levels of H3K27me3 from the X chromosome, a mark for facultative heterochromatin. In these cells, H3K9me3 is reduced and H4K20me3 is increased, both of which are marks for constitutive heterochromatin. In contrast, upon loss of A-type lamins, we found that the H3K9me3 mark is

unchanged in telomeric and pericentric domains. However, we did see a decrease in the H4K20me3 mark at these domains (Gonzalez-Suarez et al., 2009). In the Δexon9Lmna fibroblasts that were analyzed in this study, we found yet a different pattern of defects in histone marks. Telomeres in Δexon9Lmna cells exhibited decreased levels of both H3K9me3 and H4K20me3. Pericentric chromatin exhibited decreased levels of H3K9me3 while maintaining H4K20me3 levels. In addition, we observed that the structure of pericentric heterochromatin is altered in these cells. Instead of the characteristic foci-like staining areas of DAPI and heterochromatin marks, we observed either diffuse staining or large aggregates in the Δexon9Lmna fibroblasts. Overall, these studies indicate that A-type lamins play a key role in the maintenance of heterochromatin domains, but that different alterations of these proteins impact on specific chromatin-modifying activities.

Defects in telomere biology and genomic instability

There is much ongoing research trying to determine the molecular mechanisms that lead to aging. Utilizing cells from patients with HGPS or mouse models of progeria allows studies to be performed under conditions where changes in the cell that lead to aging happen rapidly. There is growing evidence that shortening of telomeres is a major contributor to the cellular aging process. Cells from patients with HGPS exhibit shorter telomeres that normal counterparts. A-type lamins play a major role in the maintenance of telomeres in these cells, as hematopoietic cells from HGPS patients which do not express lamins are able to maintain telomeres (Decker et al., 2009). Furthermore, studies performed in A-type lamin knockout mice showed that complete loss of A-type lamins leads to telomere shortening and an increase in complete loss of telomeres (Gonzalez-Suarez et al., 2009). Here, we determined whether a mouse model of progeria also exhibits telomere length defects.

Fibroblasts from the Δexon9Lmna mice present a marked reduction of average telomere length but not a consistent increase in signal free ends. Maintenance of telomere length is a complex process that requires proper accessibility of telomerase to replicating telomeres and assembly of the shelterin complex at the telomere after replication to form the T-loop structure and prevent chromosome ends from being recognized as DNA double strand breaks. The present study suggests that the expression of different forms of A-type lamins affect different processes in the maintenance of telomere homeostasis. It is possible that the expression of Δexon9Lmna mutant proteins might hinder the accessibility of telomerase to the telomeres.

Furthermore, an overall increase in genomic instability was seen upon complete loss of A-type lamins. In contrast, we found no evidence of increased genomic instability in Δexon9Lmna fibroblasts. A striking difference between these genotypes is their ability to stabilize 53BP1. We found that 53BP1 levels are markedly reduced in *LMNA* null fibroblasts, however Δexon9Lmna fibroblasts are able to maintain the levels of this protein. 53BP1 is a DNA damage response factor that is rapidly recruited to sites of DNA double strand breaks (Schultz, Chehab, Malikzay, & Halazonetis, 2000). Depletion of 53BP1 revealed a role for this protein in p53 accumulation, regulation of cell cycle checkpoints (Manis et al., 2004; Morales et al., 2003; Wang, Matsuoka, Carpenter, & Elledge, 2002), and the phosphorylation of ATM substrates in response to ionizing radiation (DiTullio et al., 2002; Fernandez-Capetillo et al., 2002). 53BP1 knockout mice exhibit a phenotype consistent with defects in DNA repair, such as increased radiosensitivity, immunodeficiency, and cancer susceptibility (Ward, Minn, van Deursen, & Chen, 2003). Accordingly, loss of 53BP1 hinders the processing of dysfunctional telomeres by NHEJ (Dimitrova, Chen, Spector, & de Lange, 2008). A role for 53BP1 in replication has also been described (Sengupta et al., 2004), with loss of 53BP1 decreasing cell survival and

enhancing chromosomal aberrations upon replication arrest (Tripathi, Nagarjuna, & Sengupta, 2007). In summary, 53BP1 appears to function at the interface of DNA replication, recombination, and repair. Thus, the decrease in 53BP1 levels observed in *LMNA* null fibroblasts could explain the increased genomic instability observed in these cells. In support of this notion, Δexon9Lmna cells, which maintain 53BP1 levels, are able to maintain genome stability. Future studies should demonstrate if in fact 53BP1 deficiency is responsible for the telomere defects and overall genomic instability observed in some mouse models of laminopathies.

Experiments are ongoing in the laboratory to introduce the Δexon9Lmna mutant construct into *LMNA* null cells to determine if the DNA repair defects observed upon loss of A-type lamins are rescued. Since 53BP1 levels are maintained in the Δexon9Lmna cells, we hypothesize that expression of this construct should stabilize 53BP1 levels in the *LMNA* null cells and therefore lead to chromosome end-to-end fusions of dysfunctional telomeres and rescue the fast phase of DNA repair as measured by comet assay. These experiments would further confirm that 53BP1 is responsible for the DNA repair defects in A-type lamins null cells and demonstrate that different expression levels of A-type lamins have different impacts on genomic instability and DNA repair. Experiments could be carried out to determine the effects that other lamins mutations have on genomic stability, DNA repair, and telomere homeostasis. Different mutant constructs that are associated with laminopathies in humans can be expressed in *LMNA* null cells to determine which can stabilize 53BP1 levels and rescue the defects that characterize these cells. These experiments would shed light into different molecular mechanisms that could be involved in the pathogenesis of different laminopathies and possibly reveal which domains in the *LMNA* gene are important for maintaining genomic stability.

4.6 References

Allsopp, R. C., Vaziri, H., Patterson, C., Goldstein, S., Younglai, E. V, Futcher, A. B., Greider, C. W., et al. (1992). Telomere length predicts replicative capacity of human fibroblasts. *Proceedings of the National Academy of Sciences of the United States of America*, 89(21), 10114–8. Retrieved from http://www.pubmedcentral.nih.gov/articlerender.fcgi?artid=50288&tool=pmcentrez&rendertype=abstract

Benetti, R., Gonzalo, S., Jaco, I., Schotta, G., Klatt, P., Jenuwein, T., & Blasco, M. A. (2007). Suv4-20h deficiency results in telomere elongation and derepression of telomere recombination. *The Journal of cell biology*, 178(6), 925–36. doi:10.1083/jcb.200703081

Blasco, M. A. (2007). The epigenetic regulation of mammalian telomeres. *Nature reviews. Genetics*, 8(4), 299–309. doi:10.1038/nrg2047

Decker, M. L., Chavez, E., Vulto, I., & Lansdorp, P. M. (2009). Telomere length in Hutchinson-Gilford progeria syndrome. *Mechanisms of ageing and development*, 130(6), 377–83. doi:10.1016/j.mad.2009.03.001

Dimitrova, N., Chen, Y.-C. M., Spector, D. L., & de Lange, T. (2008). 53BP1 promotes non-homologous end joining of telomeres by increasing chromatin mobility. *Nature*, 456(7221), 524–8. doi:10.1038/nature07433

DiTullio, R. A., Mochan, T. A., Venere, M., Bartkova, J., Sehested, M., Bartek, J., & Halazonetis, T. D. (2002). 53BP1 functions in an ATM-dependent checkpoint pathway that is constitutively activated in human cancer. *Nature cell biology*, 4(12), 998–1002. doi:10.1038/ncb892

Fernandez-Capetillo, O., Chen, H.-T., Celeste, A., Ward, I., Romanienko, P. J., Morales, J. C., Naka, K., et al. (2002). DNA damage-induced G2-M checkpoint activation by histone H2AX and 53BP1. *Nature cell biology*, 4(12), 993–7. doi:10.1038/ncb884

García-Cao, M., O'Sullivan, R., Peters, A. H. F. M., Jenuwein, T., & Blasco, M. A. (2004). Epigenetic regulation of telomere length in mammalian cells by the Suv39h1 and Suv39h2 histone methyltransferases. *Nature genetics*, 36(1), 94–9. doi:10.1038/ng1278

Gonzalez-Suarez, I., Redwood, A. B., Perkins, S. M., Vermolen, B., Lichtensztejin, D., Grotsky, D. a, Morgado-Palacin, L., et al. (2009). Novel roles for A-type lamins in telomere biology and the DNA damage response pathway. *The EMBO journal*, 28(16), 2414–27. doi:10.1038/emboj.2009.196

Gonzalo, S., García-Cao, M., Fraga, M. F., Schotta, G., Peters, A. H. F. M., Cotter, S. E., Eguía, R., et al. (2005). Role of the RB1 family in stabilizing histone methylation at constitutive heterochromatin. *Nature cell biology*, 7(4), 420–8. doi:10.1038/ncb1235

Huang, S., Risques, R. A., Martin, G. M., Rabinovitch, P. S., & Oshima, J. (2008). Accelerated telomere shortening and replicative senescence in human fibroblasts overexpressing mutant and wild-type lamin A. *Experimental cell research*, 314(1), 82–91. doi:10.1016/j.yexcr.2007.08.004

Liu, B., Wang, J., Chan, K. M., Tjia, W. M., Deng, W., Guan, X., Huang, J., et al. (2005). Genomic instability in laminopathy-based premature aging. *Nature medicine*, 11(7), 780–5. doi:10.1038/nm1266

Liu, B., & Zhou, Z. (2008). Lamin A/C, laminopathies and premature ageing. *Histology and histopathology*, 23(6), 747–63. Retrieved from http://www.ncbi.nlm.nih.gov/pubmed/18366013

Manis, J. P., Morales, J. C., Xia, Z., Kutok, J. L., Alt, F. W., & Carpenter, P. B. (2004). 53BP1 links DNA damage-response pathways to immunoglobulin heavy chain class-switch recombination. *Nature immunology*, 5(5), 481–7. doi:10.1038/ni1067

Morales, J. C., Xia, Z., Lu, T., Aldrich, M. B., Wang, B., Rosales, C., Kellems, R. E., et al. (2003). Role for the BRCA1 C-terminal repeats (BRCT) protein 53BP1 in maintaining genomic stability. *The Journal of biological chemistry*, 278(17), 14971–7. doi:10.1074/jbc.M212484200

Mounkes, L. C., Kozlov, S., Hernandez, L., Sullivan, T., & Stewart, C. L. (2003). A progeroid syndrome in mice is caused by defects in A-type lamins. *Nature*, 423(6937), 298–301. doi:10.1038/nature01631

Parnaik, V. K. (2008). Role of nuclear lamins in nuclear organization, cellular signaling, and inherited diseases. *International review of cell and molecular biology*, 266, 157–206. doi:10.1016/S1937-6448(07)66004-3

Probst, A. V, & Almouzni, G. (2008). Pericentric heterochromatin: dynamic organization during early development in mammals. *Differentiation; research in biological diversity*, 76(1), 15–23. doi:10.1111/j.1432-0436.2007.00220.x

Reddy, K. L., Zullo, J. M., Bertolino, E., & Singh, H. (2008). Transcriptional repression mediated by repositioning of genes to the nuclear lamina. *Nature*, 452(7184), 243–7. doi:10.1038/nature06727

Schultz, L. B., Chehab, N. H., Malikzay, a, & Halazonetis, T. D. (2000). p53 binding protein 1 (53BP1) is an early participant in the cellular response to DNA double-strand breaks. *The Journal of cell biology*, 151(7), 1381–90. Retrieved from http://www.pubmedcentral.nih.gov/articlerender.fcgi?artid=2150674&tool=pmcentrez&rendertype=abstract

Sengupta, S., Robles, A. I., Linke, S. P., Sinogeeva, N. I., Zhang, R., Pedeux, R., Ward, I. M., et al. (2004). Functional interaction between BLM helicase and 53BP1 in a Chk1-mediated

pathway during S-phase arrest. *The Journal of cell biology*, 166(6), 801–13. doi:10.1083/jcb.200405128

Shumaker, D. K., Dechat, T., Kohlmaier, A., Adam, S. A., Bozovsky, M. R., Erdos, M. R., Eriksson, M., et al. (2006). Mutant nuclear lamin A leads to progressive alterations of epigenetic control in premature aging. *Proceedings of the National Academy of Sciences of the United States of America*, 103(23), 8703–8. doi:10.1073/pnas.0602569103

Tripathi, V., Nagarjuna, T., & Sengupta, S. (2007). BLM helicase-dependent and -independent roles of 53BP1 during replication stress-mediated homologous recombination. *The Journal of cell biology*, 178(1), 9–14. doi:10.1083/jcb.200610051

Wang, B., Matsuoka, S., Carpenter, P. B., & Elledge, S. J. (2002). 53BP1, a mediator of the DNA damage checkpoint. *Science (New York, N.Y.)*, 298(5597), 1435–8. doi:10.1126/science.1076182

Ward, I. M., Minn, K., van Deursen, J., & Chen, J. (2003). p53 Binding protein 53BP1 is required for DNA damage responses and tumor suppression in mice. *Molecular and cellular biology*, 23(7), 2556–63. Retrieved from http://www.pubmedcentral.nih.gov/articlerender.fcgi?artid=150747&tool=pmcentrez&rendertype=abstract

CHAPTER FIVE

General conclusions and future questions

5.1 General conclusions

The work in this thesis has uncovered that a novel pathway - cathepsin L-mediated degradation of 53BP1- is active in two pathological scenarios: loss of BRCA1 in breast cancer cells, and loss of A-type lamins function. Our data indicates that this pathway could have diagnostic and therapeutic value in breast cancers with the poorest prognosis and in degenerative diseases brought on by mutations of A-type lamins, termed laminopathies. Triple negative (TN) and BRCA-mutated breast cancers are characterized by early onset, increased aggressiveness, are difficult to treat, and lead to increased metastasis compared to other breast cancers (Constantinidou, Jones, & Reis-Filho, 2010; Nanda, 2011). Adding to the treatment difficulties is the fact that many of these tumors rescue HR function and gain resistance to DNA damaging strategies, such as PARP inhibitors. Recent landmark studies have shown that loss of 53BP1 is one way in which HR is rescued in BRCA1-deficient cells, which leads to PARPi resistance (Bouwman et al., 2010; Bunting et al., 2010; Cao et al., 2009). Therefore, raising the levels of 53BP1 in BRCA1-deficient cells should render them susceptible to DNA damaging compounds. Until work in our laboratory identified CTSL as a novel regulator of 53BP1, very little was known about how levels of 53BP1 are controlled in the cell.

Here, we demonstrate that BRCA1-deficient cancer cells activate CTSL-mediated degradation of 53BP1 to rescue HR defects and overcome the growth arrest that accompanies BRCA1 loss. We show that CTSL is responsible for the degradation of 53BP1 upon depletion of BRCA1, and that treatment of cells with vitamin D or cathepsin inhibitors stabilizes 53BP1 in BRCA1-deficient cells that bypass growth arrest. Raising 53BP1 levels in this context shifts DNA repair from HR to NHEJ, thereby increasing genomic instability following irradiation or

PARPi treatment and compromising cell proliferation. Inhibition of CTSL via vitamin D or specific inhibitors could represent a novel therapeutic strategy for treatment of TN and BRCA1-mutated breast cancers. These results are summarized in **Figure 5-1.** Furthermore, we have identified a novel biomarker signature for stratification of subsets of patients with TN and BRCA1-mutated breast cancers. This biomarker signature consists of monitoring the nuclear levels of 53BP1, CTSL and VDR. We found that high nuclear CTSL correlates inversely with levels of 53BP1 in TNBC, especially in breast tumors exhibiting low levels of nuclear VDR. Overall, the proposed method will allow distinguishing tumors in which the pathway is active – high CTSL, low 53BP1, low VDR- from those in which the pathway is inactive –high CTSL, high 53BP1, high VDR-. Identification of these types of tumors is expected to have great importance for diagnosis and customization of therapy for cancer patients.

Very little is known about the molecular mechanisms that lead to laminopathies. Work in this thesis has provided evidence that CTSL-mediated degradation of 53BP1 contributes to genomic instability and possibly, to the pathogenesis of some of these diseases. Previous studies in our laboratory had shown that complete loss A-type lamins (*LMNA* knockout mouse model) leads to telomere shortening and defects in telomere structure, and increase in overall genomic instability, and downregulation of 53BP1 (Gonzalez-Suarez et al., 2009). Here, we found that cells from the Δexon9Lmna mouse model of progeria exhibit several phenotypic differences from *LMNA* null or HGPS cells. We show that Δexon9Lmna mutation leads to telomere shortening and defects in heterochromatin structure, but does not increase overall genomic instability. Importantly, cells from these mice maintain levels of 53BP1, providing a possible mechanism as to how genomic stability is maintained in this model of progeria and putatively in other types of laminopathies. The differences in these mouse models are starting to shed some

light into how different alterations in A-type lamins could contribute to the pathogenesis of the variety of lamin-related diseases. I will discuss in the following sections some questions that remain unanswered and the plans for the future of this project.

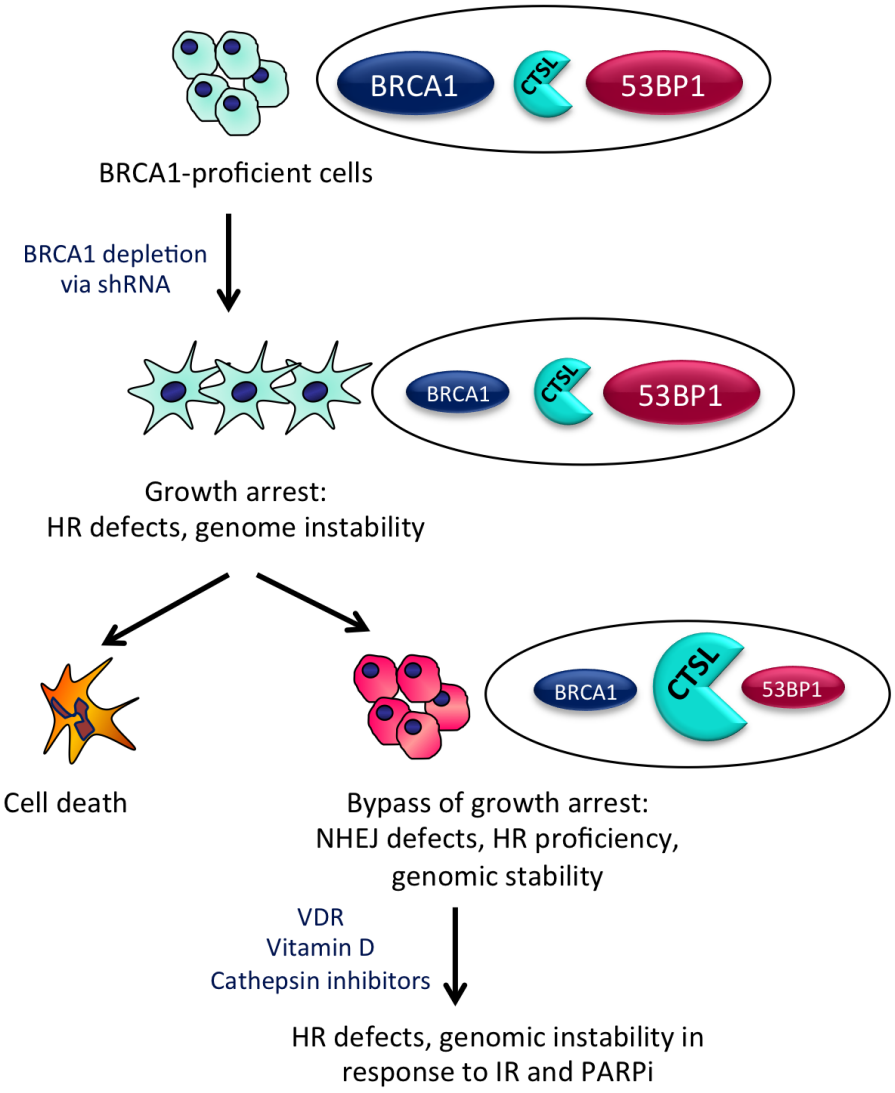

Figure 5-1. Activation of CTSL-mediated degradation of 53BP1 allows BRCA1-deficient cells to overcome genomic instability and growth arrest. Depletion of BRCA1 in breast cancer cells leads to defects in HR, genomic instability and growth arrest. Over time, BRCA1-deficient cells activate CTSL-mediated degradation of 53BP1, which rescues HR defects while inhibiting NHEJ. This allows BRCA1-deficient cells to overcome growth arrest. Inhibition of CTSL activity via treatment with vitamin D or specific inhibitors stabilizes 53BP1 protein levels and induces genomic instability in response to IR and PARPi.

5.2 How is CTSL upregulated?

Very little is known about how CTSL is regulated in the cell, so investigating how CTSL is upregulated upon depletion of BRCA1 is a very interesting question. BRCA1 is involved in genetic and epigenetic mechanisms that impact many cellular processes, including transcriptional regulation, maintenance of heterochromatin, regulation of DNA methylation, and miRNA biogenesis (Kawai & Amano, 2012; Mullan, Quinn, & Harkin, 2006; Shukla et al., 2010; Zhu et al., 2011). Given that in our study the activation of CTSL upon loss of BRCA1 can take upwards of two weeks to occur, we believe that CTSL is not likely a direct transcriptional target of BRCA1. Rather, we speculate that loss of BRCA1 might result in alterations in chromatin structure that make the CTSL gene more permissive to transcriptional activation over time. It is possible that changes in BRCA1 levels could have an effect on the chromatin structure of the CTSL gene promoter. Chromatin immunoprecipitation (ChIP) analyses can be performed on the CTSL promoter to determine changes in chromatin marks or to detect the binding of chromatin modifying factors, such as HDACs and histone methyltransferases. In addition, it would be important to monitor DNA methylation levels of a bona-fide CpG island identified at the CTSL promoter (Jean, Rousselet, & Frade, 2006). Demethylation of this region upon loss of BRCA1 could potentially be behind the increase in CTSL expression. The effect that loss of BRCA1 has on CTSL promoter activity could also be measured using a luciferase reporter construct and promoter mutants can be made to determine which domains of the CTSL promoter are important for its upregulation.

There is evidence that Ras impacts CTSL levels. Studies by other groups have shown that activation of Ras leads to increased expression of CTSL as well as increased levels of nuclear

CTSL (Chambers, Colella, Denhardt, & Wilson, 1992; Goulet et al., 2004). Experiments are under way in our laboratory to determine if Ras or any of its downstream effectors are activated upon loss of BRCA1 in breast tumor cells and if overexpression of Ras activates CTSL-mediated degradation of 53BP1, which would reveal a novel role for Ras in the regulation of DNA repair factors and genomic stability. Experiments can also be performed to determine if inhibition of Ras using compounds such as farnesyltransferase inhibitors can block CTSL-mediated degradation of 53BP1. There is also evidence that the transcription factor STAT3 (Kreuzaler et al., 2011) and the tumor suppressor protein p53 (Yu, Harris, & Levine, 2006) regulate CTSL mRNA and protein levels, an avenue that needs to be investigated in the context of BRCA1 or lamins-deficiency.

It is also unknown how loss of A-type lamins leads to transcriptional upregulation of CTSL. Given that A-type lamins have a role in the positioning of chromatin in the nucleus, the increased transcription of CTSL could be due to altered nuclear localization of the gene. Furthermore, since loss of BRCA1 or A-type lamins has similar effects on CTSL and 53BP1 levels, we can identify similar mRNA expression changes in both situations. A microarray analysis could reveal novel regulators of CTSL, which could impact DNA repair. Since our experiments have shown that loss of 53BP1 is responsible for overcoming the growth arrest, an experiment should be carried out to determine if downregulation of 53BP1 brought on by depletion of A-type lamins would be sufficient to bypass the growth arrest upon loss of BRCA1. Furthermore, since loss of A-type lamins leads to transcriptional downregulation of BRCA1, which could be responsible for the activation of CTSL-mediated degradation in *LMNA* null cells, reconstitution of BRCA1 in *LMNA* null cells could restore the levels of 53BP1.

5.3 How does nuclear CTSL impact on DNA repair?

We have also provided evidence that depletion of CTSL increases the levels of BRCA1 in breast cancer cells (**Figure 2-6**). Based on these data, we speculated that CTSL transcriptional upregulation upon depletion of BRCA1 would impact on BRCA1 protein stability, similarly to the effect of CTSL on 53BP1. To test this model, our laboratory plans to manipulate expression of CTSL in cells (either upregulation or depletion) and monitor the half-life of BRCA1 and 53BP1 proteins. The results of these studies will uncover new links between proteases and DNA repair factors. Another intriguing question that remains unanswered is whether the nuclear form of CTSL is directly responsible for the degradation of 53BP1 upon BRCA1 depletion. We have preliminary evidence from immunohistochemistry of MCF7 cells embedded in paraffin blocks that nuclear CTSL is upregulated in BOGA cells (**Figure 2-16**), however subcellular fractionation experiments have been unsuccessful in locating CTSL in the nucleus. Experiments to locate CTSL in the nucleus will continue. We have also constructed a CTSL mutant lacking the signal peptide for endoplasmic reticulum targeting, which would target it to the nucleus. Experiments using this construct will be performed to determine if nuclear CTSL degrades 53BP1 and BRCA1. An alternative possibility is that upregulation of CTSL leads to 53BP1 accumulation in the cytoplasm where it is degraded by other means. It is unclear in this context whether the degradation of 53BP1 by CTSL is direct or indirect. To determine if the degradation is direct, we can perform *in vitro* degradation assays with purified 53BP1 and varying concentrations of CTSL to assess the degree of proteolysis. We can then perform mass spectrometry to identify sites where CTSL cleaves 53BP1, if the cleavage is direct.

5.4 Does CTSL regulate BRCA1 and 53BP1 during the cell cycle?

While levels of BRCA1 are known to fluctuate during the cell cycle, being low in G0/G1 and peaking during G2 (Liu et al., 2010), very little is known about the levels of CTSL and 53BP1 during the cell cycle. Since NHEJ is primarily active during G0/G1, one would likely speculate that levels of 53BP1 would be high during this phase of the cell cycle. Our preliminary results, however, indicate that 53BP1 levels are reduced in G0/G1, possibly due to degradation by CTSL. We found that growth arresting MCF7 cells in G0/G1 by serum deprivation leads to decreased levels of BRCA1, upregulation of CTSL, and downregulation of 53BP1 (**Figure 2-17**). We hypothesize that the downregulation of BRCA1 during G0/G1 induces CTSL transcriptional upregulation, which then degrades 53BP1. Experiments are being done to determine the levels of these proteins during the remainder of the cell cycle to investigate if BRCA1 and 53BP1 mirror each other to maintain a competitive balance for proper DNA repair. Depleting CTSL in growth-arrested cells will allow us to determine if CTSL is responsible for the degradation of 53BP1. Given that CTSL may degrade BRCA1, it is possible that there is a feedback loop where the upregulation of CTSL in cells that have low BRCA1 further lowers the levels of BRCA1. Overall, these studies might reveal a functional interplay between BRCA1, CTSL, and 53BP1 during the cell cycle.

5.5 Does vitamin D or CTSL inhibitor treatment reduce tumor growth in mouse models of tumorigenesis?

Future experiments will focus on determining if vitamin D or CTSL inhibitor treatment in conjunction with PARPi or other DNA damaging strategies is effective in reducing tumor growth *in vivo*. Based on our *in vitro* findings and the identification of novel biomarkers in

TNBC and BRCA1-mutated tumors, we expect that these kinds of tumors implanted in mice will respond to treatment by CTSL inhibition. Raising 53BP1 levels in BRCA1-mutated tumors or in TNBC tumors that have high nuclear CTSL and low 53BP1 should render the cancer cells susceptible to PARPi or radiation therapy. Since vitamin D has an effect on many cellular processes aside from inhibition of CTSL, including cell cycle regulation, it will be especially important to determine if specific CTSL inhibitors could reduce tumor growth.

There are several mouse models of tumorigenesis that can be utilized to examine this. An orthotopic model can be used to implant BOGA cells into mammary fat pads of mice followed by treatment and tumor growth measurement. The human-in-mouse model could be used to implant pieces of triple-negative tumors into mice and determine how tumor growth is affected by vitamin D or CTSL inhibitor treatment. Triple-negative tumors have already been utilized in this mouse model (Ma et al., 2012), and would be the closest scenario possible to treatment of humans. BRCA1 conditional knockout mice are also available to determine how BRCA1 deficient tumors that arise in these mice would respond to treatment, and the mice could also be crossed to CTSL knockout mice to determine the effect of complete loss of CTSL on tumor growth. All tumors would be collected and subjected to immunohistochemistry to measure levels of nuclear CTSL, VDR, and 53BP1 to determine if the treatment outcome coincides with our hypothesis based on the tumor tissue microarray data and our *in vitro* findings.

5.6 Are 53BP1 levels maintained in other laminopathies?

Maintenance of 53BP1 levels appears to be a mechanism to ensure genomic stability in the context of A-type lamins deficiency. Complete loss of A-type lamins leads to the degradation of 53BP1 and genomic instability, however expression of a very small amount of mutant A-type

lamins that do not contain exon 9 is sufficient to maintain 53BP1 levels and genomic stability. An important experiment to perform would be to express the Δexon9Lmna construct in *LMNA* null cells to determine if 53BP1 levels and NHEJ defects are rescued. This experiment would demonstrate that exon 9 of *LMNA* is not required for stabilization of 53BP1. We also have a library of mutant *LMNA* constructs that are associated with different laminopathies that can be expressed in *LMNA* null cells to determine which mutants stabilize 53BP1. These experiments could also reveal which laminopathies are characterized by genomic instability and serve to identify a domain in the *LMNA* gene that is responsible for maintaining 53BP1 levels and genomic stability.

5.7 References

Bouwman, P., Aly, A., Escandell, J. M., Pieterse, M., Bartkova, J., Van der Gulden, H., Hiddingh, S., et al. (2010). 53BP1 loss rescues BRCA1 deficiency and is associated with triple-negative and BRCA-mutated breast cancers. *Nature structural & molecular biology*, *17*(6), 688–95. doi:10.1038/nsmb.1831

Bunting, S. F., Callén, E., Wong, N., Chen, H.-T., Polato, F., Gunn, A., Bothmer, A., et al. (2010). 53BP1 inhibits homologous recombination in Brca1-deficient cells by blocking resection of DNA breaks. *Cell*, *141*(2), 243–54. doi:10.1016/j.cell.2010.03.012

Cao, L., Xu, X., Bunting, S. F., Liu, J., Wang, R.-H., Cao, L. L., Wu, J. J., et al. (2009). A selective requirement for 53BP1 in the biological response to genomic instability induced by Brca1 deficiency. *Molecular cell*, *35*(4), 534–41. doi:10.1016/j.molcel.2009.06.037

Chambers, A. F., Colella, R., Denhardt, D. T., & Wilson, S. M. (1992). Increased expression of cathepsins L and B and decreased activity of their inhibitors in metastatic, ras-transformed NIH 3T3 cells. *Molecular carcinogenesis*, *5*(3), 238–45. Retrieved from http://www.ncbi.nlm.nih.gov/pubmed/1586450

Constantinidou, A., Jones, R. L., & Reis-Filho, J. S. (2010). Beyond triple-negative breast cancer: the need to define new subtypes. *Expert review of anticancer therapy*, *10*(8), 1197–213. doi:10.1586/era.10.50

Gonzalez-Suarez, I., Redwood, A. B., Perkins, S. M., Vermolen, B., Lichtensztejin, D., Grotsky, D. a, Morgado-Palacin, L., et al. (2009). Novel roles for A-type lamins in telomere biology and the DNA damage response pathway. *The EMBO journal*, *28*(16), 2414–27. doi:10.1038/emboj.2009.196

Goulet, B., Baruch, A., Moon, N.-S., Poirier, M., Sansregret, L. L., Erickson, A., Bogyo, M., et al. (2004). A cathepsin L isoform that is devoid of a signal peptide localizes to the nucleus in S phase and processes the CDP/Cux transcription factor. *Molecular cell*, *14*(2), 207–19. Retrieved from http://www.ncbi.nlm.nih.gov/pubmed/15099520

Jean, D., Rousselet, N., & Frade, R. (2006). Expression of cathepsin L in human tumor cells is under the control of distinct regulatory mechanisms. *Oncogene*, *25*(10), 1474–84. doi:10.1038/sj.onc.1209196

Kawai, S., & Amano, A. (2012). BRCA1 regulates microRNA biogenesis via the DROSHA microprocessor complex. *The Journal of cell biology*, *197*(2), 201–8. doi:10.1083/jcb.201110008

Kreuzaler, P. A., Staniszewska, A. D., Li, W., Omidvar, N., Kedjouar, B., Turkson, J., Poli, V., et al. (2011). Stat3 controls lysosomal-mediated cell death in vivo. *Nature cell biology*, *13*(3), 303–9. doi:10.1038/ncb2171

Liu, W., Zong, W., Wu, G., Fujita, T., Li, W., Wu, J., & Wan, Y. (2010). Turnover of BRCA1 involves in radiation-induced apoptosis. *PloS one*, *5*(12), e14484. doi:10.1371/journal.pone.0014484

Ma, C. X., Cai, S., Li, S., Ryan, C. E., Guo, Z., Schaiff, W. T., Lin, L., et al. (2012). Targeting Chk1 in p53-deficient triple-negative breast cancer is therapeutically beneficial in human-in-mouse tumor models. *The Journal of clinical investigation*, *122*(4), 1541–52. doi:10.1172/JCI58765

Mullan, P. B., Quinn, J. E., & Harkin, D. P. (2006). The role of BRCA1 in transcriptional regulation and cell cycle control. *Oncogene*, *25*(43), 5854–63. doi:10.1038/sj.onc.1209872

Nanda, R. (2011). "Targeting" triple-negative breast cancer: the lessons learned from BRCA1-associated breast cancers. *Seminars in oncology*, *38*(2), 254–62. doi:10.1053/j.seminoncol.2011.01.007

Shukla, V., Coumoul, X., Lahusen, T., Wang, R.-H., Xu, X., Vassilopoulos, A., Xiao, C., et al. (2010). BRCA1 affects global DNA methylation through regulation of DNMT1. *Cell research*, *20*(11), 1201–15. doi:10.1038/cr.2010.128

Yu, X., Harris, S. L., & Levine, A. J. (2006). The regulation of exosome secretion: a novel function of the p53 protein. *Cancer research*, *66*(9), 4795–801. doi:10.1158/0008-5472.CAN-05-4579

Zhu, Q., Pao, G. M., Huynh, A. M., Suh, H., Tonnu, N., Nederlof, P. M., Gage, F. H., et al. (2011). BRCA1 tumour suppression occurs via heterochromatin-mediated silencing. *Nature*, *477*(7363), 179–84. doi:10.1038/nature10371

CHAPTER SIX

Materials and methods

6.1 Cell culture and cell treatments

All cells were maintained by standard tissue culture procedure in DMEM supplemented with 10% fetal bovine serum or bovine growth serum with antibiotics and antimycotics. MCF7 and MDA-MB-231 cells were gifts from Jason Weber (Washington University). The HCC1937 cells were gifts from Junran Zhang (Case Western Reserve University). The Δexon9Lmna mouse embryonic and adult fibroblasts were generated in the laboratory of Colin L. Stewart as described in Mounkes, Kozlov, Hernandez, Sullivan, & Stewart (2003). MCF7 cells transduced with sh scr or sh BRCA1 were fingerprinted and shown to correspond to parental MCF7 cells (data not shown). For growth arrest by serum deprivation, MCF7 cells were incubated in DMEM + 0.1% FBS + antibiotics/antimycotics for 48 hours. DNA content was monitored after ethanol fixation and propidium iodide labeling (1 mg/ml in water).

Cells were subjected to the following treatments:

Vitamin D. Cells were incubated with 10^{-7} M 1α,25-dihydroxyvitamin D_3 (D1530, Sigma-Aldrich) for 24-48 hours, as indicated. Aliquots of 1 nmol 1α,25-dihydroxyvitamin D_3 were resuspended in 1 mL of BGS and diluted in DMEM to a final concentration of 10% BGS. BGS was the vehicle in control media.

E-64. Cells were incubated with the broad-spectrum cathepsin inhibitor E-64 (E3132, Sigma-Aldrich) diluted in water at a concentration of 10 µM for 24 hours.

PARPi. Cells were treated with the PARPi EB-47 (E8405, Sigma-Aldrich) diluted in water at a concentration of 1.2 µg/mL for 48 hours.

Ionizing radiation. For determining the extent of genomic instability, cells were irradiated with 2 Gy and analysis of metaphase spreads was performed 24 hours post-irradiation. For assaying formation of IRIF, cells were irradiated with 8 Gy and fixed and processed for immunofluorescence 1 hour, 3 hours, or 6 hours post-irradiation as indicated. For comet assays, cells were irradiated with 8 Gy.

6.2 Lentiviral transductions/Transient transfection

Lentiviral transductions were performed as previously described (Gonzalez-Suarez et al., 2009). Briefly, 293T cells were transfected with viral packaging (pHR'8.2ΔR) and envelope (pCMV-VSV-G) plasmids along with the vector containing the sh RNA of interest or sh control. After 48 hours, viral media was collected and used to infect target cells in one 4-6 hour infection. Cells were allowed to recover for 48 hours and treated with the appropriate selection drug (0.5 mg/mL G418 or 2 μg/mL puromycin). Viral packaging and envelope plasmids were gifts from Sheila Stewart. Except for one shBRCA1 (sequence: TCAGTACAATTAGGTGGGCTT) that was constructed by Junran Zhang, the rest were purchased from the Genome Institute at Washington University (sh BRCA sequences #1: GAGAATCCTAGAGATACTGAA, #2:TATAGCTGTTGGAAGGACTAG, #3:CCCTAAGTTTACTTCTCTAAA, #4:GCCCACCTAATTGTACTGAAT, #5:CCCACCTAATTGTACTGAATT). The sh53BP1 and sh CTSL constructs were purchased from Washington University.

HA-BRCA1 (Plasmid 14999, Addgene) transient transfections were carried out using the X-tremeGENE HP transfection reagent (06366236001, Roche).

6.3 Analysis of aberrant chromosomes

Cells were treated with vitamin D or E-64 for 24 hours, irradiated, and allowed to recover for 24 hours. Cells treated with PARPi were pre-treated with vitamin D for 24 hours followed by combined treatment with vitamin D and PARPi for 48 hours. Following all treatments, cells were arrested in mitosis by treatment with colcemid for 4 hours and metaphase spreads prepared by hypotonic swelling in 0.56% KCl, followed by **fixation in 3:1 methanol: acetic acid. Cell suspensions were dropped onto slides and** stained for 25 minutes in Wright-Giemsa Stain (9380-32, Ricca Chemical Company) and then washed in water. Slides were allowed to dry and were mounted using Eukitt Mounting Reagent (03989, Sigma) and analyzed at room temperature on a Leica DM5000 B microscope using a 100x oil objective (NA 1.30). Images were acquired with the Leica DFC350 FX digital camera using the Leica Application Suite Version 4.1.0

6.4 Comet Assay

Neutral comet assays were performed using CometSlide assay kits (Trevigen). Treated cells were irradiated with 8 Gy and incubated at 37ºC for different periods of time to allow DNA to repair (0, 30, 60, 90 min). Cells were embedded in agarose, lysed, and subjected to neutral gel electrophoresis. Cells were stained with ethidium bromide and visualized using a fluorescence microscope. Olive comet moments were calculated by multiplying the percentage of DNA in the tail by displacement between the means of the head and tail distributions as described in Olive, Banáth, & Durand (1990). The program CometScore™ Version 1.5 (TriTek) was used to calculate olive moments. A total of 30 comets were analyzed per sample in each experiment.

6.5 Immunoblotting

Cells were lysed in RIPA buffer (50mM Tris-HCl pH 8.0, 150mM NaCl, 1% NP-40, 0.5% sodium deoxycholate, 0.5% SDS) supplemented with PMSF, protease inhibitors (Sigma), and 20mM DTT. Protein detection was carried out using the following antibodies: BRCA1 (sc-6954, Santa Cruz), 53BP1 (NB100-304, Novus), CTSL (sc-6500, Santa Cruz), β-Tubulin (T8328, Sigma), Lamin A/C (sc-20681, Santa Cruz), Actin (69100, ImmunO), and P107 (sc-318, Santa Cruz).

6.6 Immunofluorescence

For immunofluorescence of RAD51, 53BP1, H3K9me3 and H4K20me3 cells were plated on coverslips and fixed in 3.7% formaldehyde and 0.2% Triton-X 100 in PBS for 10 minutes at room temperature. Coverslips were washed and blocked for 1 hour at 37ºC in 1% BSA and 0.1% Triton-X 100 in PBS. Primary antibody incubation with antibodies recognizing RAD51 (1:200, sc-8349, Santa Cruz), 53BP1 (1:1000, NB100-304, Novus), H3K9me3 (#07-442, Upstate), or H3K20me3 (#07-463, Upstate) was carried out for 1 hour at 37ºC, followed by washing in PBS and incubation with Alexa Fluor 488 goat anti-rabbit (1:1000, A11008, Invitrogen) secondary antibody for 1 hour at 37ºC. After washing in PBS, coverslips were mounted using Vectashield with DAPI (H-1200, Vector Labs). BRCA1 immunofluorescence was performed following a protocol from the Fernandez-Capetillo laboratory. Briefly, cells were washed twice with PBS, and incubated in CSK I buffer (10 mM PIPES pH6.8, 100 mM NaCl, 300 mM sucrose, 3 mM $MgCl_2$, 1 mM EGTA, and 0.5% Triton X-100) for 5 minutes. Coverslips were washed 5 times with cold PBS and fixed in modified STF buffer (150 mM 2-Bromo-2-nitro-1,3,-propanediol, 108 mM diazolidinyl urea, 10 mM Na citrate, and 50 nM EDTA pH 5.7) for 30 minutes at room

temperature. Coverslips were then washed twice with cold PBS and permeabilized (PB buffer: 100 mM Tris-HCl pH 7.4, 50 mM EDTA pH 8.0, and 0.5% Triton X-100) for 15 minutes at room temperature followed by 2 washes in PBS. Blocking, antibody staining, and mounting were carried out as described above, with BRCA1 antibody (sc-6954, Santa Cruz) diluted at 1:200 and Alexa Fluor 594 goat anti-mouse secondary antibody (A11005, Invitrogen) diluted at 1:1000.

Microscopy and photo capture was performed at room temperature on either a Nikon Eclipse 90i microscope using 60x oil or 100x oil objective lenses (NA 1.4 and 1.45, respectively) with a Photometrics Cool Snap ES2 digital camera and MetaMorph (Version 7.1.2.0) or a Leica DM5000 B microscope using 63x oil or a 100x oil objective lenses (NA 1.4 and 1.3, respectively) with a Leica DFC350FX digital camera and the Leica Application Suite (Version 4.1.0).

6.7 Proliferation assays

To quantify growth upon depletion of BRCA1, cells were plated in triplicate at 150,000 cells/well and counted 96 hours later. Cell proliferation was measured in each cell line 4 times within a 14-day period. To quantify the growth of the sh 53BP1/sh BRCA1 cells, $4x10^6$ cells were plated in 15 cm dishes and counted every 96 hours for 20 days. In order to extrapolate proliferation to the respective time periods, we used the equation $N=N_0e^{kt}$ where N is the final number of cells, N_0 is the starting number of cells, k is ln2/DT (doubling time), and t is time in days (Sherley, Stadler, & Stadler, 1995). For each 96 hour period we calculated the doubling time and used it to estimate the number of cells (N) that would result from initially plating 150,000 (N_0) and culture them for a given period of time. The doubling times for the control

cells remained constant throughout the time period, while the doubling times for the shBRCA1 cells started increasing once the cells overcame the growth arrest.

6.8 Quantitative reverse-transcription PCR

RNA was isolated using the RNAqueous-4PCR Kit (Ambion). cDNA was generated from 500 ng of total RNA using TaqMan Reverse Transcription Reagents (Applied Biosystems). BRCA1, 53BP1, CTSL and 18S expression was determined using TaqMan Gene Expression Assays (Hs01556193_m1, Hs00996818_m1, Hs00377632_m1, Hs99999901_s1, respectively, Applied Biosystems). For the analysis, all reactions (in triplicate) were carried out by amplifying target gene and endogenous controls in the same plate. Relative quantitative evaluation of target gene was determined by comparing the cycle thresholds.

6.9 Tissue tumor microarrays (TMA)

A total of 249 tissue samples from patients with sporadic breast carcinoma were obtained at Hospital Universitari Arnau de Vilanova in Lleida, Spain from 1998 to 2012. An informed consent was obtained from each patient and the study was approved by the local Ethical Committee. The series of 249 tumor samples included formalin-fixed, paraffin-embedded blocks for all patients, 165 core biopsies, before the initiation of neoadjuvant treatment, and 84 surgical specimens, before the initiation of adjuvant treatment. Tumors were classified according to the expression of the following proteins: Ki67, ERα and Her2 into four molecular subtypes: Luminal A (n=99), Luminal B (n=69), Her2 (n=45), Triple-Negative (n=36). Luminal A tumors are steroid hormone receptor–positive, negative for Her2, contain less than 30% of Ki67 positive cells, and tend to have a good prognosis. Luminal B tumors are steroid hormone receptor–

positive, negative for Her2, contain more than 30% Ki67 positive cells, and tend to have a worse prognosis than luminal A. In contrast, Her2 tumors are positive for Her2 and have been shown to have a poor prognosis. Triple-Negative tumors are negative for steroid hormone receptors and Her2 and have the worst prognosis. Moreover, tissue samples were also obtained from 18 breast cancers from patients carrying a BRCA1 germline mutation (Luminal A, n=1; Luminal B, n=1; Her2, n=2; Triple-Negative, n=15), and from 14 breast cancers from patients carrying a BRCA2 germline mutation (Luminal A, n=6; Luminal B, n=2; Her2, n=3; Triple-Negative, n=3). These patients had been treated in Hospital Santa Creu I Sant Pau, Barcelona, Spain.

A Tissue arrayer device (Beecher Instrument, MD) was used to construct the TMA. Briefly, all samples were histologically reviewed and representative areas were marked in the corresponding paraffin-blocks. Two selected cylinders (0.6 mm of largest diameter) from two different areas were included for each case.

6.10 Immunohistochemical analysis

TMA blocks were sectioned at a thickness of 3 μm, dried for 1h at 65ºC before being dewaxed in xylene and rehydrated through descending concentrations of ethanol, and washed with phosphate-buffered saline. Ki67, ERα and HER2 were used to determine molecular subtype. Comparative studies of CTSL, VDR, and 53BP1 expression were carried out on sequential serial sections. Antigen retrieval for CTSL and ERα was achieved by heat treatment at 95ºC for 20 min in a high pH solution (DAKO). Heat-induced antigen retrieval for 53BP1 and Ki67 was performed in a low pH solution (DAKO). Before staining the sections, endogenous peroxidase was blocked. Primary antibodies and incubation times were as follows: CTSL (1:50; S-20, Santa Cruz Biotechnology, incubation overnight at 4ºC); 53BP1 (1:2500; NB100-304,

Novus Biologicals, incubation 20 minutes at room temperature); VDR (1:2000; ABCAM, incubation 20 min at room temperature); Ki67 (Ready-to-use; M1B, DAKO, incubation 20 minutes at room temperature); ERα (Ready-to-use; 1D5, DAKO, incubation 20 minutes at room temperature), and HER2 (Herceptest Kit, DAKO). The reaction was visualized with the Streptovidin-Biotin Complex (DAKO) for CTSL and Envision Flex (DAKO) for 53BP1, Ki67 and ERα. Sections were counterstained with haematoxylin. Appropriate positive and negative controls were also tested.

Immunohistochemical scores provide a semiquantitative measurement of protein expression per tumor by taking into consideration the percentage of positive cells and the intensity of their staining. A histological score ranging from 0 (no immune reaction) to 300 (maximal immunoreactivity) was obtained with the formula Histoscore (Hscore) = 1X (% light staining) + 2X (% moderate staining) + 3X (% strong staining). The reliability of such scores for the interpretation of immunohistochemical staining in TMAs has been reported (Pallares et al., 2009).

Her2 staining was evaluated according to a standard protocol (HercepTest; DAKO) and scored as 4 intensities (i.e. negative=0; weak=1+; moderate=2+; and strong=3+), considering negative Her2 expression for intensity values of 0, 1+ and 2+ when there was no amplification by FISH, and positive for intensity values of 3+ and 2+, when 2+ was amplified by FISH. For each marker, there were a variable number of non-assessable cases due to technical problems including no representative tumor sample left in the cylinders, detachment, cylinders missed while constructing the array, necrosis, and absence of viable tumor cells in the TMA sections. TMA validation methods and results are available upon request.

6.11 MTS assay

Cells were plated in quadruplicate (500 or 1000 cells/well) in 96 well plates and treated with vitamin D or vehicle for 48 hours prior to measurement of proliferation. On the day of measurement of proliferation, an appropriate volume of MTS reagent was made just before addition to cells. Prior to addition of MTS reagent, cell media was replaced with 100µL of pre-warmed DMEM without phenol red. Per 1mL of PBS, 2mg of MTS powder was dissolved and 50µL of PMS was added and mixed. 20µL of MTS reagent was added to each well and absorbance at 490nm was read every hour for 4 hours after addition of the reagent.

6.12 *In vivo* tumor study

4T1 cells (gift from David Piwnica-Worms) were cultured as above. 50,000 4T1 cells per animal in 50µL of PBS were injected into mammary fat pads of female 6-8 week old female BALB/c mice. Vitamin D treatment began 6 days after tumor injection. Mice were injected i.p. with vehicle (PBS) or a mixture of a high dose (60ng) of the vitamin D precursor, 25-hydroxyvitamin D, and a low dose (1ng) of the active form of vitamin D, 1,25-dihydroxyvitamin D_3 once per week. Two other times per week mice were injected with only the active vitamin D. Tumor volume was measured using calipers daily.

6.13 Chromatin immunoprecipitation (ChIP)

ChIP analyses were carried our as described in García-Cao, O'Sullivan, Peters, Jenuwein, & Blasco (2004) with several modifications. Chromatin was extracted from a total number of $4x10^6$ MEFs and subjected to immunoprecipitation with various antibodies. To isolate chromatin, protein and DNA were crosslinked by treating adherent cells for 15 minutes at room

temperature (rt) with 1% formaldehyde in PBS. Crosslinking was terminated by adding glycine (final concentration of 0.125-0.150 M) for 5 minutes at rt. Cells were washed with cold PBS once and scraped off plates in cold PBS supplemented with PMSF and protease inhibitor cocktail. Cells were pelleted and lysed with lysis buffer (1% SDS, 10mM EDTA, 50mM Tris-HCl pH 8.0, PMSF, protease inhibitor cocktail) for 10 minutes on ice. Lysed cells were then sonicated using a Bioruptor sonicator (Diagenode) at 30 second intervals for 15 minutes on high to obtain DNA fragments between 250-1000 base pairs in length. Sonicated lysates were centrifuged at maximum speed for 15 minutes at rt and the chromatin containing supernatant was collected and the pellet was discarded.

Next, 200µL of lysate was transferred to a 2mL Eppendorf tube and diluted 1:10 in dilution buffer (1.1% Triton X-100, 0.01% SDS, 1.2mM EDTA pH 8.0, 167mM NaCl, 16.7mM Tris-HCl pH 8.0, PMSF, protease inhibitor cocktail) and precleared for 5 hours at 4ºC on a rotating platform using a 25% slurry of Protein A/G PLUS-Agarose Immunoprecipitation Reagent (sc-2003, Santa Cruz) was blocked with E. coli genomic DNA and BSA. Following preclearing, supernatant was collected by centrifugation at rt for 4 minutes at 4000rpm. Next, 4µL of antibody of interest (anti-H3K9me3, #07-442, Upstate or anti-H4K20me3 #07-463, Upstate) was added to the solution at incubated on a rotating platform for 1 hour at 4º. After the first hour, 60µL of the protein A/G beads slurry was added and incubated on a rotating platform overnight at 4ºC. The solution was then centrifuged as before and the unbound fraction in the supernatant was saved to be used as inputs. The pelleted fraction containing the beads was washed with 2mL of each buffer for 4 minutes at rt on a rocking platform as follows: once in low salt immune complex buffer (0.1% SDS, 1% Triton X-100, 2mM EDTA, 20mM Tris-HCl pH 8.0, 150mM NaCl), once in high salt immune complex buffer (0.1% SDS, 1% Triton X-100,

2mM EDTA, 20mM Tris-HCl pH 8.0, 500mM NaCl), once in LiCl immune complex wash buffer (0.25M LiCl, 1% NP-40, 1% sodium deoxycholate, 1mM EDTA, 10mM Tris-HCl pH 8.0), and twice in TE buffer (10mM Tris pH 8.0, 1mM EDTA). Elution of the immune complexes was done by adding 250µL of elution buffer (1% SDS, 50mM $NaHCO_3$), vortexing slowly at rt for 15 minutes, centrifuging for 4 minutes at 4000rpm, and collecting the supernatant. The elution procedure was repeated again to acquire a total volume of bound fraction of 500µL. Crosslinks were then reversed by adding 20µL of 5M NaCl and incubating at 65ºC overnight (inputs were included as well).

RNA and proteins were removed by adding 10µL of 0.5M EDTA, 20µL of 1M Tris-HCl pH 6.5, 2µL of RNAse (10µg/µL), and 2µL of proteinase K (20µg/µL) to each sample and incubating at 45ºC for 1 hour. DNA was recovered by phenol/chloroform extraction and ethanol precipitation. 500µL of phenol:chloroform:isoamyl alcohol 25: 24:1 was added and the solution was vortexed at high speed then centrifuged for 5 minutes at 10,000 rpm. The supernatant was collected and 500µL of chloroform:isoamyl alcohol was added and the sample was vortexed and centrifuged. This supernatant was transferred to a 2mL tube where we added 50µL of 5M NaCl, 1.5mL of 100% ethanol, and 1µL of glycogen and incubated at -20ºC for 1 hour to precipitate DNA. The solution was centrifuged at maximum speed for 15 minutes at rt and the DNA pellet was washed with 70% ethanol. The pellet was air dried and resuspended in 30µL of TE buffer. Immunoprecipitated DNA was slot-blotted onto a Hybond N^+ membrane and hybridized to a telomeric probe (gift from T. de Lange, Rockefeller University, NY, USA) or a major satellite probe. The signal was quantitated using the ImageQuant software (Molecular Dynamics). Serial dilutions of the unbound fraction from the no antibody control were processed for inputs. We calculated the amount of telomeric DNA immunoprecipitated relative to the signal of the

corresponding inputs. The ChIP values are represented as a percentage of the total input telomeric DNA, therefore correcting for the difference in the number of telomere repeats.

6.14 Terminal Restriction Fragment (TRF) analysis

To measure telomere length we prepared cells in agarose plugs and carried out TRF analysis as described (Blasco et al., 1997). Cells were collected, washed in PBS, and resuspended in 50µL PBS and incubated at 50ºC for 5 minutes to warm them. 50µL of 2% low melt agarose in PBS heated to 50ºC was added to the cells and incubated for 5 minutes at 50ºC. The mixtures was transferred to a plug mold (#170-3713, Bio-Rad) and allowed to solidify by cooling for 5 minutes at rt and then for 15 minutes at 4ºC. The plugs were transferred to 1.7mL tubes and treated with 500µL of proteinase K (2mg/ml) and incubated at 4ºC overnight. Plugs were then washed in TE buffer 4 times for 1 hour each and PMSF was added to the third and fourth washed to inactivate the proteinase K. Samples were then stored at 4ºC in TE buffer until digestion. To digest, plugs were washed in water for 1 hour, then equilibrated in MboI enzyme buffer for 1 hour. Next the plugs were incubated in 300µL of restriction enzyme buffer containing 50U of MboI overnight at 37ºC. Following digestion, the plugs were washed for 30 minutes with water and 30 minutes with 0.5X TBE buffer. Pulsed-field gel electrophoresis was performed using 1% low melt agarose in 0.5X TBE buffer for 23 hours at 6 V/cm^2. Following electrophoresis, the gel was denatured 3 times for 30 minutes each (0.5M NaOH, 1.5M NaCl in water) and neutralized 3 times for 30 minutes each (0.5M Tris-HCl, 1.5M NaCl in water, pH adjusted to 7.0) at rt. The Whatman TurboBlotter system was used to transfer the DNA to nylon membrane and DNA was crosslinked to the membrane using the Stratalinker UV crosslinker. DNA was then hybridized to a telomeric probe.

6.15 Quantitative Fluorescence *in situ* Hybridization (Q-FISH)

Q-FISH was performed as described previously (Herrera, Samper, & Blasco, 1999). Cells were cultured in 10cm dishes to 70% confluence and colcemid was added to the media (100µL in 10mL media) for 4 hours to arrest cells in metaphase. Cells were trypsinized after collected media and PBS wash, and centrifuged. The supernatant was aspirated to leave 1mL of media and the cell pellet, which was gently resuspended by flicking the tube. Cells were swollen in 9mL of pre-heated (37ºC) hypotonic buffer (0.56% KCl) for 10 minutes at 37ºC. 3 drops of fixing solution (cold 3:1 methanol:acetic acid) was added to the cells and cells were centrifuged at 4ºC. The supernatant was aspirated to leave 1mL and cells were resuspended as above. 11mL of fixing solution was added dropwise while gently vortexing, followed by centrifugation, aspiration of the supernatant, and addition of 11 more mL of fixing solution. Cells were stored at least overnight at -20ºC until hybridization.

Cells were pelleted and resuspend in fresh fixing solution. Cells were pelleted again and cells were dropped onto microscope slides containing 45% acetic acid and allowed to dry overnight. Next, slides were washed 3 times for 5 minutes each in PBS, fixed in 4% formaldehyde in PBS for 10 minutes, and washed another 3 times for 5 minutes each in PBS. Slides were incubated in pre-heated acidified pepsin (200mL water, 200mg pepsin, 168µL 12M HCl) for 10 minutes at 37ºC and then washed 3 times for 5 minutes each in PBS. Slides were fixed again as above and washed 3 times in PBS, then the slides were dehydrated by incubating for 5 minutes each in 70%, 90%, and then 100% ethanol and allowed to air dry. 10µL of probe solution (2.5µL 1M Tris-HCl pH 7.4, 21.4µL $MgCl_2$ buffer, 175µL deionized formamide, 5µL telomere probe, 12.5µL blocking reagent, 33.6µL distilled water), ($MgCl_2$ Buffer: 25mM $MgCl_2$,

9mM citric acid, 82mM Na_2HPO_4, adjusted pH to 7.0), (PNA telomere probe: TelC-Cy3, #F1002-5, Panagene), (blocking reagent: 10g Boehringer reagent in 100mL maleic acid buffer, pH 7.5), (maleic acid buffer: 100mM maleic acid, 150mM NaCl, pH 7.5) was added in 2 drops to coverslips and applied to slides. Slides were then heated on a slide warmer for exactly 3 minutes each at 80ºC for denaturation, then incubated in a humidified chamber in the dark for 2 hours at rt. Slides were then washed twice for 15 minutes while shaking at rt in buffer 1 (280mL formamide, 4mL 1M Tris-HCl pH 7.2, 4mL of 10% in water BSA, 112mL distilled water) and then 3 times for 5 minutes in buffer 2 (0.08% Tween-20 in TBS) while shaking at rt. Slides were dehydrated as above and mounted in Vectashield with DAPI. Fluorescent images were taken on a Nikon 90i upright microscope and intensity of telomere fluorescence was measured used the TFL-Telo program (a gift from P. Lansdorp, Vancouver, Canada) (Zijlmans et al., 1997). Images and telomere fluorescence values were measured from at least 50 metaphases in all cases.

6.16 Statistical analysis

For the in vitro experiments, a "two-tailed" student's t-test was used to calculate statistical significance of the observed differences. Microsoft Excel v.2010 was used for the calculations. In all cases, differences were considered statistically significant when $p<0.05$. For the TMA studies, a Kruskal-Wallis test was used to test the statistical significance of the observed differences in CTSL, VDR and 53BP1 Hscores between molecular breast tumor subtypes. Tumors were partitioned according to cut-off nuclear Hscores for CTSL, 53BP1 and VDR selected by their median values as >0, <150 and <120, respectively. Once cut-off points were applied, Fisher Exact Test was used to assess the statistical significance of the differences in the distribution of the two categories of CTSL, 53BP1 and VDR Hscores above or below cut

off points for all breast tumor types. In the analysis of BRCA1 and BRCA2 samples, we used the Mann-Whitney test to analyze Hscore differences between them as well as differences of each of them with the sample of sporadic tumors, and we used the Fisher exact test to assess differences in the distributions of groups defined by the same cut-off points used for the sporadic tumors. The subsample of TNBC was also compared with the sample of germinal BRCA1 mutated cancers using the same statistical tests. The Pearson correlation coefficient together with linear regression models assessed the statistical significance of the relationship between nuclear CTSL and 53BP1 Hscores. R package was used to all TMA statistical tests. Differences were considered significant when $p<0.05$.

6.17 References

Blasco, M. A., Lee, H. W., Hande, M. P., Samper, E., Lansdorp, P. M., DePinho, R. A., & Greider, C. W. (1997). Telomere shortening and tumor formation by mouse cells lacking telomerase RNA. *Cell*, 91(1), 25–34. Retrieved from http://www.ncbi.nlm.nih.gov/pubmed/9335332

García-Cao, M., O'Sullivan, R., Peters, A. H. F. M., Jenuwein, T., & Blasco, M. A. (2004). Epigenetic regulation of telomere length in mammalian cells by the Suv39h1 and Suv39h2 histone methyltransferases. *Nature genetics*, 36(1), 94–9. doi:10.1038/ng1278

Gonzalez-Suarez, I., Redwood, A. B., Perkins, S. M., Vermolen, B., Lichtensztejin, D., Grotsky, D. a, Morgado-Palacin, L., et al. (2009). Novel roles for A-type lamins in telomere biology and the DNA damage response pathway. *The EMBO journal*, 28(16), 2414–27. doi:10.1038/emboj.2009.196

Herrera, E., Samper, E., & Blasco, M. A. (1999). Telomere shortening in mTR-/- embryos is associated with failure to close the neural tube. *The EMBO journal*, 18(5), 1172–81. doi:10.1093/emboj/18.5.1172

Mounkes, L. C., Kozlov, S., Hernandez, L., Sullivan, T., & Stewart, C. L. (2003). A progeroid syndrome in mice is caused by defects in A-type lamins. *Nature*, 423(6937), 298–301. doi:10.1038/nature01631

Olive, P. L., Banáth, J. P., & Durand, R. E. (1990). Heterogeneity in radiation-induced DNA damage and repair in tumor and normal cells measured using the "comet" assay. *Radiation research*, 122(1), 86–94. Retrieved from http://www.ncbi.nlm.nih.gov/pubmed/2320728

Pallares, J., Santacana, M., Puente, S., Lopez, S., Yeramian, A., Eritja, N., Sorolla, A., et al. (2009). A review of the applications of tissue microarray technology in understanding the molecular features of endometrial carcinoma. *Analytical and quantitative cytology and histology / the International Academy of Cytology [and] American Society of Cytology*, 31(4), 217–26. Retrieved from http://www.ncbi.nlm.nih.gov/pubmed/19736869

Sherley, J. L., Stadler, P. B., & Stadler, J. S. (1995). A quantitative method for the analysis of mammalian cell proliferation in culture in terms of dividing and non-dividing cells. *Cell proliferation*, 28(3), 137–44. Retrieved from http://www.ncbi.nlm.nih.gov/pubmed/7734623

Zijlmans, J. M., Martens, U. M., Poon, S. S., Raap, A. K., Tanke, H. J., Ward, R. K., & Lansdorp, P. M. (1997). Telomeres in the mouse have large inter-chromosomal variations in the number of T2AG3 repeats. *Proceedings of the National Academy of Sciences of the United States of America*, 94(14), 7423–8. Retrieved from http://www.pubmedcentral.nih.gov/articlerender.fcgi?artid=23837&tool=pmcentrez&rendertype=abstract